Trigonocephaly in a select South African population: A morphometric analysis utilising specific anatomical cranial landmarks

Courtney Barnes
Student number: 218008430

Supervisor: Prof L. Lazarus
Co-supervisor: Prof A. Madaree

Submitted in fulfilment of the degree of

Master of Medical Science (Clinical Anatomy)

in the School of Laboratory Medicine and Medical Sciences,
College of Health Sciences, Department of Clinical Anatomy,
University of KwaZulu-Natal, Durban, South Africa

2024

PREFACE

This study is a representation of original work by the author and has not been submitted to other universities in any form. The work is under review in accredited journals in line with the thesis guidelines of the University of KwaZulu-Natal. Acknowledgment in the text has been made where the work of others was used.

The research described in the project was supervised by Prof L. Lazarus (Department of Clinical Anatomy, School of Laboratory Medicine and Medical Sciences, College of Health Sciences, University of KwaZulu-Natal, Durban, South Africa), and Prof A. Madaree (Department of Plastic and Reconstructive Surgery, School of Clinical Medicine, College of Health Sciences, University of KwaZulu-Natal, Durban, South Africa), and was conducted in the above-mentioned institution (on the Westville campus) and the Inkosi Albert Luthuli Central Hospital, Durban, South Africa.

DECLARATION

I, Ms Courtney Barnes, declare that:

i. The research reported in this dissertation, except where otherwise indicated, is my original work.
ii. This dissertation has not been submitted for any degree or examination at any other university.
iii. This dissertation does not contain other persons' data, pictures, graphs or other information, unless specifically acknowledged as being sourced from other persons.
iv. This dissertation does not contain other persons' writing, unless specifically acknowledged as being sourced from other researchers. Where other written sources have been quoted, then:
   a. Their words have been re-written but the general information attributed to them has been referenced.
   b. Where their exact words have been used, their writing has been placed inside quotation marks, and referenced.
v. Where I have reproduced a publication of which I am an author, co-author or editor, I have indicated in detail which part of the publication was actually written by myself alone and have fully referenced such publications.
vi. This dissertation does not contain text, graphics or tables copied and pasted from internet, unless specifically acknowledged, and the source being in the dissertation and in the Reference sections.

Signed:

[redacted] 30 January 2024

Courtney Barnes (218008430) **Date**

[redacted]

Professor Lelika Lazarus

[redacted]

Professor Anil Madaree

ACKNOWLEDGEMENTS

This research project has been possible due to the support and motivation of many important people in my life. I would like to take this opportunity to thank these people:

- God, for listening to my prayers and giving me the knowledge and perseverance to complete this research.
- My parents, Mr Murray Barnes and Mrs Melissa Barnes, for their love, support, and motivation throughout my life. Thank you so much for always being my safety net and reminding me what I am capable of.
- Professor Lelika Lazarus, for her continuous guidance, support, and for always believing in my capabilities as a researcher.
- Professor Anil Madaree, for his clinical expertise, time, and patience throughout this research project.
- The AME Healthcare staff at the Inkosi Albert Luthuli Central Hospital, for their radiological assistance.
- Dr Partson Tinarwo, for his assistance with the statistical data analysis.
- My family for always being interested and encouraging throughout my life and my research journey.
- My closest friend, Miss Vensuya Bisetty, for her advice, support, and keeping me sane throughout this journey.
- My close running group of friends, Mr Tindall Kruger, Mr Solly Nzima, Miss Shannon Williams, and Mr Richard Heath, for always keeping me grounded and entertained.
- The College of Health Sciences (CHS) for their financial assistance for part funding of this project.

TABLE OF CONTENTS

LIST OF FIGURES

LIST OF TABLES

LIST OF ABBREVIATIONS

2D	Two dimensional
3D	Three dimensional
ACF	Anterior cranial fossa
BREC	Biomedical Research Ethics Committee
CHS	College of Health Sciences
CT	Computed tomography
DICOM	Digital Imaging and Communication in Medicine
EBA	Endocranial bifrontal angle
FA	Frontal angle
IALCH	Inkosi Albert Luthuli Central Hospital
ICC	Intraclass coefficients
MCF	Middle cranial fossa
MPR	Multiplanar Reconstruction
MRI	Magnetic resonance imaging
PACS	Picture Archiving and Communication System
PCF	Posterior cranial fossa
ROI	Region of Interest
SD	Standard deviation

ABSTRACT

Trigonocephaly is a congenital abnormality that is caused by the premature fusion of the metopic suture. A triangular shaped forehead, shortening of the anterior cranial fossa (ACF), hypotelorism, narrowing of the bitemporal region, and widening of the occipitoparietal region are some of the cranial and facial deformities that patients with trigonocephaly present with. Literature on the morphometry of the ACF and cranial base is scarce in patients with trigonocephaly; most studies focus on the morphometric changes that occur to the entire cranium rather than the cranial base. Therefore, this study aimed to investigate the morphometric changes that occurred to the ACF and orbits in trigonocephaly patients and to determine whether compensatory growth of the middle and posterior cranial fossae (MCF and PCF) was evident via volumetric assessment. Additionally, the identification of various cranial parameters in order to assess the severity of patients with trigonocephaly remains controversial. Thus, this study also aimed to describe an improved grading system in the assessment of trigonocephaly within a select South African population.

Dimensions of the ACF and of the orbits, and volumetric assessment of all three cranial fossae were measured using specific anatomical cranial landmarks on preoperative computed tomography (CT) scans of 15 patients with a radiographic confirmed diagnosis of non-syndromic, isolated trigonocephaly between 2012 and 2023, and eight non-affected age-matched pediatric patients were selected as the control group. ACF dimensions in younger and trigonocephaly patients who were classified as severe, were observed to be larger compared to control patients, whilst in older and trigonocephaly patients who were classified as severe, ACF dimensions were observed to be smaller compared to control patients. MCF volume showed significance ($p=0.050$), whilst ACF and PCF volumes, respectively showed no significance ($p=0.170$ and $p=0.821$) when trigonocephaly patients were compared to controls. Additionally, maximum compensatory growth occurred in the PCF compared to the MCF in trigonocephaly patients. The overall dimensions of the orbit showed no significance between trigonocephaly and control patients. However, significant findings were observed in the correlation analysis between the interorbital distance and other orbital parameters and ACF angles when trigonocephaly patients were compared to control patients. Furthermore, more complex orbital morphologies were observed in trigonocephaly patients in younger age groups, compared to less complex orbital morphologies which were observed in older age groups.

This study provides novel morphometric and morphological data within a specific South African population. The data obtained could further assist craniofacial surgeons by providing a relationship between the degree of severity and choice of surgical intervention. Additionally, the orbital data obtained could indicate to surgeons the morphological changes that occur in the orbits, and provide an insight into the evolution of the deformity in pediatric patients with trigonocephaly in order to obtain as near to normal orbital features.

CHAPTER 1: INTRODUCTION

1.1. Introduction

Approximately 240 000 new-borns die globally within 28 days of birth per year due to congenital disorders (World Health Organization, 2023). Congenital disorders result in an additional 170 000 deaths of paediatric patients between one month and five years of age (World Health Organization, 2023). Craniosynostosis is a common congenital disorder caused by the premature fusion of one or more cranial sutures (Mendoza *et al*., 2013). As a result, this condition typically results in an abnormally shaped skull as well as a certain degree of damage to the brain, and abnormal facial features (Kajdic *et al*., 2018). Craniosynostosis can be classified according to the number of cranial sutures that have fused prematurely or the presence of underlying conditions (Kajdic *et al*., 2018).

Trigonocephaly, otherwise known as metopic synostosis, is classified as the second most common type of craniosynostosis, forming approximately 25% of all non-syndromic, isolated craniosynostosis occurrences (Beckett *et al*., 2012; Naran *et al*., 2017; Chandler *et al*., 2021). Trigonocephaly is caused by the premature fusion of the metopic suture (Van der Meulen, 2012; Wang *et al*., 2016). The occurrence of this premature fusion results in a number of cranial and facial abnormalities, such as a ridge over the middle of the forehead, creating a triangular-shaped forehead, shortening of the anterior cranial fossa (ACF), supra-orbital retrusion, hypotelorism, narrowing of the bitemporal region, and widening of the occipitoparietal region (Van der Meulen, 2012; Wang *et al*., 2016). The incidence of trigonocephaly is one in every 5000 live births and is observed to be more predominant in males compared to females (Van der Meulen, 2012; Ghizoni *et al*., 2016; Baş *et al*., 2021).

Due to the fact that trigonocephaly is the second most common type of craniosynostosis, there has been sparse literature documenting the dimensions of the ACF and orbits in trigonocephaly, especially in a South African population. This study appears to be unique in that it will record and compare the dimensions of the ACF and orbits in a specific South African population; several aspects of this study remain novel.

A reduced length and volume of the ACF is typical in trigonocephaly, therefore restoring both the normal shape and volume of the ACF, is one of the primary concerns in the treatment of trigonocephaly (Van der Meulen, 2012). As a result, knowledge of the dimensions of the ACF plays a vital role in the surgical correction of trigonocephaly, especially when assessing the severity of trigonocephaly into severe, moderate and mild types (Naran *et al*., 2017). Additionally, ACF morphometry can provide an indication to surgeons regarding the amount of damage trigonocephaly has caused to the brain during development, as patients with isolated trigonocephaly have been observed to possess the highest percentage of neurodevelopmental complications (Van der Meulen, 2012; Naran *et al*., 2017).

The volume of the ACF could have a relationship with the degree of severity of trigonocephaly. Restriction in the growth of the anterior third of the skull is typical in trigonocephaly (Naran *et al*., 2017). There has been sparse literature with regards to the volumetric comparison of the ACF and the entire cranial fossae volume in trigonocephaly patients. Moreover, previous literature has reported on the volume of the entire anterior cranium but not on the volume of the ACF specifically. Naran *et al*. (2017) observed a significantly smaller volumetric ratio when the volume of the anterior third of the skull was compared to the total cranial skull volume in patients with trigonocephaly compared to controls. Furthermore, due to the increase in the compensatory growth of the middle and posterior thirds of the skull in trigonocephaly, Naran *et al*. (2017) also observed a significantly larger volumetric ratio when the volume of the middle third of the skull was compared to the total cranial skull volume; however, the volumetric ratio of the posterior third of the skull compared to the total cranial skull volume showed no difference in trigonocephaly patients compared to controls.

Orbital morphometry is another important aspect to consider in patients with trigonocephaly. Hypotelorism, which occurs due to the ethmoid bone being underdeveloped, is present at the medial orbital walls in the majority of trigonocephaly cases, resulting in the orbits having various morphological appearances (Van der Meulen, 2012; Ezaldein *et al*., 2014; Štefánková *et al*., 2015). The majority of the literature mainly focuses on the surgical correction of the forehead and not on the surgical correction of hypotelorism (Ezaldein *et al*., 2014). There is a relationship between hypotelorism and the degree of severity, as orbital dysmorphology is more prone to decline with increasing severity of trigonocephaly, therefore resulting in more functional defects of the eye in trigonocephaly patients (Ezaldein *et al*., 2014). The interorbital distance is also affected in patients with this condition, and plays a role in the postoperative care of trigonocephaly patients, in order to determine the success rate of the hypotelorism correction (Maltese *et al*., 2014).

Plastic surgeons need to take specific metopic indices into consideration when assessing trigonocephaly patients for surgical correction. Metopic indices could help guide surgeons on the invasiveness of their surgical procedures and potentially reduce recovery time (Wang *et al*., 2016). Some cranial landmarks that are used to create the metopic indices can be palpable, therefore reducing the risk of exposing trigonocephaly patients to radiation through computed tomography (CT) scans.

This study aimed to record and compare the morphometry of the ACF and orbits, as well as the morphology of the orbits, in a select group of South African patients with non-syndromic, isolated trigonocephaly, using preoperative CT scans. Furthermore, this study aimed to describe an improved grading system in the assessment of the severity of trigonocephaly in a select South African population.

1.1.1. Research question

What are the dimensions of the ACF and orbits in trigonocephaly patients as opposed to a normal paediatric cohort in a South African population?

1.1.2. Aim

To record and compare the morphometry of the ACF and orbits, as well as the morphology of the orbits, in a group of select South African patients with non-syndromic, isolated trigonocephaly, using preoperative CT scans.

1.1.3. Objectives

a) To determine and compare the dimensions of the ACF in non-syndromic, isolated trigonocephaly to a normal age-matched paediatric group in terms of length, height, width, and volume.
b) To describe an improved grading system in the assessment of the severity of trigonocephaly.
c) To determine and compare the volume of the ACF to the entire cranial fossae volume in trigonocephaly patients and a normal age-matched paediatric group.
d) To determine and compare the compensatory growth percentages of the volumes of the MCF and PCF in trigonocephaly patients and a normal age-matched paediatric group.
e) To determine and compare the dimensions of the orbits in trigonocephaly to a normal age-matched paediatric group in terms of height, width, surface area, and interorbital distance.
f) To determine the different morphologies of the orbits in trigonocephaly patients.

1.2. Literature review

1.2.1. Gross anatomy

1.2.1.1. Development of the calvarium

The skull is composed of two parts, viz., the neurocranium, which encloses the brain, and the viscerocranium, which is responsible for forming the facial skeleton. The neurocranium can then further be divided into a cartilaginous part and a membranous part (Jin *et al.*, 2016). The membranous part is responsible for forming the calvarium, and consists of the paired frontal and parietal bones, temporal bone (squamous portion), and occipital bone (interparietal portion) (Jin *et al.*, 2016). The majority of the bones in the skull are connected by fibrous joints called sutures, which assist in facilitating the growth of the skull as opposed to movement during skull development (Gray and Standring, 2016).

Additionally, sutures are responsible for permitting the flexibility of the head during parturition in order to ensure normal delivery; as well as supporting the growth of the new-born brain in the postnatal period (Sharma, 2013). The calvarium consists of four main sutures, viz., the metopic, sagittal, coronal, and lambdoid sutures. The metopic suture divides the paired frontal bones from each other and varies with regards to its fusion period (Ghizoni *et al*., 2016). Typical fusion of the metopic suture is between three and nine months of age, but in some cases can start to fuse at two months of age, and is entirely closed by the third year of age (Ghizoni *et al*., 2016).

1.2.1.2. Development of the cranial fossae

The cartilaginous part of the neurocranium (chondrocranium) of the skull is initially comprised of various separate cartilages (Fig. 1A). Cartilages that are located anterior to the notochord, which terminate at the position of the pituitary gland in the middle of the sella turcica, are derived from neural crest cells. As a result, these cartilages are responsible for forming the prechordal chondrocranium. Cartilages that are located posterior to this termination are derived from the paraxial mesoderm and are responsible for forming the chordal chondrocranium. Thus, the skull base is formed by the fusion of these cartilages which undergo ossification via endochondral ossification. The parachordal cartilage and the bodies of three occipital sclerotomes are responsible for forming the base of the occipital bone (Fig. 1A). Anterior to the base of the occipital bone lie the hypophyseal cartilages and the trabeculae cranii, which eventually fuse to in order to form the body of the sphenoid and ethmoid bones, respectively. As a result of this fusion, an extended center plate of cartilage from the nasal area to the anterior aspect of the foramen magnum is formed. Furthermore, various additional mesenchymal condensations appear laterally on each side of the center plate. The most anterior condensation, the ala orbitalis, is responsible for forming the lesser wing of the sphenoid bone, whilst the posterior condensation, the ala temporalis, is responsible for forming the greater wing of the sphenoid bone. An additional condensation called the periotic capsule forms the petrous and mastoid parts of the temporal bone. These condensations eventually fuse with the center plate and each other, except for openings via which cranial nerves exit the skull (Fig. 1A and B) (Sadler and Langman, 2004).

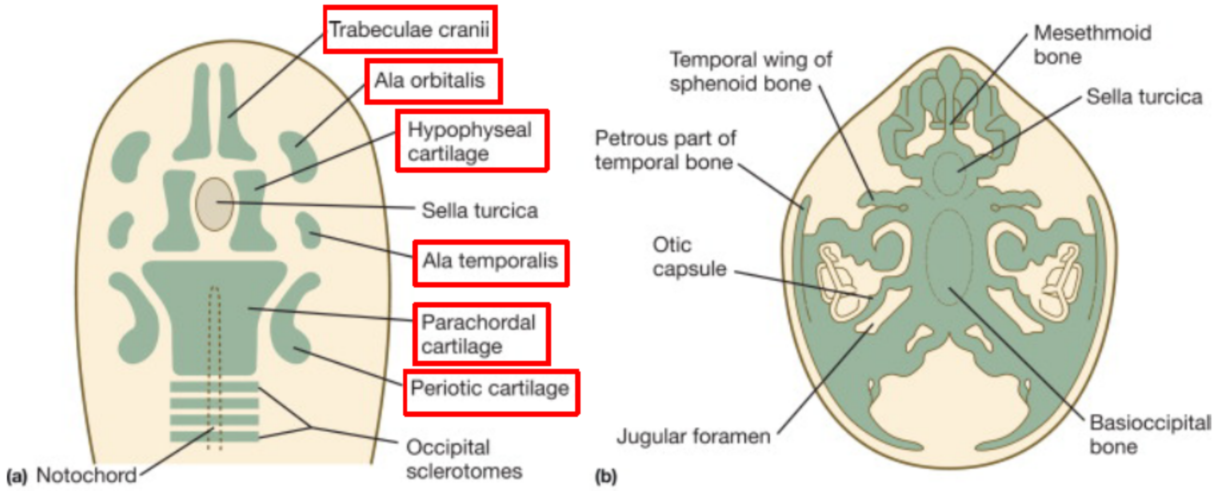

Figure 1: Development of the skeletal components of the chondrocranium. Superior view of a six week (A) and eight week embryo (B)

(Adapted from Carlson, 1996)

1.2.1.3. Anterior cranial fossa

The floor of the cranial cavity is separated into three distinct impressions known as the anterior, middle, and posterior cranial fossae. The ACF is the most anteriorly positioned impression and provides support to the frontal lobes of the cerebrum (Gray and Standring, 2016). The orbital portion of the frontal bone, the cribriform plate and crista galli of the ethmoid bone, and the lesser wings and anterior portion of the body (jugum sphenoidale and prechiasmatic sulcus) of the sphenoid bone are responsible for forming the ACF (Gray and Standring, 2016; Kasai *et al*., 2019). The cribriform plate of the ethmoid bone is positioned in the middle of the two orbital plates but is dipped below the orbital plates, therefore dividing the ACF from the nasal cavity (Hughes *et al*., 2010). The boundaries of the ACF floor consist of the following: (a) the frontal bone anteriorly; (b) the lesser wings of the sphenoid bone and frontal bone laterally; (c) the ethmoid bone and the body of the sphenoid bone medially; and (d) the sphenoid bone posteriorly (Smith and Bhatnagar, 2019).

1.2.1.4. Orbits

The orbits are paired structures in the upper portion of the face situated anterior to the MCF and are separated by the nasal cavity and paranasal air sinuses (Luibil *et al*., 2023). The orbits house the eyeball, the optic nerve, the extra-ocular eye muscles, the lacrimal apparatus, and the nerves and vessels supplying these structures. There are seven bones that are responsible for forming the bony orbit, viz., the maxilla, zygomatic, frontal, ethmoid, lacrimal, sphenoid, and palatine bones (Moore *et al*., 2010; Luibil *et al*., 2023). Jointly, these bones make the bony orbit to be pyramidal in shape. The optic foramen forms the apex of the pyramid-shaped bony orbit, whilst its base forms the walls of the orbits which are created by: (a) the frontal bone and lesser wing of the sphenoid bone superiorly (roof); (b) the frontal process of the maxilla medially (medial wall); (c) the zygomatic process of the maxilla, the zygomatic bone, and palatine bone inferiorly (floor); and (d) the zygomatic bone, the frontal process of the zygomatic bone, and the zygomatic process of the frontal bone laterally (lateral wall), which is the thickest of the orbital walls (Gray and Standring, 2016; Luibil *et al*., 2023). Each orbit has four boundaries, viz., the supraorbital boundary which is formed by the frontal bone, the lateral boundary which is formed by the frontal process of the zygomatic bone and completed superiorly by the zygomatic process of the frontal bone; the zygomaticofrontal suture is positioned in the palpable depression of these two bones, the infraorbital boundary which is formed on the lateral side by the zygomatic bone and on the medial side by the maxilla, and the medial boundary which is formed superiorly by the frontal bone and inferiorly by the lacrimal crest of the frontal process of the maxilla (Gray and Standring, 2016).

1.2.2. Outline of craniosynostosis

Craniosynostosis is a congenital anomaly caused by the premature fusion of the cranial sutures (Mendoza *et al*., 2013). It can result in cosmetic complications and also have functional repercussions, due to its effect on the growth of the brain, intra-cranial pressure, and its ability to cause visual and respiratory impairments (Mendoza *et al*., 2013). Studies have found that intracranial pressure may be increased in approximately 14% of single suture craniosynostoses. This is a result of the diminished cranial size and the unequal distribution between the production of cerebrospinal fluid and its exit rate (Sharma, 2013). Therefore, the most vital aspect of this congenital disorder is diagnosing patients as early as possible, in order for early surgical intervention to take place (Mendoza *et al*., 2013). This ensures that there is minimal brain damage, restoration of normal intracranial pressure, and decreased visual and respiratory deficiencies.

Craniosynostosis can usually be classified according to whether there is an underlying mechanism, the presence of other conditions, or the number of sutures that have fused (Kajdic *et al*., 2018). Primary craniosynostosis is an occurrence of craniosynostosis that results due to an initial defect in the process of ossification, whereas secondary craniosynostosis results due to the presence of known systemic disorders with hematologic or metabolic impairment, such as rickets or hypothyroidism (Kajdic *et al*., 2018). Additionally, if only one suture fuses prematurely it is classified as simple craniosynostosis, while complex craniosynostosis relates to the premature fusion of more than one suture (Ghizoni *et al*., 2016). Furthermore, primary craniosynostosis can be classified further into syndromic or non-syndromic craniosynostosis according to phenotypic characteristics (Sumkovski *et al*., 2019). Syndromic craniosynostosis, which accounts for less than 5% of all craniosynostoses, is typically associated with a clear family history of the congenital disorder, the fusion of more than one suture, and other abnormalities, such as Apert, Crouzon, or Pfeiffer syndromes (Ghizoni *et al*., 2016; Sumkovski *et al*., 2019); whereas non-syndromic craniosynostosis, which is more commonly observed, results from an isolated condition and involves the premature fusion of only one suture (Sumkovski *et al*., 2019) (Fig. 2).

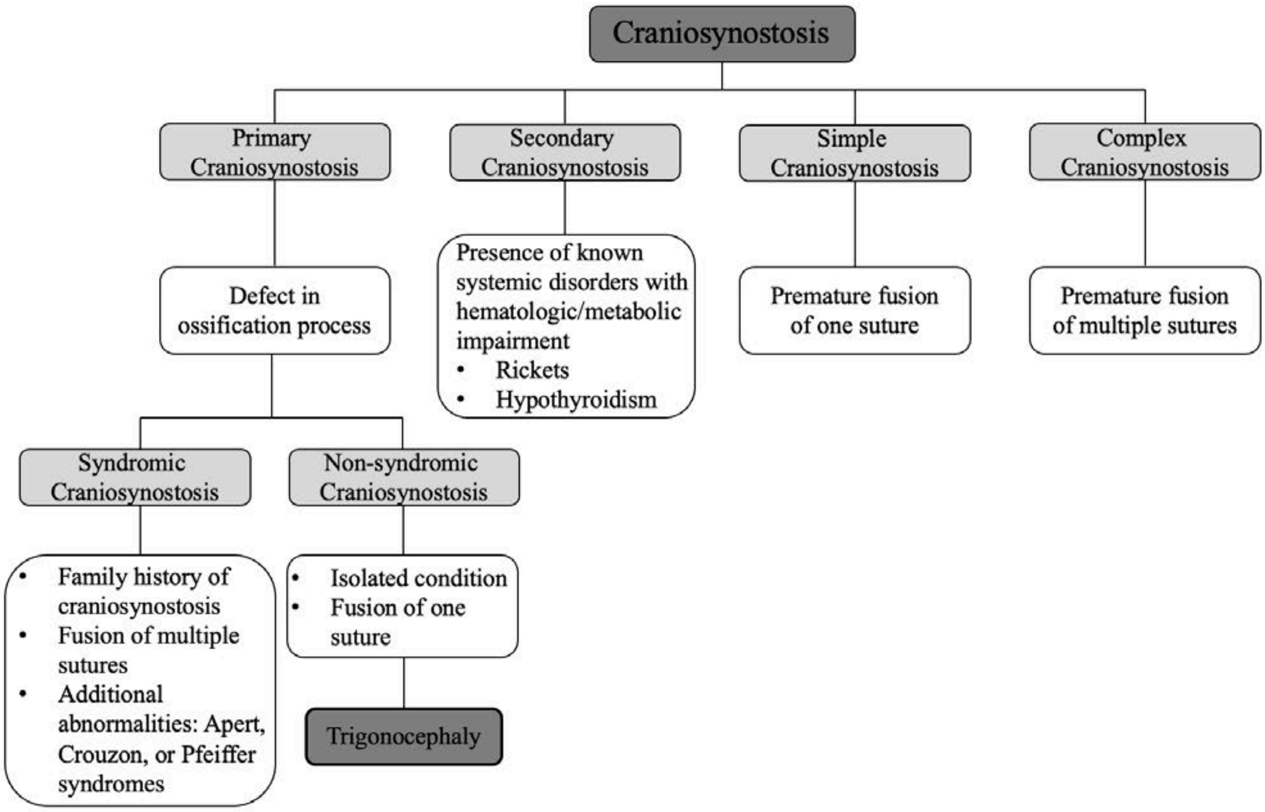

Figure 2: Schematic diagram on the classification of craniosynostosis

The prevalence of craniosynostosis has been reported to occur in one in every 2100-2500 live births (Mendoza *et al*., 2013; Ghizoni *et al*., 2016; Kajdic *et al*., 2018). The collective prevalence of craniosynostosis has significantly increased with no clear cause (Kajdic *et al*., 2018). Both environmental factors (for example, intrauterine fetal head constraint, prenatal exposures to teratogens, maternal smoking, or the use of fertility drugs such as clomiphene citrate) and genes (single gene mutations, abnormalities in chromosomes, and polygenic background) could all be influential factors in the aetiology of craniosynostosis (Reefhuis *et al*., 2003; Ghizoni *et al*., 2016; Kajdic *et al*., 2018). Genetic causes are responsible for 20% of all craniosynostoses, and are linked to various complications such as abnormalities of the limbs, cardiac region, trachea, and central nervous system (Ko, 2016; Kajdic *et al*., 2018).

1.2.3. Trigonocephaly

The term trigonocephaly arises from the Greek words "trigonon" meaning triangle, and "kephale" meaning head (Van der Meulen, 2012). Trigonocephaly, otherwise known as metopic synostosis, is the second most common type of craniosynostosis (Beckett *et al*., 2012; Naran *et al*., 2017; Chandler *et al*., 2021). It can occur in isolation (non-syndromic), with the fusion of other sutures, or due to the presence of a morphological abnormality such as Crouzon or Saethre-Chotzen syndrome (Ghizoni *et al*., 2016). The metopic suture is typically the first suture to fuse physiologically, starting at about three months of age. However, the premature fusion of this suture results in a ridge located over the middle of the forehead and limits the lateral growth of the frontal bones (Van der Meulen, 2012; Wang *et al*., 2016) (Fig. 2). This restricted growth of the frontal bones in combination with an increased compensatory growth of the cranial sutures that are unaffected results in the characteristic head shape of trigonocephaly (Freudlsperger *et al*., 2015).

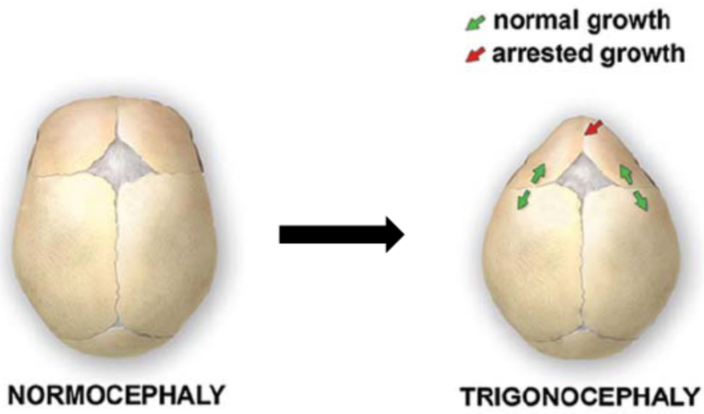

Figure 3: Restricted growth of the skull as a result of trigonocephaly

(Adapted from Kajdic et al., 2018)

Therefore, trigonocephaly can be characterized by a triangular-shaped forehead, shortening of the anterior cranial fossa, supra-orbital retrusion, hypotelorism, narrowing of the bitemporal region, and widening of the occipitoparietal region (Van der Meulen, 2012; Wang *et al*., 2016; Madaree *et al*., 2023) (Fig. 3A). The anterior fontanelle also fuses prematurely in approximately 50% of cases (Baş *et al*., 2021). The underdeveloped lateral orbital rims in trigonocephaly promotes the supra-orbital retrusion and bitemporal indentations (Van der Meulen, 2012). In some cases, hypotelorism is present at the medial orbital walls, and may be paired with incomplete development of the ethmoid bone. According to Van der Meulen (2012), the orbits in trigonocephaly patients are teardrop shaped and are angled towards the middle of the forehead (Fig. 3B).

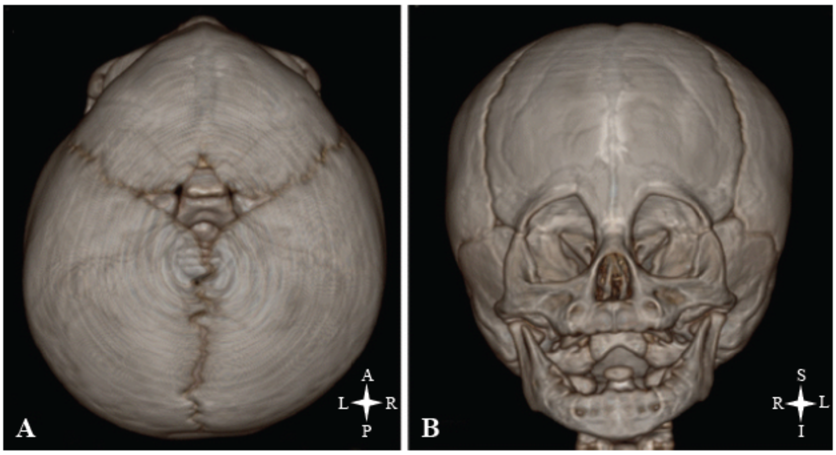

Figure 4: CT scan showing a superior (A) and anteroposterior (B) view of trigonocephaly

(Adapted from Van der Meulen, 2012)

The clinical facial features of trigonocephaly include:

- A significant metopic ridge, which is the most vital palpable soft tissue feature (Fig. 3A, 4D) (Van der Meulen, 2012; Spazzapan *et al*., 2016)
- A forehead resembling a heel shape, which is a soft tissue feature (Fig. 4A and B) (Spazzapan *et al*., 2016)
- Temples that show evidence of being depressed bilaterally due to bitemporal narrowing, which is a soft tissue feature as well as being visible radiologically (Fig. 4B, 4D) (Spazzapan *et al*., 2016)
- An extremely longer philtrum, which is a soft tissue feature (Fig. 4D) (Spazzapan *et al*., 2016)
- Evidence of hypotelorism at the medial orbital walls, which can be classified according to the morphology of the orbits, and is more accurately visible via three dimensional (3D) CT imaging (Fig. 3A and 4F) (Van der Meulen, 2012; Spazzapan *et al*., 2016)
- Constricted frontal lobes, which can be visible on magnetic resonance imaging (MRI), therefore resulting in developmental delays (Fig. 4C and 4E) (Spazzapan *et al*., 2016).

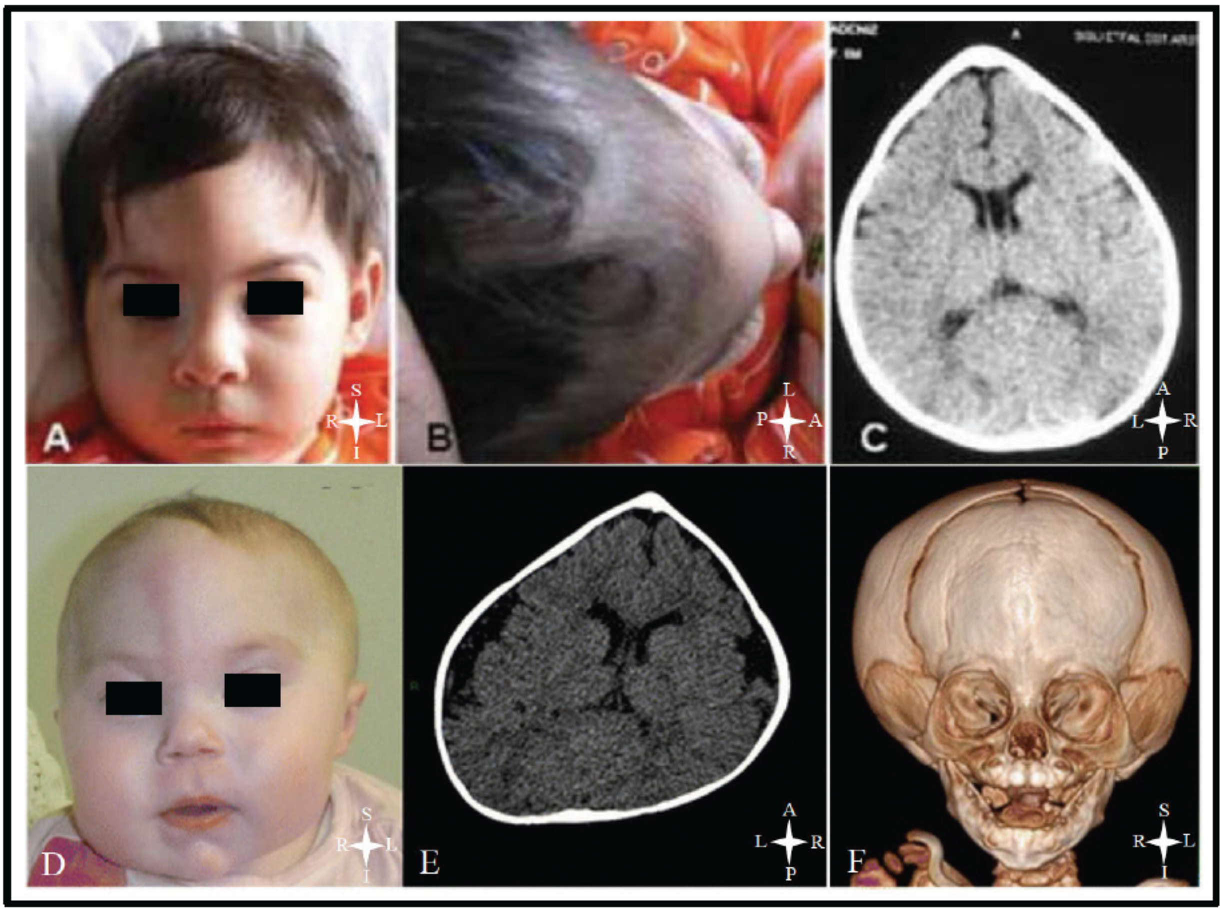

Figure 5: The clinical and soft tissue features of trigonocephaly patients. (A) and (B) Resembling the metopic ridge and a heel keel shaped forehead. (B) and (D) Resembling bilaterally depressed temples, and (D) also resembling the metopic ridge and a longer philtrum. (C) and (E) Resembling constricted frontal lobes. (F) Resembling hypotelorism at the medial orbital walls.

(Adapted from Spazzapan et al., 2016)

1.2.4. Severity assessment of trigonocephaly

According to a study by Wang *et al*. (2016), the severity assessment of trigonocephaly has been dependent on the judgement of the clinician and includes the use of aesthetic markers. This concurs with previous literature in which the Whitaker classification (1987) (which depends on the judgement of the clinician in order to determine if surgical intervention is required) was used as an assessment tool for craniosynostosis (Wang *et al*., 2016; Baş *et al*., 2021). There is no doubt that the Whitaker classification can provide a reliable severity assessment of trigonocephaly; however, it could restrict preoperative assessment of the severity of trigonocephaly as well as postoperative assessment of surgical correction (Wang *et al*., 2016). Furthermore, the use of specific cranial dimensions, in combination with the Whitaker classification, has shown to increase the accuracy and reliability in the assessment of various other craniosynostoses such as positional plagiocephaly, scaphocephaly, and brachycephaly (Wang *et al*., 2016). Therefore, these cranial measurements could also serve as an additional assessment tool to clinicians in assessing the severity of trigonocephaly. Previous literature has described various definitions of metopic indices which have been utilised in assisting clinicians in assessing patients with trigonocephaly both preoperatively and postoperatively (Table 1).

Table 1: Specific metopic indices utilised in the assessment of trigonocephaly in existing literature

Study	Parameter	Explanation
Beckett *et al*. (2012)	Endocranial bifrontal angle	"Angle of the frontal bone in a single axial plane at the level of the superior-most aspect of the crista galli with the vertex located on the endocranial side of the frontal bone at the metopic suture and terminal points at the lateral borders of the respective orbital apertures."
Van der Meulen (2012)	Frontal angle	"The angle between the two lines drawn through the pterion (bilaterally) and nasion."
Wang *et al*. (2016)	Metopic index	"The midfronto-zygomatic diameter divided by the eurion-eurion diameter."
Chandler *et al*. (2021)	Endocranial bifrontal angle	"Angle of the frontal bone in a single axial plane at the level of the superior-most aspect of the crista galli with the vertex located on the endocranial side of the frontal bone at the metopic suture and terminal points at the lateral borders of the respective orbital apertures."
	Frontal angle	"Angle of the frontal bone in a single axial plane with the vertex located on the exocranial side of the most anterior point of the frontal bone and terminal points at the coronal sutures."

The frontal angle (FA) and endocranial bifrontal angle (EBA) are the most commonly used indices, to assess the severity of trigonocephaly, that have been found in the literature thus far. Van der Meulen (2012) classified trigonocephaly into three categories according to the FA, viz., severe type (<89°), moderate type (90°-95°), and mild type (96°-103°). A normal FA was observed to be 104° or more (Van der Meulen, 2012). Furthermore, a study by Beckett *et al*. (2012) described that two severity patterns exist in trigonocephaly, as characterised by the EBA, viz., severe type (100°-124°) and moderate type (124°-148°). Similar findings have also been found by Ezaldein *et al*. (2014), regarding the EBA, who also observed a normal EBA to be greater than 149°. Severe trigonocephaly showed substantial orbitofrontal narrowing and medially tilted orbital rims when compared to a control group, as opposed to moderate trigonocephaly that did not show any substantial difference in the morphology of the orbitofrontal region when compared to a control group (Beckett *et al*., 2012). In a study by Chandler *et al*. (2021), the EBA and the FA indices both showed significance (p=0.001) when classifying the severity of trigonocephaly.

The common assessment indices that have been described in the literature thus far are able to classify the severity of trigonocephaly in similar ways (Chandler *et al*., 2021). Although the use of CT scans is the most commonly used method to assess trigonocephaly, some studies have proposed that not all trigonocephaly cases (possibly including moderate and mild types) require the use of CT scans for assessment (Wang *et al*., 2016). Furthermore, if some cranial indices can be determined via palpable cranial landmarks, it would not only reduce the amount of radiation patients are exposed to but also reduce the risk of any side effects that may occur thereof (Wang *et al*., 2016).

1.2.5. Prevalence and aetiology

Recently, studies have illustrated that trigonocephaly has increased in the past decade, due to an unknown cause, therefore, making it the second most common isolated single suture synostosis to date (Van der Meulen, 2012; Baş *et al*., 2021). Additionally, various hypotheses have been described by previous literature to understand the specific aetiology of non-syndromic, isolated trigonocephaly, which to date is still currently unknown (Table 2). Furthermore, trigonocephaly is observed to be more predominant in males compared to females with a ratio of 3:1 (Van der Meulen, 2012; Ghizoni *et al*., 2016). Similar findings were also observed by Baş *et al*. (2021), who determined that the male to female trigonocephaly ratio was 3.5:1. In another study by Maltese *et al*. (2014), the male to female trigonocephaly ratio was documented to be 5.4:1.

Table 2: Various hypotheses of the increased prevalence of non-syndromic, isolated trigonocephaly in existing literature

Study	Country	Possible hypotheses
Penfold and Simpson (1975)	Australia	• Thyroid hormone replacement therapy for hypothyroidism
Johnsonbaugh *et al*. (1978)	United States of America	
Rasmussen *et al*. (2007)		
Boulet *et al*. (2008)	United States of America, Georgia	• Increased maternal age • Birth weight > 2 500g
Di Rocco *et al*. (2009)	France	• Improvement in clinical diagnostic techniques and technology • Environmental factors • Pharmacological factors
Kolar (2011)	United States of America, Texas	• Improvement in diagnostic techniques and technology
Van der Meulen (2012)	Netherlands	• Intrinsic bone malformation as a result of genetic, metabolic or pharmaceutical means • Fetal head constriction in the final stage of pregnancy • Intrinsic brain deformity
Sharma (2013)	India	• Abnormalities in cranial sutures • Abnormalities in the development of the base of the skull which affects the cranial sutures via the attachment to the dura mater
Cornelissen *et al*. (2016)	Netherlands	• Increased awareness amongst health care professionals resulting in a greater detection rate
Ghizoni *et al*. (2016)	Brazil	• Genetic factors – mutations in the following genes, viz., FGFRs, TWIST1, LRIT3, ALX4, IGFR1, EFNA4, RUNX2, and FREM1 • Maternal environmental factors (intrauterine fetal head constriction)
Kajdic *et al*. (2018)	Slovenia	• Environmental factors (intrauterine fetal head constriction, abnormal position of the fetus, oligohydramnios – decreased amniotic fluid, prenatal exposures to teratogens, and antiepileptic drugs such as valproic acid and phenytoin) • Genetic factors (gene mutations, chromosomal abnormalities, and hereditary background)

1.2.6. Craniometric morphometry

1.2.6.1. ACF

Chandler *et al*. (2021) documented the dimensions of the entire anterior cranium in trigonocephaly and control groups. The majority of patients in both the trigonocephaly and control groups were males. It was concluded that no significant decrease in the volume of the anterior cranium was observed when patients with trigonocephaly were compared to age-matched controls; however, the ACF area decreased significantly in patients with trigonocephaly compared to controls (Chandler *et al*., 2021). Furthermore, the height, length, and width of the anterior cranium all showed significance when trigonocephaly patients were compared to controls (Chandler *et al*., 2021). These findings differed from Naran *et al*. (2017), who analysed the differences in the volumes of the entire cranial vault, where it was concluded that trigonocephaly patients had a significantly smaller volume of the anterior third of the skull compared to control patients (Table 3). Although a shortened ACF is a characteristic of trigonocephaly, the degree of severity of trigonocephaly could have an impact on the volume of the ACF.

The following craniometric parameters of the anterior cranium, and middle and posterior cranial volumes were described by previous literature:

- ***ACL (Anterior cranial length)***
  Chandler *et al*. (2021) described the length of the anterior cranium as the distance from the center of the sella turcica to the anterior most position of the skull. More specifically, Hughes *et al*. (2010) described the length of the ACF as the distance from the nasion to the posterior clinoid process.

- ***ACH (Anterior cranial height)***
  The height of the anterior cranium was described as the height from the center of the sella turcica to the highest point of the metopic suture (Chandler *et al*., 2021).

- ***ACW (Anterior cranial width)***
  Chandler *et al*. (2021) described the width of the anterior cranium as the distance between the coronal sutures on the perpendicular plane to the sagittal plane determined by a position one centimetre above the upper portion of the orbital rim and the internal occipital protuberance.

- ***ACV (Anterior cranial vault volume)***
  Naran *et al*. (2017) explained that the border that divided the anterior cranial vault volume from the middle cranial vault volume was described by outlining the posterior boundaries of the lesser wings of the sphenoid bone and continuing in a lateral direction to the border of the cranial vault. Thereafter, this border then passed superiorly and perpendicularly to the Frankfort

Horizontal plane (which is defined as the zygomatico-maxillary suture line passing at the lower orbital rim, with the point being positioned on the orbits inferior margin) (Fig. 5). A similar method using the Frankfort Horizontal plane as a reference plane was also utilized by Chandler *et al*. (2021) to calculate the anterior cranial vault volume. By using this technique, it allowed for the volume of the cranium to be more accurately divided when control patients were compared to trigonocephaly patients (Naran *et al*., 2017).

- ***MCV (Middle cranial vault volume)***
  Similarly, Naran *et al*. (2017) described that the petrous ridges of the temporal bone were joined medially on the dorsum sellae and then laterally extended to the vault, in order to divide the middle and posterior cranial vault volumes. Thereafter, this border passed superiorly and perpendicularly to the Frankfort Horizontal plane (Naran *et al*., 2017) (Fig. 5).

- ***PCV (Posterior cranial vault volume)***
  The posterior cranial vault volume was measured from the petrous ridges of the temporal bone to the most posterior aspect of the cranial vault (Naran *et al*., 2017) (Fig. 5).

Growth restriction of the ACF as well as the underlying brain is a characteristic feature of trigonocephaly (Naran *et al*., 2017). In a craniometric study of the cranial base, Naran *et al*. (2017) analysed the ratio of the volume of the anterior third of the skull to the total cranial skull volume. It was observed that the volumetric ratio in trigonocephaly patients (0.09±0.02) was significantly smaller compared to control patients (0.012±0.02) (p=0.0128). Furthermore, the volumetric ratio of the posterior third of the skull to the total cranial skull volume showed no difference in trigonocephaly patients compared to control patients (Naran *et al*., 2017).

Knowledge of ACF morphometry could provide a relationship between the degree of severity of trigonocephaly and the restricted volume of the anterior third of the skull. This could further assist clinicians by acting as a guideline in surgical correction, and also as an indication of how severe trigonocephaly has impacted the developing brain neurologically (Naran *et al*., 2017).

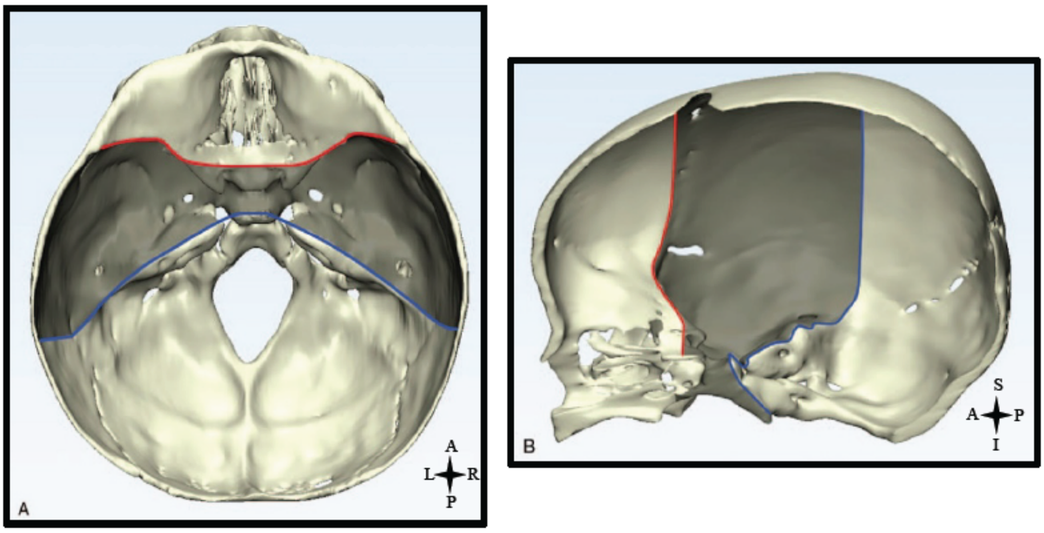

Figure 6: Volumetric boundaries of the cranial vault. (A) The border dividing the anterior from the middle cranial vault volumes was explained by outlining the posterior boundaries of the lesser wings of the sphenoid bone, continuing in a lateral direction to the border of the cranial vault. (B) The line then passed superiorly on a perpendicular plane to the Frankfort Horizontal plane

(Adapted from Naran et al., 2017)

1.2.6.2. Orbits

Orbital dysmorphology, such as ethmoidal hypoplasia, hypotelorism, orbits shaped like a tear drop, and both orbital rims laterally depressed is evident in trigonocephaly. The orbits are typically positioned closer together than normal and the degree of hypotelorism can vary from mild to severe forms (Štefánková *et al*., 2015). Most treatment methods for trigonocephaly mainly focus on the forehead and not on the orbital dysmorphology, therefore, there is sparse literature and understanding on the correlation between the bony orbital structure and trigonocephaly (Ezaldein *et al*., 2014). A study by Ezaldein *et al*. (2014) investigated the relationship between 3D orbital dysmorphology and the severity of trigonocephaly and concluded the following, viz., the orbital width showed no significant differences when moderate and severe trigonocephaly types were compared to a control group, and when the orbital height between control and trigonocephaly groups were compared, no significance was found, however, when severe and moderate trigonocephaly cases were compared to controls there was a decrease in the orbital height in severe cases (Table 4). The interorbital distance is also affected in trigonocephaly patients. In a study by Maltese *et al*. (2014), the interorbital distance in trigonocephaly patients was investigated preoperatively and at a later stage postoperatively. It was concluded that preoperatively, the interorbital distance in trigonocephaly patients decreased significantly compared to control patients, with interorbital distances measuring 13.8 ± 1.3mm and 18.6 ± 1.4mm, respectively (Maltese *et al.*, 2014).

The following orbital parameters were described by previous literature:

- ***OW (Orbital width)***
  The orbital width was described as the distance between the zygomaticofrontal suture and the dacryon (which is the intersection of the frontal, maxillary and lacrimal bone sutures found on the medial border of the orbit) on the same side (Ezaldein *et al*., 2014) (Fig. 6 – black line).

- ***OH (Orbital height)***
  The orbital height was described as the distance between the zygomatico-maxillary suture and the supraorbital notch (Ezaldein *et al*., 2014) (Fig. 6 – yellow line).

- ***IOD (Interorbital distance)***
  The interorbital distance was described by Pala *et al*. (2015) as the distance between the medial borders of the two orbits (Fig. 6 – red line).

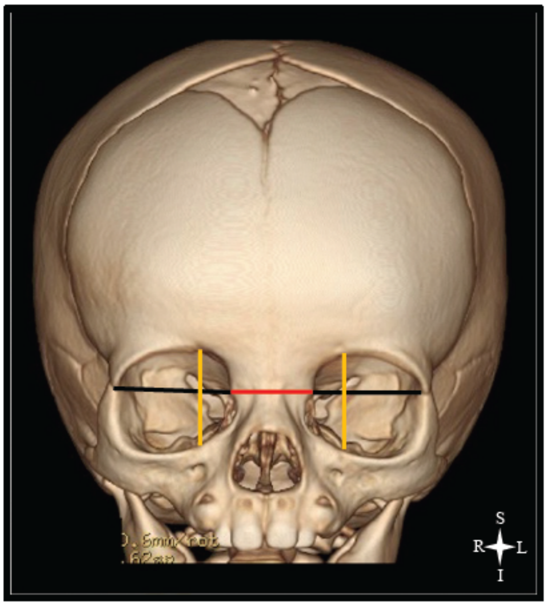

Key:
Black line – Orbital width
Yellow line – Orbital height
Red line – Interorbital distance

Figure 7: Orbital landmarks used to measure the orbital width and height as present in hypotelorism, a characteristic feature of trigonocephaly

(Adapted from Teager et al., 2018)

Orbital dysmorphology declines with increasing severity of trigonocephaly, and also introduces more functional defects (Ezaldein *et al*., 2014). Providing extension and improvement to the lateral orbital walls is a vital treatment aspect in surgical correction (Ezaldein *et al*., 2014). The morphometry of the orbit could greatly assist clinicians in the type of surgical procedure that is required in relation to the severity of trigonocephaly. Furthermore, accomplishing normal orbital morphology may have a direct impact on the way the globe will lie in the orbit. Therefore, as a result, this will ensure that the convergence of light is optimized past the cornea which will minimize the refractory error (Ezaldein *et al*., 2014).

1.2.7. Summary of previous literature

Table 3: Craniometric morphometry of the anterior third of the skull in trigonocephaly patients compared to a control group reported in the literature

Author	Sample size (n)	Sex	Mean age (months)	Control (mean)	Trigonocephaly (mean)	p-value
Naran *et al*. (2017)	Total: 39 (20 affected patients, 19 controls)	M and F	6.1 (affected patients) 5.7 (controls)	*Volume ratio (Anterior third/Total Skull Volume)*		
				0.012	0.09	0.0128*
Applegren *et al*. (2018)	Total: 203 (87 affected patients, 116 controls)	M and F	Total mean age for affected patients and controls: 6.4	*Volume of anterior third (mm^3)*		
				409 820	389 250	0.029*
Chandler *et al*. (2021)	Total: 211 (167 affected patients, 44 controls)	M and F	7.2 (affected patients) 7.6 (controls)	*Length (mm)*		
				45.35	49.35	0.003*
				Height (mm)		
				73.30	79.71	0.010*
				Width (mm)		
				91.32	83.77	0.001*
				Volume of anterior third (mm^3)		
				173 582.01	164 173.59	0.294

** Indicates statistical significance with a p-value less than 0.05*

Table 4: Orbital dimensions in different severities of trigonocephaly compared to a control group

Study	Sample size (n)	Sex	Trigonocephaly (mean)	Control (mean)	Control and moderate vs severe p-value
Ezaldein *et al*. (2014)	Total: 46 (23 affected patients, 23 controls)	18 Males 5 Females	*Orbital width (mm)*		
			Moderate Left = 27.21 Right = 26.58 Severe Left = 28.03 Right = 27.94	Left = 28.34 Right = 28.13	Left = 0.4336 Right = 0.3569
			Orbital height (mm)		
			Moderate Left = 30.94 Right = 30.80 Severe Left = 29.23 Right = 28.79	Left = 30.54 Right = 30.87	Left = 0.0460* Right = 0.0337*

**Indicates statistical significance with a p-value less than 0.05*

1.3. Materials and Methods

This study follows a retrospective cohort design. A total of 15 preoperative patient CT scans were obtained from the database of the Department of Plastic and Reconstructive Surgery at the Inkosi Albert Luthuli Central Hospital (IALCH), Durban, South Africa. Due to the whole ACF of the skull being affected in trigonocephaly, a control group was required in order to entirely assess the severity of the deformity. The control group was composed of normal age-matched paediatric patients who had undergone clinical CT scanning of the head, for conditions not affecting the bones of the skull. Only those who had met the inclusion criteria were selected for analysis. The morphometry and volumetric measurements of the ACF were determined utilising specific anatomical cranial landmarks on 2D CT scans in the axial and sagittal planes, whilst the dimensions of the orbits were determined on 2D CT scans in the axial and coronal planes. Measurements were repeated three times in order to ensure maximum accuracy and reliability.

1.3.1. Inclusion and Exclusion Criteria

1.3.1.1. Inclusion Criteria

Patients

- Paediatric patients with a preoperative confirmed diagnosis of non-syndromic, isolated trigonocephaly and confirmed fusion of the metopic suture who had presented to the craniofacial unit at IALCH between 2012 and 2023, with a CT slice thickness between 1 to 5mm.

Controls

- Unaffected paediatric patients who had undergone clinical CT scanning of the head with comparable CT scan information available.
- CT scans with a slice thickness of 0.6mm.

1.3.1.2. Exclusion Criteria

Patients

- Paediatric patients diagnosed with syndromic craniosynostoses.
- Postoperative CT scans of paediatric patients who had undergone surgical treatment.
- Poor image quality CT scans where the anatomy of the skull and orbits could not be clearly identified.

Controls

- Paediatric patients with an abnormally shaped skull.

- Poor image quality CT scans where the anatomy of the skull and orbits could not be clearly identified.
- CT scans with a slice thickness of less than or greater than 0.6mm.

1.3.2. Sample size

Patients

Preoperative CT scans of a confirmed diagnosis of non-syndromic, isolated trigonocephaly who presented to the IALCH craniofacial unit between 2012 and 2023 which met the inclusion criteria were included in this study. Of the total 55 patients that were identified, only 15 had met the inclusion criteria. The median age at the time when the CT scan was taken was 11 months (range: 5-36 months).

Controls

Preoperative CT scans of unaffected age-matched paediatric patients who had undergone clinical scanning of the head with comparable information and which met the inclusion criteria. Of the total 14 unaffected patients that were identified, only 8 had met the inclusion criteria. The median age at the time when the CT scan was taken was 22 months (range: 1-48 months).

1.3.3. Variables

Demographic factors

Demographic factors such as sex, age and race were determined, and any variations pertaining to these factors were documented.

Laterality

Dimensions of the right and left orbits in trigonocephaly patients and non-affected controls were recorded, and any variations pertaining to laterality were documented.

1.3.4. Image acquirement and analysis

Acquirement

CT scans of selected patients were retrieved from a Picture Archiving and Communication System (PACS) at the IALCH and saved onto a hard drive in the DICOM (Digital Imaging and Communication in Medicine) format. CT scans were obtained during routine scanning of the head using either a 128-slice SOMATOM Definition Adaptive scanner or SOMATOM Definition Flash CT Scanner (Siemens Healthineers, Forcheim, Germany, 2007). The CT scans of the selected patients had a slice thickness ranging from 1 to 5mm, and CT scans of the control group had a slice thickness of 0.6mm.

Analysis

CT scans were examined and analysed using the Horos Project Software version 3.3.6 on an external MacBook computer unit. The DICOM viewer was used to calibrate and manually verify the CT scan images. CT scans were aligned in the orbitomeatal plane, which is described as a line that passes through the lateral canthus of the eye and the middle of the external acoustic meatus (Otake *et al*., 2018). All measurements on the CT scan images were completed in the bone window setting and 3D MPR (Multiplanar Reconstruction) setting using the built-in length, angle, closed polygon, and region of interest (ROI) volume tools.

1.3.5. Morphometric analysis

ACF Measurements

- Length and width

  The midpoint of the limbus sphenoidale (LS) was selected as a reference landmark and extrapolated to the level at which the ACF was observed to be its maximum length. At the level at which the lesser wings of the sphenoid bone were observed to be the most prominent, the maximum anterior-posterior distance (length) was measured in an axial plane from the referenced landmark and perpendicularly extrapolated to the inner table of the frontal bone (ITF) (Fig. 7). At the level at which the lesser wings of the sphenoid bone were observed to be the most prominent, the maximum transverse distance (width) was measured in an axial plane between the inner tables of the frontal bones, in the same plane that the maximum anterior-posterior distance was measured (Fig. 7).

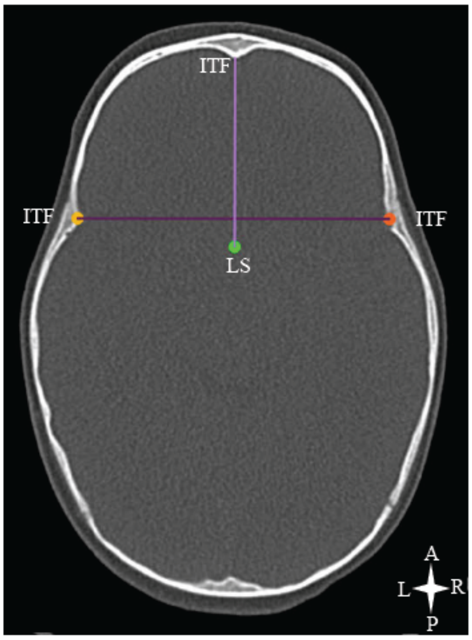

Figure 8: ACF measurements on an axial CT scan of a normal patient (length: LS to ITF; width: ITF to ITF). Key: LS – midpoint of limbus sphenoidale (transcended point); ITF – inner table of frontal bone

- Height

  The maximum superior-inferior distance was measured in a sagittal plane by extrapolating a perpendicular line vertically from the midpoint of the limbus sphenoidale (reference landmark) to the inner table of the frontal bone.

- Volume

  The volume of the ACF was measured in an axial plane, and the ACF was manually divided in each individual slice of the CT scan images. The level at which the fused coronal suture (FCS), on either side, was observed to be the most prominent was selected as the posterior boundary that divided the ACF from the MCF. The posterior boundary was determined by constructing a horizontal line from the FCS on one side of the skull to the coronal suture on the opposite side of the skull. The posterior boundary was transferred to every single slice of the CT images where the ACF was visible. The start slice was chosen when the ACF was first visible, and the end slice was chosen when the midpoint of the limbus sphenoidale was no longer visible. The ACF was manually outlined on each CT image slice by using the closed polygon tool. All slices were selected and the volume of the ACF was automatically calculated using the ROI volume tool (Fig. 8).

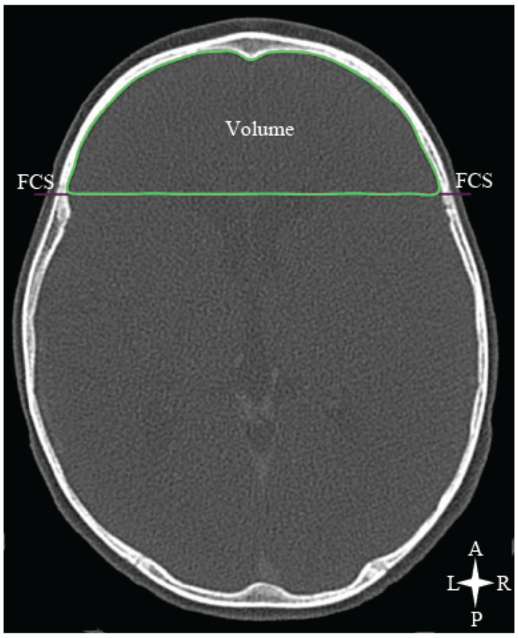

Figure 9: Volume measurement of the ACF on an axial CT scan of a normal patient
Key: FCS – fused coronal suture

- Angles

  The angles of the ACF were measured in the same plane as the selected reference landmark. The frontal angle (FA) was measured as the angle of the frontal bone in an axial plane with the vertex positioned on the exocranial aspect on the most anterior point of the frontal bone and terminal points at which the lesser wings of the sphenoid bone were observed to be the most prominent, on the external surface. The endocranial bifrontal angle (EBA) was measured as the angle of the frontal bone in an axial plane with the vertex positioned on the endocranial aspect on the most anterior point of the frontal bone and terminal points at which the lesser wings of the sphenoid bone were observed to be the most prominent, on the internal surface (Fig. 9).

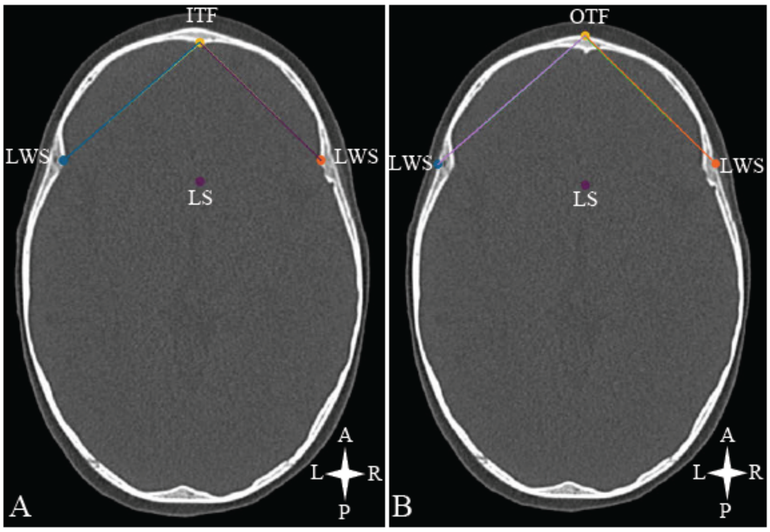

Figure 10: Angles of the ACF on an axial CT scan of a normal patient (EBA: vertex at ITF and terminal points at LWS; FA: vertex at OTF and terminal points at LWS). Key: ITF – inner table of frontal bone; OTF – outer table of frontal bone; LWS – lesser wing of sphenoid bone; LS – midpoint of limbus sphenoidale (transcended landmark used as a reference plane)

Additional Volumetric measurements

- MCF volume

  The volume of the MCF was measured in an axial plane, and the MCF was manually divided in each individual slice of the CT scan images. The level at which the superior margin of the petrous part of the temporal bone was observed to be the most prominent was selected as the posterior boundary that divided the MCF from the PCF. The start slice was chosen when the foramen ovale was first visible, and the end slice was chosen when the superior orbital fissure, immediately inferior to the lesser wing of the sphenoid bone, was no longer visible. The MCF was manually outlined on each CT image slice by using the closed polygon tool. All slices were selected and the volume of the MCF was automatically calculated using the ROI volume tool.

- PCF volume

  The volume of the PCF was measured in an axial plane, and the PCF was manually divided in each individual slice of the CT scan images. The level at which the inferior margin of the petrous part of the temporal bone was observed to be the most prominent was selected as the anterior boundary that divided the PCF from the MCF. The level at which the groove for the transverse sinus was observed to be the most prominent was selected as the most posterior boundary of the PCF. The start slice was chosen when the foramen magnum was first visible, and the end slice was chosen when the petrous part of the temporal bone was no longer visible. The midpoint of the posterior margin of the dorsum sellae was also determined in order to ensure accurate division between the PCF and MCF in the midline. The PCF was manually outlined on each CT image slice by using the closed polygon tool. All slices were selected and the volume of the PCF was automatically calculated using the ROI volume tool.

Orbital Measurements and Morphology

- Height and width

  These measurements were taken in a coronal plane, at the level at which the inferior orbital margin and zygomaticofrontal suture were observed to be the most prominent. The superior-inferior distance (height) was measured by extrapolating a perpendicular line vertically from a point on the inferior orbital margin towards a point on the superior orbital margin. The transverse distance (width) was measured by constructing a horizontal line from the zygomaticofrontal suture to the dacryon (medial orbital wall) of the same orbit. Both these measurements were determined for right and left orbits (Fig. 10).

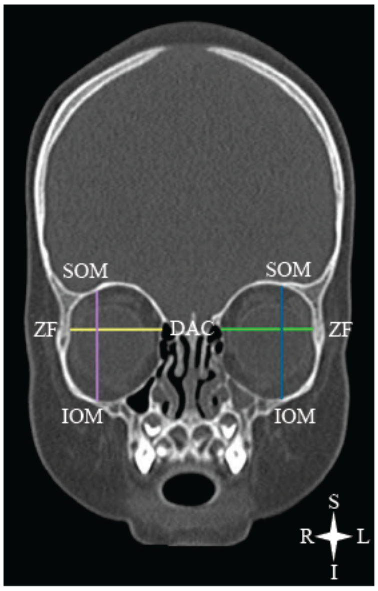

Figure 11: Orbital measurements on a coronal CT scan of a normal patient (height: IOM to SOM; width: ZF to DAC). Key: IOM – inferior orbital margin; SOM – superior orbital margin; ZF – zygomaticofrontal suture; DAC – dacryon

- Surface area

  This measurement was taken in a 2D coronal plane, at the level at which the zygomaticofrontal suture was observed to be the most prominent. The surface area of each orbit was calculated by manually outlining the orbital rim using the closed polygon tool, which thereafter automatically calculated the surface area of each orbit.

- Interorbital distance

  This measurement was taken in an axial plane, at the level at which the dacryon (medial orbital wall) of each orbit was observed to be the most prominent. The interorbital distance was measured by constructing a horizontal line from the dacryon of one orbit to the dacryon of the opposite orbit.

- Orbital morphology

  The morphology of the orbits in trigonocephaly patients was determined using the orbital index, which was calculated according to the equation: mean orbital height/mean orbital width x 100. Thereafter, the morphology of the orbits were classified into various morphological appearances according to different age groups, and differences in the morphology of the orbits pertaining to laterality was also observed and recorded.

1.3.6. Statistical Analysis

The R Statistical Computing Software of the R Core Team (R Studio, Boston, MA, USA, 2021) was used to perform statistical data analysis. The results were expressed as descriptive statistics, and the appropriate statistical tests were performed. Descriptive statistics were recorded as minimum, maximum, standard deviation, means and medians. Mean or median differences were respectively applied to morphometrical data to indicate a normal or skewed distribution of data. The t-test and Ranksum test were used to describe comparisons between trigonocephaly patients and the control group, the Fischer's exact test was used to determine relationships between demographic variables, and the ANOVA and Kruskal-Wallis tests were used in the comparisons of different degrees of severity in trigonocephaly patients. Compensatory growth via volumetric assessment was determined and expressed as percentages. Correlation analysis was also used to determine the relationship between various morphometrical data. A p-value of less than 0.05 was considered statistically significant. Intra-observer and inter-observer reliability tests were expressed as intraclass coefficient (ICC) values in order to determine the reliability of the morphometrical data as well as the intra-observer and inter-observer error. All statistical analyses were determined via consultation with a university statistician.

1.3.7. Ethical Considerations

The relevant gatekeeper permissions were acquired from IALCH and institutional ethical approval for this study was obtained from the Biomedical Research Ethics Committee (BREC) at the University of KwaZulu-Natal (Ethical approval number: BREC/00004342/2022). Informed consent from patients was not required, as this study used retrospective CT scans, and information regarding the identity of patients was anonymised to ensure confidentiality. The POPI Act (2020) was not breached.

1.4. Structure of thesis

The following thesis was conducted according to the guidelines set by the College of Health Sciences (CHS) at the University of KwaZulu-Natal, Durban, South Africa. The manuscripts have also been prepared according to the formatted guidelines of the respective scientific journals. This thesis is structured as follows:

1.4.1. Chapter 1: Introduction

This chapter created a clear understanding of the development of trigonocephaly, as well as the characteristics and craniofacial features associated with it. Additionally, a complete literature review, outline, aims, objectives, research question and outline of the methodology are included in this chapter.

1.4.2. Chapter 2: Scientific Manuscript 1

This chapter is composed of an original scientific manuscript entitled: *"A morphometric analysis of the cranial base and severity in trigonocephaly"*. This manuscript investigated and recorded the morphometry of the ACF, viz., length, width, height, and volume, as well as the volumes of the MCF and PCF in patients with non-syndromic, isolated trigonocephaly (n=15) and an age-matched control group (n=8) within a specific South African population. Additionally, metopic indices of the ACF were determined in order to assist in improving the current severity assessment of trigonocephaly within the above-mentioned population. The results were assessed across demographic variables in order to determine statistically significant relationships.

This manuscript was submitted to the *Journal of Craniofacial Surgery* (Manuscript number: pending)

1.4.3. Chapter 3: Scientific Manuscript 2

This chapter is composed of a second original scientific manuscript entitled: *"Hypotelorism-associated orbital morphometry and morphology in trigonocephaly"*. This manuscript investigated and recorded the morphometry of the orbits, viz., height, width, surface area, and interorbital distance in patients with non-syndromic, isolated trigonocephaly (n=15) and an age-matched control group (n=8), as well as the morphology of the orbits in trigonocephaly patients within a specific South African population. The results were assessed across demographic variables in order to determine statistically significant relationships.

This manuscript was submitted to the *International Journal of Oral and Maxillofacial Surgery* (Manuscript number: pending)

1.4.4. Chapter 4: Synthesis

This chapter further examined the key findings of Chapters 2 and 3 and concluded the findings of the morphometry of the ACF and orbits, as well as the morphology of the orbits in patients with trigonocephaly within a specific South African population. The limitations of this study and future recommendations have been depicted in this chapter. Appendices are listed following Chapter 4.

The references for Chapter 1 are listed below.

1.5. References

1. Applegren, N. D., Shock, L. A., Aldridge, K. J., Derrick, C. D., Tanaka, T., Baker, C. L., Muzaffar, A. R. 2018. Relationship of a metopic ridge and anterior cranial volume measured by a non-invasive laser shape digitizer. *Journal of Craniofacial Surgery*, 29(1), pp. 76-81. doi: 10.1097/SCS.0000000000004065.
2. Baş, N. S., Baş, S. 2021. Craniometric Measurements and Surgical Outcomes in Trigonocephaly Patients Who Underwent Surgical Treatment. The *Cureus Journal of Medical Science,* 13(3), pp. e13676. doi: 10.7759/cureus.13676.
3. Beckett, J. S., Chadha, P., Persing, J. A., Steinbacher, D. M. 2012. Classification of Trigonocephaly in Metopic Synostosis. *Journal of Plastic and Reconstructive Surgery*, 130(3), pp. 442e-447e. doi: 10.1097/PRS.0b013e31825dc244.
4. Boulet, S. L., Rasmussen, S. A., Honein, M. A. 2008. A population-based study of craniosynostosis in metropolitan Atlanta, 1989-2003. *American Journal of Medical Genetics Part A*, 146A(8), pp. 984-991. 10.1002/ajmg.a.32208. doi: 10.1002/ajmg.a.32208.
5. Carlson, B. M., Patten, B. M. 1996. Patten's Foundations of Embryology. 6th ed. McGraw-Hill.
6. Chandler, L., Park, K. E., Allam, O., Mozaffari, M. A., Khetpal, S., Smetona, J., Pourtaheri, N., Lu, X., Persing, J. A., Alperovich, M. 2021. Distinguishing craniomorphometric characteristics and severity in metopic synostosis patients. *International Journal of Oral and Maxillofacial Surgery*, 50, pp. 1040-1046. doi: 10.1016/j.ijom.2020.11.022.
7. Cornelissen, M., Den Ottelander, B., Rizopoulos, D., Van der Hulst, R., Van der Molen, A. M., Van der Horst, C., Delye, H., Van Veelen, M. L., Bonsel, G., Mathijssen, I. 2016. Increase of prevalence of craniosynostosis. *Journal of Cranio-Maxillofacial Surgery*, 44, pp. 1273-1279. doi: 10.1016/j.jcms.2016.07.007.
8. Di Rocco, F., Arnaud, E., Renier, D. 2009. Evolution in the frequency of nonsyndromic craniosynostosis. *Journal of Neurosurgery Pediatrics*, 4(1), pp. 21-25. doi: 10.3171/2009.3.PEDS08355.

9. Ezaldein, H. H., Metzler, P., Persing, J. A., Steinbacher, D. M. 2014. Three-dimensional orbital dysmorphology in metopic synostosis. *Journal of Plastic, Reconstructive and Aesthetic Surgery*, 67, pp. 900-905. doi: 10.1016/j.bjps.2014.03.009.
10. Freudlsperger, C., Steinmacher, S., Bächl, H., Somlo, E., Hoffmann, J., Engel, M. 2015. Metopic synostosis: Measuring intracranial volume change following fronto-orbital advancement using three-dimensional photogrammetry. *Journal of Cranio-Maxillofacial Surgery*, 43(5), pp. 593-598. doi: 10.1016/j.jcms.2015.02.017.
11. Ghizoni, E., Denadai, R., Raposo-Amaral, C. A., Joaquim, A. F., Tedescni, H., Raposo-Amaral, C. E. 2016. Diagnosis of infant synostotic and nonsynostotic cranial deformities: a review for pediatricians. *Revista Paulista De Pediatria*, 34(4), pp. 495-502. doi: 10.1016/j.rpped.2016.01.004.
12. Gray, H., Standring, S. 2016. Gray's anatomy: The anatomical basis of clinical practice. 41st ed. Elsevier, Amsterdam, pp. 416, 429.
13. Hughes, D. C., Kadnthodil, M. J., Connolly, D. J. A., Griffiths, P. D. 2010. Dimensions and ossification of the normal anterior cranial fossa in children. *American Journal of Neuroradiology*, 31, pp. 1268-1272. doi: 10.3174/ajnr.A2107.
14. Jin, S. W., Sim, K. B., Kim, S. D. 2016. Development and Growth of the Normal Cranial Vault: An Embryologic Review. *Journal of Korean Neurosurgical Society*, 59(3), pp. 192-196. doi: 10.3340/jkns.2016.59.3.192.
15. Johnsonbaugh, R. E., Bryan, R. N., Hierlwimmer, R., Georges, L. P. 1978. Premature craniosynostosis: a common complication of juvenile thyrotoxicosis. *The Journal of Pediatrics*, 93(2), pp. 188-191. doi: 10.1016/s0022-3476(78)80493-4.
16. Kajdic, N., Spazzapan, P., Velnar, T. 2018. Craniosynostosis – Recognition, clinical characteristics, and treatment. *Bosnian Journal of Basic Medical Sciences*, 18(2), pp. 110-116. doi: 10.17305/bjbms.2017.2083.
17. Kasai, E., Kondo, S., Kasai, K. 2019. Morphological variation in the anterior cranial fossa. *Clinical and Experimental Dental Research*, 5, pp. 136-144. doi: 10.1002/cre2.163.
18. Ko, J.M. 2016. Genetic Syndromes Associated with Craniosynostosis. *Journal of Korean Neurosurgical Society*, 59(3), pp. 187-191. doi: 10.3340/jkns.2016.59.3.187.
19. Kolar, J. C. 2011. An epidemiological study of nonsyndromal craniosynostoses. *The Journal of Craniofacial Surgery*, 22(1), pp. 47-49. doi: 10.1097/SCS.0b013e3181f6c2fb.
20. Luibil, N., Lopez, M. J., Patel, B. C. 2023. Anatomy, Head and Neck, Orbit. In: StatPearls [Internet]. Treasure Island (FL): StatPearls Publishing.
21. Madaree, A., Bisetty, V., Mohan, N., Barnes, C., L, Lazarus. 2023. An Exploration of the Practice of CT Modalities to Evaluate Anterior Cranial Deformities in Craniosynostosis. In: Microscopy Techniques for Biomedical Education and Healthcare Practice: Principles in Light,

Fluorescence, Super-Resolution and Digital Microscopy, and Medical Imaging. Cham: Springer Nature, Switzerland, pp. 125-142.

22. Maltese, G., Tarnow, P., Tovertjärn, R., Kölby, L. 2014. Correction of hypotelorism in isolated metopic synostosis. *Journal of Plastic Surgery and Hand Surgery*, 48(1), pp. 63-66. doi: 10.3109/2000656X.2013.812967.
23. Mendoza, C. S., Safdar, N., Myers, E., Kittisarapong, T., Rogers, G. F., Linguraru, M. G. 2013. An optimal set of landmarks for metopic craniosynostosis diagnosis from shape analysis of pediatric CT scans of the head. *International Society for Optics and Photonics*, 8670, pp. 86702T. doi: 10.1117/12.2008039.
24. Moore, K., Agur, A., Dalley, A. 2010. Clinically oriented anatomy. 6th ed. Philadelphia: Wolters Kluwer Health: Lippincott, Williams and Wilkins.
25. Naran, S., Mazzaferro, D., Wes, A., Vossough, A., Bartlett, S., Taylor, J. 2017. A Craniometric Analysis of Cranial Base and Cranial Vault Differences in Patients with Metopic Craniosynostosis. *Journal of Craniofacial Surgery*, 28(8), pp. 2030-2035. doi: 10.1097/SCS.0000000000003888.
26. Otake, S., Taoka, T., Maeda, M., Yuh, W. T. C. 2018. A guide to identification and selection of axial planes in magnetic resonance imaging of the brain. *Neuroradiology Journal*, 31(4), pp. 336-344. doi: 10.1177/1971400918769911.
27. Pala, H. G., Artunç-Ülkümen, B., Koyuncu, F. M., Uyar, Y., Bülbül-Baytur, Y. 2015. Normal ranges of biorbital and interorbital distances in healthy Turkish pregnancies at 19-23 weeks of gestation and correlation with craniofacial structures. *Journal of the Turkish-German Gynecological Association*, 16, pp. 170-173. doi: 10.5152/jtgga.2015.15062.
28. Penfold, J. L., Simpson, D. A. 1975. Premature craniosynostosis – a complication of thyroid replacement therapy. *The Journal of Pediatrics*, 86(3), pp. 360-363. doi: 10.1016/s0022-3476(75)80963-2.
29. Rasmussen, S. A., Yazdy, M. M., Carmichael, S. L., Jamieson, D. J., Canfield, M. A., Honein, M. A. 2007. Maternal thyroid disease as a risk factor for craniosynostosis. *Obstetrics and Gynecology*, 110(2 Part 1), pp. 369-377. doi: 10.1097/01.AOG.0000270157.88896.76.
30. Reefhuis, J., Honein, M. A., Shaw, G. M., Romitti, P. A. 2003. Fertility Treatments and Craniosynostosis: California, Georgia, and Iowa. *American Academy of Pediatrics*, 111(1), pp. 1163-1166. doi: 10.1542/peds.111.S1.1163.
31. Sadler, T. W., Langman, J. 2004. Langman's Medical Embryology. 9th ed. Lippincott Williams and Wilkins, Pennsylvania, pp. 175-176.
32. Sharma, R. 2013. Craniosynostosis. *Indian Journal of Plastic Surgery*, 46(1), pp. 18-27. doi: 10.4103/0970-0358.113702.
33. Smith, T. D., Bhatnagar, K. P. 2019. Handbook of Clinical Neurology. Volume 164. Elsevier, Amsterdam, pp. 17-28.

34. Spazzapan, P., Arnaud, E., Baujat, G., Nizon, M., Malan, V., Brunelle, F., Di Rocco, F. 2016. Clinical and neuroradiological features of the 9p deletion syndrome. *Child's Nervous System*, 32(2), pp. 327-335. doi: 10.1007/s00381-015-2957-2.
35. Śtefánková, E., Horn, F., Neščáková, E., Kabát, M.,Petrík, M., Trnka, J. 2015. Anthropometry of craniosynostosis. *Polish Journal of Neurology and Neurosurgery*, 49(4), pp. 229-238. doi: 10.1016/j.pjnns.2015.05.006.
36. Sumkovski, R., Kocevski, I., Micunovic, M. 2019. Trigonocephaly: Case Report, Review of Literature and a Technical Note. *Open Access Macedonian Journal of Medical Sciences*, 7(1), pp. 117-120. doi: 10.3889/oamjms.2019.031.
37. Teager, S. J., Constantine, S., Lottering, N., Anderson, P. J. 2018. Physiologic closure time of the metopic suture in South Australian infants from 3D CT scans. *Child's Nervous System*, 35, pp. 329-335. doi: https://doi.org/10.1007/s00381-018-3957-9.
38. Van der Meulen, J., Van der Hulst, R., Van Adrichem, L., Arnaud, E., Chin-Shong, D., Duncan, C., Habets, E., Hinojosa, J., Mathijssen, I., May, P., Morritt, D., Nishikawa, H., Noons, P., Richardson, D., Wall, S., Van der Vlugt, J., Renier, D. 2009. The increase of metopic synostosis: a pan-European observation. *The Journal of Craniofacial Surgery*, 20(2), pp. 283-286. doi: 10.1097/scs.0b013e31818436be.
39. Van der Meulen, J. 2012. Metopic synostosis. *Child's Nervous System*, 28, pp. 1359-1367. doi: 10.1007/s00381-012-1803-z.
40. Wang, J. Y., Dorafshar, A. H., Liu, A., Groves, M. L., Ahu, E. S. 2016. The metopic index: an anthropometric index for the quantitative assessment of trigonocephaly from metopic synostosis. *Journal of Neurosurgery Pediatrics*, 18, pp. 275-280. doi: 10.3171/2016.2.PEDS15524.
41. World Health Organization. 2023. *Congenital disorders*. Available at: https://www.who.int/news-room/fact-sheets/detail/birth-defects (Accessed: 22 October 2023).

INTERFACE PAGE

Chapter 1 comprised an overview of previous literature on trigonocephaly, the morphometry and volumes of the anterior, middle, and posterior cranial thirds, as well as the morphometry of the orbits in trigonocephaly patients. This overview revealed that literature on the morphometry of the cranial fossae and orbits in patients with trigonocephaly is scarce, especially in a South African population. Furthermore, no previous study has investigated the volumes of the cranial fossae alone and recorded the different morphological appearances of the orbits in patients with trigonocephaly.

CHAPTER 2: SCIENTIFIC MANUSCRIPT 1

Contributions of the chapter

This chapter includes an original manuscript that investigates and records the morphometry of the ACF, viz., length, width, height, and volume, as well as the volumes of the MCF and PCF in patients with non-syndromic, isolated trigonocephaly and an age-matched control group within a select South African population. Additionally, metopic indices of the ACF are determined in order to assist in improving the current severity assessment of trigonocephaly within the above-mentioned population. The results of this study is assessed across demographic variables in order to determine statistically significant relationships.

The following manuscript has been submitted and is currently under review in the Journal of Craniofacial Surgery.

Title: A morphometric analysis of the cranial base and severity in trigonocephaly
Authors: C Barnes, A Madaree, L Lazarus
Journal: The Journal of Craniofacial Surgery
Manuscript Number: Pending

This manuscript has been written and structured according to the author guidelines defined by the Journal of Craniofacial Surgery. The American Medical Association (AMA) style was used to format references, as required by the journal.

A morphometric analysis of the cranial base and severity in trigonocephaly

Courtney Barnes B. Med Sci; H. Med Sci[1], Anil Madaree MBChB; FRCS; FCS; PhD[2], Lelika Lazarus M Med Sci; PD Dip in HE, PhD[1]

[1]Department of Clinical Anatomy, School of Laboratory Medicine and Medical Sciences, University of KwaZulu-Natal, Durban, South Africa.
[2]Department of Plastic and Reconstructive Surgery, University of KwaZulu-Natal, Durban, South Africa.

Corresponding Author: Anil Madaree MBChB; M Med; FRCS; PhD[2]
Department of Plastic and Reconstructive Surgery
University of KwaZulu-Natal
Durban, South Africa
MADAREE@ukzn.ac.za
+27 (0)31 240 1168, +27 (0)83 625 0629

Disclosure of funding received: The authors wish to acknowledge the financial assistance of the College of Health Sciences (CHS) for part funding of this project.

2.1. Abstract

Trigonocephaly occurs when the metopic suture fuses prematurely. Few studies have documented the morphometry of the entire anterior cranium in patients with trigonocephaly and not on the morphometric changes to the cranial fossae alone. Thus, this study aimed to determine and compare the dimensions of the anterior cranial fossa (ACF) in trigonocephaly patients and an age-matched control group, and describe an improved grading system in the assessment of the severity of trigonocephaly. Additionally, volumetric assessments of the middle and posterior cranial fossae (MCF and PCF) were analysed to determine the amount of compensatory growth in these regions. Specific anatomical landmarks were used to measure the length, width, height, angles and volume of the ACF, as well as the volumes of the MCF and PCF on preoperative two-dimensional computed tomography scans of 15 non-syndromic, isolated trigonocephaly patients between 2012 and 2023 and eight controls. Comparative assessment of the ACF revealed larger dimensions in younger more severe trigonocephaly patients when compared to a control group. Smaller dimensions of the ACF were recorded in the older group of patients who presented with moderate and severe trigonocephaly compared to the control cohort. The volume of the MCF was found to be significant ($p=0.05$) (Student t-test), and the volume of the PCF was larger in trigonocephaly patients compared to the control group. The PCF showed the most amount of compensatory growth (30.4%) in trigonocephaly patients. The frontal and endocranial bifrontal angles were used to assess the different degrees of severity in trigonocephaly patients. The morphometric data obtained could assist craniofacial surgeons in improving the current grading system in the assessment of the degree of severity, and help understand the changes that occur in the ACF to decide which type of corrective treatment is most suitable.

Keywords: cranial fossae, compensatory growth, non-syndromic, severity, trigonocephaly

2.2. Introduction

Trigonocephaly, otherwise known as metopic synostosis, is the second most common type of craniosynostosis forming approximately 25% of all non-syndromic, isolated craniosynostosis occurrences[1-3]. Previous literature has reported that the prevalence of trigonocephaly was one in every 10 000-15 000 live births[4-6], however, recently, the prevalence has increased in the past decade, due to an unknown cause, affecting one in every 5000 live births[5-7]. Additionally, trigonocephaly is observed to be more predominant in males as opposed to females with a male to female ratio of 3:1[5-7]. Both environmental factors (intrauterine head constraint, prenatal exposures to teratogens, or the use of fertility drugs) and genetics (single gene mutations and chromosomal abnormalities) could have an impact on the aetiology of this condition, however, genetic causes are only responsible for approximately 20% of all craniosynostoses[7-9]. Trigonocephaly can occur in isolation (non-syndromic), with the fusion of other sutures, or due to the presence of a morphological abnormality such as Crouzon or Saethre-Chotzen syndrome[7]. Typically, at about three months of age, the metopic suture is one of the first sutures to fuse, however, the premature fusion of this suture results in a ridge over the middle of the forehead and limits the lateral growth of the frontal bones[6,10]. Therefore, trigonocephaly is characterised by a triangular shaped forehead, shortening of the anterior cranial fossa (ACF), supra-orbital retrusion, hypotelorism, narrowing of the bitemporal region, and widening of the occipitoparietal region[6,10].

The abnormality of the morphometry and morphology of the cranial base, specifically the ACF, in trigonocephaly varies and is dependent on the paediatric age, the extent of premature metopic suture fusion, compensatory growth of other regions of the cranium, and the degree of severity[2,7,11]. Currently, clinicians still majorly rely on their judgement to assess the degree of severity of trigonocephaly as well as to determine if surgical intervention is required[5,10]. However, the use of specific cranial dimensions, in conjunction with the clinician's judgement, has shown to increase the accuracy and reliability in the assessment of various other craniosynostoses such as positional plagiocephaly, scaphocephaly and brachycephaly[10]. Additionally, numerous studies have identified various metopic indices that can assist surgeons in assessing the severity of trigonocephaly[1-3,5,6,10,12].

Furthermore, there is sparse literature on the volumetric changes of the cranial fossae in trigonocephaly patients, and the few studies that have carried out volumetric assessments involved proportioning the cranial vault into thirds and not solely investigating the volumes of the ACF, middle and posterior cranial fossae (MCF and PCF) between trigonocephaly patients and a control group[2,3,13]. Due to the restricted growth of the ACF, as well as bitemporal narrowing and occipitoparietal widening, there could possibly be compensatory growth of both the MCF and PCF in patients with trigonocephaly.

This study provides an insight into the morphometry of the ACF in trigonocephaly patients. A comparative assessment of dimensions between trigonocephaly patients and age-matched control patients will also inform clinicians on the degree of severity of this condition. As a result, this will assist in improving the current grading system to assess the severity of trigonocephaly within the select population group. The data obtained in this study may also further assist craniofacial surgeons by providing a relationship between the degree of severity and which technique of surgical correction to undertake.

This study aimed to determine and compare the dimensions of the ACF in trigonocephaly and age-matched control patients in a specific South African population, as well as describe an improved grading system in the assessment of the severity of trigonocephaly. Additionally, volumetric assessments of the MCF and PCF were analysed in order to determine the amount of compensatory growth of these cranial fossae in trigonocephaly patients due to the restricted growth of the ACF.

2.3. Materials and Methods

2.3.1. Patients

This study followed a retrospective cohort design and was conducted using two dimensional (2D) preoperative computed tomography (CT) scans obtained from the database of the Department of Plastic and Reconstructive Surgery at the Inkosi Albert Luthuli Central Hospital (IALCH), Durban, South Africa. Ethical approval for this study was obtained from the Biomedical Research Ethics Committee (BREC) at the University of KwaZulu-Natal (Ethical approval number: BREC/00004342/2022). This study was composed of CT scans of 15 patients with a radiographic confirmed diagnosis of non-syndromic, isolated trigonocephaly who presented to the craniofacial unit at IALCH between 2012 and 2023. CT scans of eight non-affected age-matched pediatric patients who had undergone scanning of the head for conditions where the skull was unaffected were selected as the control group. Only patients who had met the inclusion criteria were included in this study. For affected patients, those who had an additional underlying diagnosis of a genetic syndrome, syndromic craniosynostosis, and who had undergone surgical treatment were excluded. For the control group of patients, those who had an abnormally shaped skull, poor imaging quality of the CT scans where the anatomy of the skull and orbits could not be clearly identified, and CT scans with a slice thickness of less than or greater than 0.6mm were excluded.

2.3.2. Image acquirement and analysis

CT scans of selected patients were retrieved from a Picture Archiving and Communication System (PACS) at the IALCH and saved onto a hard drive in the DICOM (Digital Imaging and Communication in Medicine) format. CT scans were obtained during routine scanning of the head using either a 128-slice SOMATOM Definition Adaptive scanner or SOMATOM Definition Flash CT Scanner (Siemens

Healthineers, Forcheim, Germany, 2007). The CT scans of the selected patients had a slice thickness ranging from 1 to 5mm, and CT scans of the control group had a slice thickness of 0.6mm. CT scans were examined and analysed using the Horos Software version 3.3.6 (Horos Project, Annapolis, MD, USA, 2019) on an external MacBook computer unit. The DICOM viewer was used to calibrate and manually verify the CT scan images. CT scans were aligned in the orbitomeatal plane. Axial CT scan images were reformatted into sagittal and coronal planes and all measurements were completed in the bone window setting and three dimensional (3D) multiplanar reconstruction setting using the built-in length, angle, closed polygon, and region of interest (ROI) volume tools. Measurements were taken three times and intra-observer and inter-observer correlation coefficients were produced in order to ensure maximum accuracy and reliability.

2.3.3. Morphometry of the ACF

Specific anatomical landmarks were identified and chosen by a plastic and reconstructive surgeon and an anatomist on CT scans in the axial and sagittal planes in order to determine the maximum anterior-posterior, transverse, and superior-inferior distances as well as the volume of the ACF.

ACF Length: The midpoint of the limbus sphenoidale (LS) was selected as a reference landmark and extrapolated to the level at which the ACF was observed to be its maximum length. At the level at which the lesser wings of the sphenoid bone were observed to be the most prominent, the maximum anterior-posterior distance was measured in an axial plane from the referenced landmark and perpendicularly extrapolated to the inner table of the frontal bone (ITF) (Fig. 1A and B).

ACF Width: The midpoint of the limbus sphenoidale (LS) was selected as a reference landmark and extrapolated to the level at which the ACF was observed to be its maximum width. At the level at which the lesser wings of the sphenoid bone were observed to be the most prominent, the maximum transverse distance was measured in an axial plane between the inner tables of the frontal bones (ITF), in the same plane that the maximum anterior-posterior distance was measured (Fig.1A and B).

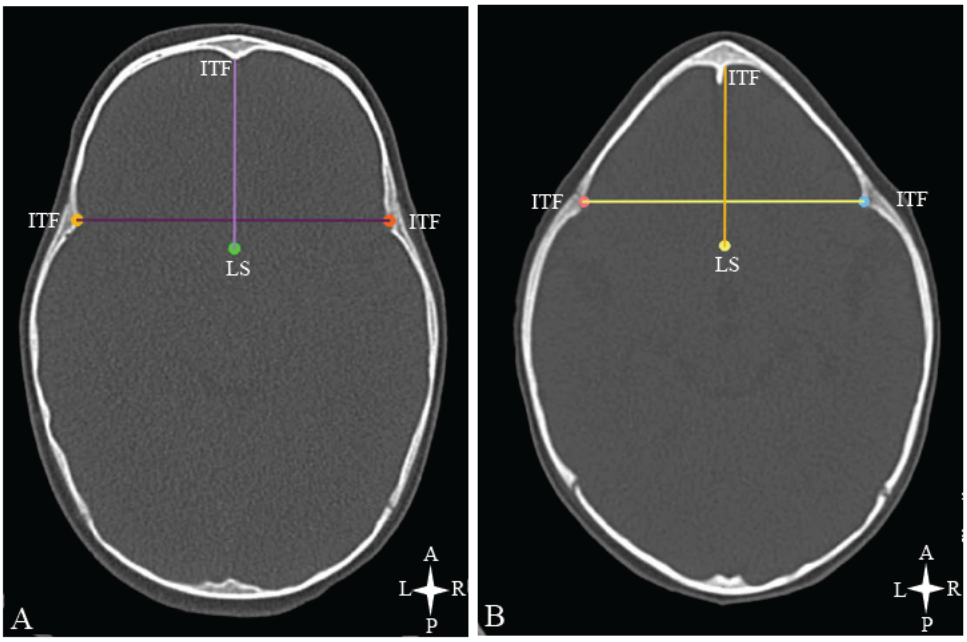

Figure 1: ACF length and width on an axial CT scan of a normal patient (A) and trigonocephaly patient (B) (length: LS to ITF; width: ITF to ITF). Key: LS – midpoint of limbus sphenoidale (extrapolated point); ITF – inner table of frontal bone

ACF Height: The maximum superior-inferior distance was measured in a sagittal plane by extrapolating a perpendicular line vertically from the midpoint of the limbus sphenoidale (reference landmark) to the inner table of the frontal bone (ITF) (Fig. 2A and B).

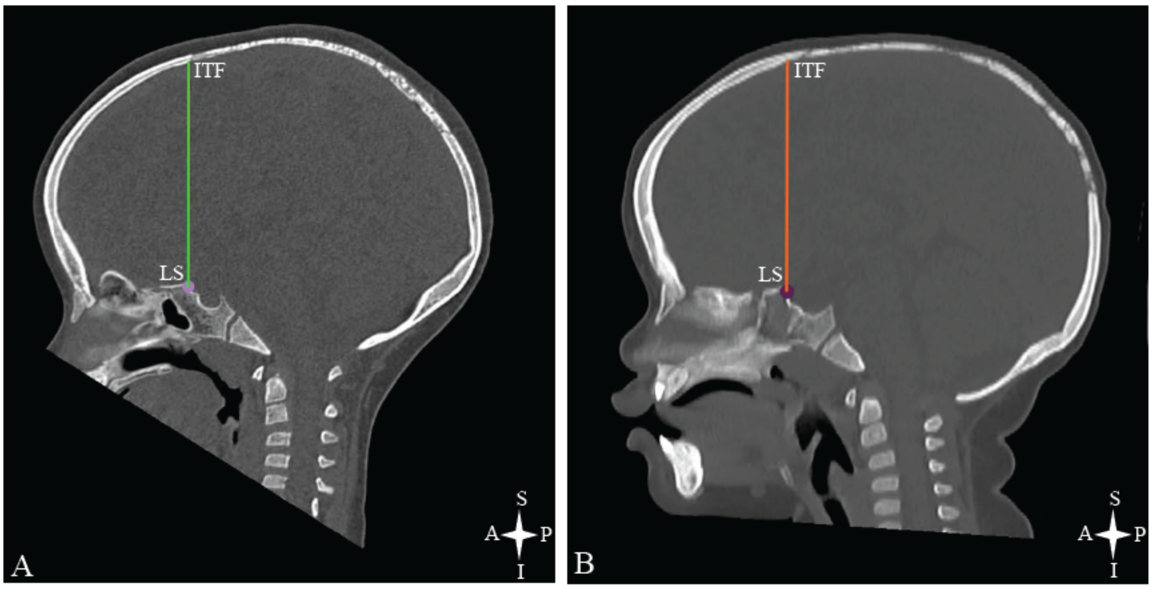

Figure 2: ACF height on a sagittal CT scan of a normal patient (A) and trigonocephaly patient (B) (height: LS to ITF). Key: LS – midpoint of limbus sphenoidale; ITF – inner table of frontal bone

ACF Volume: The volume of the ACF was measured in an axial plane, and the ACF was manually divided on each individual slice of the CT scan images. The level at which the fused coronal suture (FCS), on either side, was observed to be the most prominent was selected as the posterior boundary that divided the ACF from the MCF. The posterior boundary was determined by constructing a horizontal line from the FCS on one side of the skull to the coronal suture on the opposite side of the skull. The posterior boundary was transferred to every single slice of the CT scan images where the ACF was visible. The start slice was chosen when the ACF was first visible, and the end slice was chosen when the midpoint of the limbus sphenoidale was no longer visible. The ACF was manually outlined on each CT image slice by using the closed polygon tool. All slices were selected and the volume of the ACF was automatically calculated using the ROI volume tool (Fig. 3A and B).

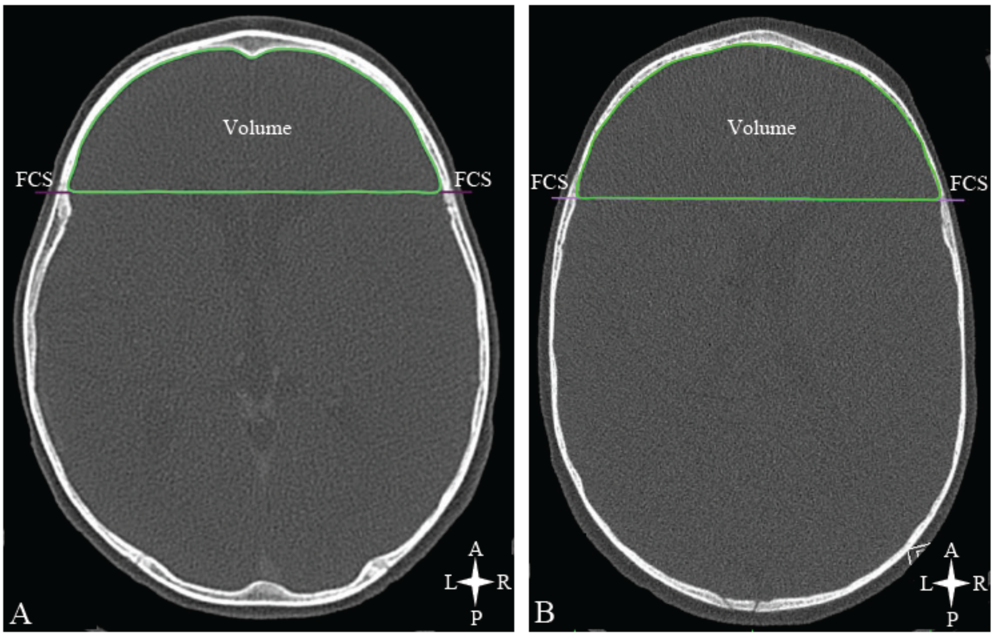

Figure 3: Volume measurement of the ACF on an axial CT scan of a normal patient (A) and trigonocephaly patient (B). Key: FCS – fused coronal suture

ACF Angles: The angles of the ACF were measured in the same plane as the selected reference landmark. The frontal angle (FA) was measured as the angle of the frontal bone in an axial plane with the vertex positioned on the exocranial aspect on the most anterior point of the frontal bone and terminal points at which the lesser wings of the sphenoid bone were observed to be the most prominent, on the external surface. The endocranial bifrontal angle (EBA) was measured as the angle of the frontal bone in an axial plane with the vertex positioned on the endocranial aspect on the most anterior point of the frontal bone and terminal points at which the lesser wings of the sphenoid bone were observed to be the most prominent, on the internal surface (Fig. 4A, B, C and D).

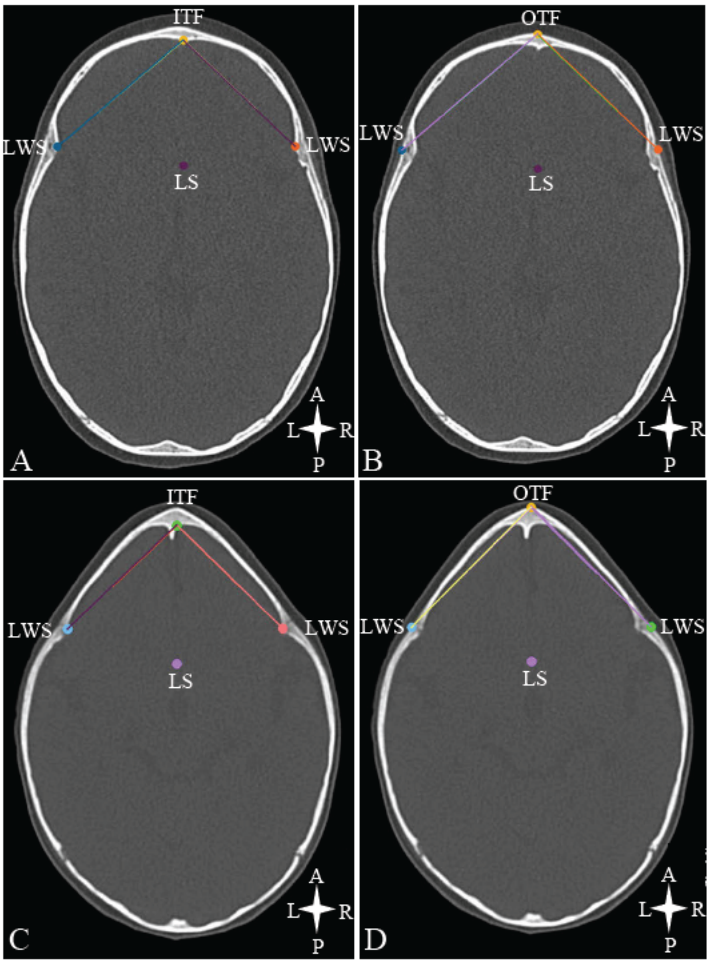

Figure 4: Angles of the ACF on an axial CT scan of a normal patient (A and B) and trigonocephaly patient (C and D) (EBA: vertex at ITF and terminal points at LWS; FA: vertex at OTF and terminal points at LWS). Key: IFT – inner table of frontal bone; OTF – outer table of frontal bone; LWS – lesser wing of sphenoid bone; LS – midpoint of limbus sphenoidale (extrapolated landmark used as a reference plane)

2.3.4. Volumetric assessment of the MCF and PCF

MCF Volume: The volume of the MCF was measured in an axial plane, and the MCF was manually divided on each individual slice of the CT scan images. The level at which the superior margin of the petrous part of the temporal bone was observed to be the most prominent was selected as the posterior boundary that divided the MCF from the PCF. The start slice was chosen when the foramen ovale was first visible, and the end slice was chosen when the superior orbital fissure, immediately inferior to the lesser wing of the sphenoid bone, was no longer visible. The MCF was manually outlined on each CT image slice by using the closed polygon tool. All slices were selected and the volume of the MCF was automatically calculated using the ROI volume tool.

PCF Volume: The volume of the PCF was measured in an axial plane, and the PCF was manually divided on each individual slice of the CT scan images. The level at which the petrous part of the temporal bone was observed to be the most prominent was selected as the anterior boundary that divided the PCF from the MCF. The level at which the groove for the transverse sinus was observed to be the most prominent was selected as the most posterior boundary of the PCF. The start slice was chosen when the foramen magnum was first visible, and the end slice was chosen when the petrous part of the temporal bone was no longer visible. The midpoint of the posterior margin of the dorsum sellae was also determined in order to ensure accurate division between the PCF and MCF in the midline. The PCF was manually outlined on each CT image slice by using the closed polygon tool. All slices were selected and the volume of the PCF was automatically calculated using the ROI volume tool.

Demographic information, viz., as age, sex, and population group were recorded and any significant findings pertaining to these factors were documented. Different pediatric age groups were taken into account when assessing the degrees of severity in trigonocephaly patients.

The cephalic index (CI) was calculated and assessed across the different degrees of severity in trigonocephaly patients. The equation: cephalic width/cephalic length x 100 was used to calculate the CI. The cephalic length was measured in the transverse plane as the maximum anterior-posterior distance with points located on the outer table of the skull. The cephalic width was measured in the transverse plane as the maximum transverse distance of the skull with points located on the outer table of the skull[14].

Trigonocephaly and control patients were further grouped by age in order to ensure a more accurate comparative assessment. There were three age groups, viz., <12 months, 12-<36 months, and 36-<72 months. The different degrees of severity of trigonocephaly patients were classified into three groups according to the FA and EBA of the ACF. According to the FA, trigonocephaly patients were classified into severe (<90°), moderate (91°-99°), and mild (100°-109°); and according to the EBA, trigonocephaly patients were classified into severe (82°-90°), moderate (91°-99°), and mild (100°-110°).

2.3.5. Statistical analysis

The results were expressed as descriptive statistics, and data was analysed for normality by means of the appropriate statistical test. Descriptive statistics were recorded as minimum, maximum, standard deviation, means and medians. Mean differences were respectively applied to indicate a normal distribution of data, and the Ranksum and Kruskal-Wallis tests were used to determine median differences in the morphometrical data between trigonocephaly and control patients to indicate a skewed distribution of data. The t-test was used to describe comparisons between trigonocephaly and control patients, the Fischer's exact test was used to determine relationships between demographic variables, and the ANOVA test was used to determine comparisons between the different degrees of severity of trigonocephaly patients. Compensatory growth via volumetric assessment was determined and expressed as percentages. Each measurement was measured three times, and intra-observer and inter-observer correlation coefficient values were calculated in order to assess the accuracy and reliability of the data that was recorded. The R Statistical Computing Software of the R Core Team (R Studio, Boston, MA, USA, 2021) was used to perform statistical data analysis. A p-value of less than 0.05 was considered statistically significant.

2.4. Results

The demographics of the study population is indicated in Table 1. A total of 15 (13 males and two females) patients with a confirmed diagnosis of non-syndromic, isolated trigonocephaly were included in the data analysis of this study. The median age at the time the CT scan was taken was 11 months (range: 5-36 months) for trigonocephaly patients, with a male to female ratio of 6.5:1. The number of patients in the three different age groups were: <12 months (n=8), 12-<36 months (n=6), and 36-<72 months (n=1). Four different population groups were documented in trigonocephaly patients, viz., Black (40%), White (33.3%), Indian (20%), and Coloured (6.7%). With regards to the degree of severity, trigonocephaly patients were classified into three types according to the FA, viz., three patients were assigned to the mild type (100°-109°), seven patients were assigned to the moderate type (91°-99°), and five patients were assigned to the severe type (<90°) (FA range: 83°-109°); and according to the EBA, viz., three patients were assigned to the mild type (100°-110°), five patients were assigned to the moderate type (91°-99°), and seven patients were assigned to the severe type (82°-90°) (EBA range: 82°-110°). The mean CI was 75.7±8.0% (range: 66%-99%) in trigonocephaly patients. A total of eight (four males and four females) control patients with no skull abnormalities were included in the data analysis of this study as the control group. The median age at the time the CT scan was taken was 22 months (range: 1-48 months) for the control group. The number of controls in the three different age groups were: <12 (n=1), 12-<36 months (n=6), and 36-<72 months (n=1). Only two different population groups were documented in the control group, viz., Black (87.5%), and Indian (12.5%). A normal FA was observed to be between 84°-96°, whilst a normal EBA was observed to be between 81°-97°. The mean CI was 74.5±3.7% (range: 69%-81%) in the control group.

Table 1: Demographic information of the study population

Demographic	Trigonocephaly (n=15)	Control (n=8)
Age CT scan was taken (months)		
<12	8 (53.3%)	1 (12.5%)
12-<36	6 (40%)	6 (75%)
36-<72	1 (6.7%)	1 (12.5%)
Mean±SD	-	20.9±13.5
Median (Q1-Q3)	11 (8.0-18.5)	22 (13.0-24.0)
Range	5-36	1-48
Sex		
Male	13 (86.7%)	4 (50%)
Female	2 (13.3%)	4 (50%)
Population group		
Black	6 (40%)	7 (87.5%)
White	5 (33.3%)	0 (0%)
Indian/Asian	3 (20%)	1 (12.5%)
Coloured	1 (6.7%)	0 (0%)
Degree of severity		
FA		
Mild	3 (20%)	-
Moderate	7 (46.7%)	-
Severe	5 (33.3%)	-
Median (Q1-Q3)	91.8º (90.5º-95.7º)	91.1º (88.8º-92.5º)
Range	83º-109º	84º-96º
EBA		
Mild	3 (20%)	-
Moderate	5 (33.3%)	-
Severe	7 (46.7%)	-
Median (Q1-Q3)	91.2º (90.4º-94.6º)	91.0º (89.0º-92.6º)
Range	82º-110º	81º-97º
Cephalic Index (%)*		
Mean±SD	75.7±8.0	74.5±3.7
Range	66-99	69-81

Abbreviation: SD – Standard deviation;
**Cephalic Index = cranial width/cranial length x 100*

2.4.1. Morphometry of the ACF

The overall comparison of the morphometry of the ACF between trigonocephaly and control patients is indicted in Table 2.

Table 2: ACF dimensions between trigonocephaly and the control group patients

Dimension	Trigonocephaly (n=15)	Control (n=8)	p-value
ACF length (mm)			
Mean±SD	50.3±3.86	51.5±4.51	0.514
ACF width (mm)			
Median[a]	89.8(82.2-93.9)	93.5(88.4-95.3)	0.583
ACF height (mm)			
Median[a]	78.4(74.0-81.7)	79.7(77.6-82.0)	0.868
ACF volume (mm^3)			
Mean±SD	59700±22200	75300±29900	0.170
ACF FA (°)			
Median[a]	91.8(90.5-95.7)	91.1(88.8-92.5)	0.212
ACF EBA (°)			
Median[a]	91.2(90.4-94.6)	91.0(89.0-92.6)	0.324

Abbreviations: ACF – Anterior cranial fossa. EBA – Endocranial bifrontal angle. FA – Frontal angle. SD – Standard deviation
[a]Ranksum test: Median value (Q1-Q3) is shown due to skewness of data

The overall length, width, height, volume, FA, and EBA of the ACF were all found to be non-significant between trigonocephaly and control groups (p=0.514; p=0.583; p=0.868; p=0.170; p=0.212; p=0.324) (Table 2).

Age comparison

Due to some of the age groups only having a single measurement, significant comparisons by age could not be performed between trigonocephaly and control patients. Therefore, the following data is expressed as descriptive statistics (Table 3). In the <12 months age group, the ACF length, width, height, and volume were larger in trigonocephaly patients compared to controls; the EBA was more acute in the trigonocephaly group compared to the control group, whilst the FA was more acute in controls compared to trigonocephaly patients. In the 12-<36 months age group, the ACF length, width, height, and volume were smaller in trigonocephaly patients compared to controls; the EBA and FA were both larger and less acute in the trigonocephaly group compared to the control group. In the 36-<72 months age group, the ACF length and width were smaller, whilst the ACF height and volume were larger in trigonocephaly compared to control patients; the EBA was larger and less acute in comparison to the FA which was smaller and more acute in trigonocephaly compared to control patients (Table 3).

Degree of severity

Due to some of the age groups only having a single measurement, significant comparisons by degree of severity could not be performed between trigonocephaly and control patients. Therefore, the following data is expressed as descriptive statistics (Table 3). The degrees of severity of trigonocephaly were further categorised in the three age groups into the different severity types according to the FA and EBA severity classifications. According to the FA: in the <12 months age group, one patient was assigned to the mild type, four patients were assigned to the moderate type, and three patients were assigned to the severe type; in the 12-<36 months age group, two patients were assigned to the mild type, three patients were assigned to the moderate type, and one patient was assigned to the severe type; in the 36-<72 months age group, only one patient was assigned to the severe type. According to the EBA: in the <12 months age group, one patient was assigned to the mild type, four patients were assigned to the moderate type, and three patients were assigned to the severe type; in the 12-<36 months age group, two patients were assigned to the mild type, one patient was assigned to the moderate type, and three patients were assigned to the severe type; in the 36-<72 months age group, only one patient was assigned to the severe type (Table 3).

2.4.2. Volumetric assessment of the cranial fossae

The volumetric dimensions of the ACF, MCF, PCF, and total cranial fossae volume is indicated in Table 4. The mean MCF volume was significantly larger in trigonocephaly patients compared to the control group (p=0.050), whilst the mean ACF and median PCF volumes did not show significance when trigonocephaly patients were compared to the control group (p=0.170 and p=0.821, respectively). However, the median PCF volume was observed to be larger in patients with trigonocephaly (47200mm^3) compared to the control group (39300mm^3). No significance was observed when the total cranial fossae volume was compared between trigonocephaly patients and the control group (p=0.973) (Table 4).

Overall compensatory growth of the MCF and PCF

Evidence of compensatory growth in the overall volumes of the MCF and PCF in trigonocephaly patients and the control group were expressed as percentages and visually recorded as line graphs (Fig. 5). For trigonocephaly patients, the PCF showed the most compensatory growth of 30.4% (range: 22.2%-52.6%), whilst the MCF showed compensatory growth of 28.8% (range: 12.1%-40.9%). In the control group, the MCF and PCF both showed very little compensatory growth of 5.6% (range: 15.3%-20.9%) and 15.7% (range: 20.8%-61.7%), respectively (Fig. 5).

Compensatory growth of the MCF and PCF according to degree of severity

Compensatory growth of the MCF and PCF was further categorised according to the different degrees of severity in trigonocephaly patients, and is indicated in Table 5. In the FA severity classification, mild patients showed the most amount of compensatory growth in the MCF (32.0±9.84%), whilst the least amount of compensatory growth was observed in severe patients (22.3±8.39%); moderate patients showed the most amount of compensatory growth in the PCF (36.2%), followed by mild patients (28.3%), and severe patients (25.4%). In the EBA severity classification, mild patients showed the same amount of compensatory growth in the MCF (32.0±9.84%) as mild patients in the FA severity, whilst the least amount of compensatory growth was observed in severe patients (21.1±6.36%); severe patients showed the most amount of compensatory growth in the PCF (41.7%), followed by moderate patients (31.4%), and mild patients (28.3%) (Table 5).

Table 3: Comparison of ACF dimensions between trigonocephaly patients and the control group by age and degree of severity

Parameter	Age group (months)					
	<12		12-<36		36-<72	
	Trigonocephaly (n=8) (Median[a])	Control (n=1) (Median[a])	Trigonocephaly (n=6) (Mean±SD)	Control (n=6) (Mean±SD)	Trigonocephaly (n=1) (Median[a])	Control (n=1) (Median[a])
ACF length (mm)	51.1(49.4-52.2)	42.2(42.2-42.2)	49.2±5.52	52.1±1.82	53.2(53.2-53.2)	57.6(57.6-57.6)
ACF width (mm)	87.8(79.6-90.1)	69.8(69.8-69.8)	92.8±8.31	92.9±4.09	97.1(97.1-97.1)	97.5(97.5-97.5)
ACF height (mm)	76.7(73.4-78.5)	60.7(60.7-60.7)	79.4±9.89	80.8±3.73	84.1(84.1-84.1)	81.5(81.5-81.5)
ACF volume (mm^3)	60600(38100-62900)	9450(9450-9450)	59900±18600	82200±14300	114000(114000-114000)	100000(100000-100000)
ACF EBA (°)	91.2(90.3-92.5)	91.5(91.5-91.5)	98.0±8.39	92.1±4.14	82.1(82.1-82.1)	81.4(81.4-81.4)
ACF FA (°)	91.7(90.3-93.3)	90.9(90.9-90.9)	97.7±7.36	91.7±3.92	83.3(83.3-83.3)	84.2(84.2-84.2)
Degree of severity						
FA						
Mild	1	-	2	-	-	-
Moderate	4	-	3	-	-	-
Severe	3	-	1	-	1	-
EBA						
Mild	1	-	2	-	-	-
Moderate	4	-	1	-	-	-
Severe	3	-	3	-	1	-

Abbreviations: ACF- Anterior cranial fossa. EBA – Endocranial bifrontal angle. FA – Frontal angle. SD – Standard deviation
[a]*Ranksum test: Median value (Q1-Q3) is shown due to skewness of data*

Table 4: Comparison of volumetric measurements of the ACF, MCF, PCF, and total cranial fossae volume between trigonocephaly and control groups

Volume (mm^3)	Trigonocephaly (n=15)	Control (n=8)	p-value
ACF volume			
Mean±SD	59700±22200	75300±29900	0.170
MCF volume			
Mean±SD	34500±8790	26400±9130	0.050*
PCF volume			
Median[a]	47200(29500-63100)	39300(31300-48700)	0.821
Total cranial fossae volume			
Mean±SD	148000±50500	147000±48900	0.973

Abbreviations: ACF- Anterior cranial fossa. MCF – Middle cranial fossa. PCF – Posterior cranial fossa. SD – Standard deviation
**Indicates statistical significance with a p-value less than 0.05*
[a]Ranksum test: Median value (Q1-Q3) is shown due to skewness of data

Table 5: Comparison of the compensatory growth of the MCF and PCF according to the FA and EBA classifications of severity in trigonocephaly patients

FA severity	Mild (100°-109°) (n=3)	Moderate (91°-99°) (n=7)	Severe (<90°) (n=5)	p-value
MCF (%) Mean±SD	32.0±9.84	23.9±6.23	22.3±8.39	0.239[b]
PCF (%) Median[a]	28.3(28.3-35.9)	36.2(26.8-40.5)	25.4(24.7-45.3)	0.987[c]
EBA severity	**Mild (100°-110°) (n=3)**	**Moderate (91°-99°) (n=5)**	**Severe (82°-90°) (n=7)**	**p-value**
MCF (%) Mean±SD	32.0±9.84	26.1±7.18	21.1±6.36	0.133[b]
PCF (%) Median[a]	28.3(28.3-35.9)	31.4(24.7-36.2)	41.7(24.9-47.2)	0.581[c]

Abbreviations: MCF – Middle cranial fossa. PCF – Posterior cranial fossa. SD – Standard deviation
[a]Ranksum test: Median value (Q1-Q3) is shown due to skewness of data
[b]ANOVA test: Conducted for mild, moderate and severe trigonocephaly patients
[c]Kruskal-Wallis test: Median value (Q1-Q3) is shown due to skewness of data

A

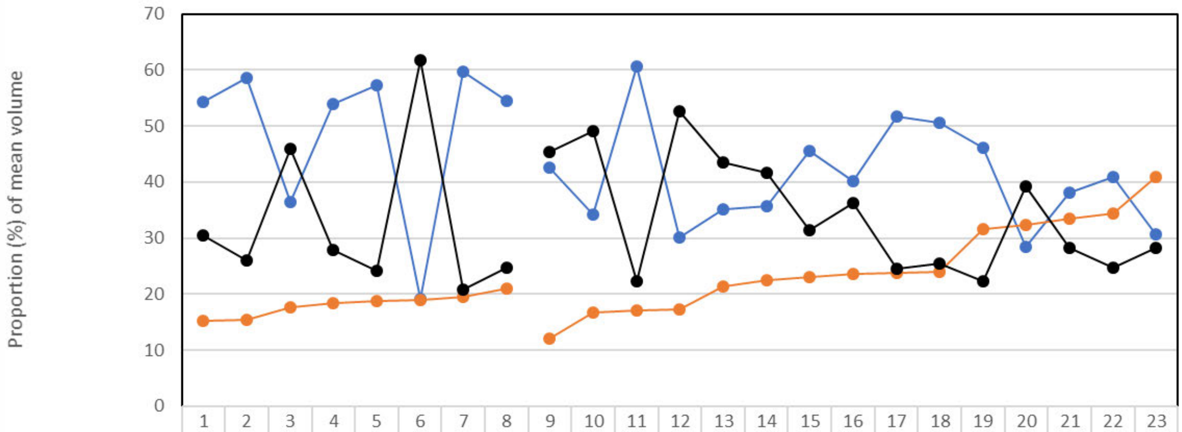

	1	2	3	4	5	6	7	8	9	10	11	12	13	14	15	16	17	18	19	20	21	22	23
Study ACF									42.6	34.3	60.7	30.1	35.1	35.8	45.5	40.2	51.7	50.7	46.1	28.5	38.2	40.9	30.7
Study MCF									12.1	16.7	17.0	17.3	21.4	22.5	23.1	23.6	23.8	23.9	31.6	32.4	33.5	34.4	40.9
Study PCF									45.3	49.0	22.2	52.6	43.5	41.7	31.4	36.2	24.5	25.4	22.3	39.2	28.3	24.7	28.3
Control ACF	54.2	58.6	36.4	53.9	57.2	19.2	59.6	54.4															
Control MCF	15.3	15.4	17.6	18.3	18.7	19.0	19.6	20.9															
Control PCF	30.5	26.0	46.0	27.8	24.1	61.7	20.8	24.7															

B

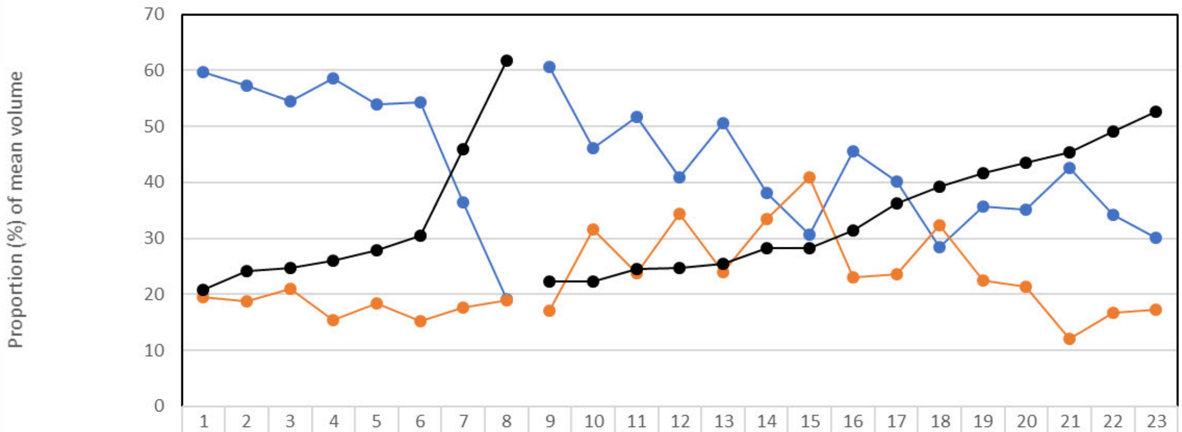

	1	2	3	4	5	6	7	8	9	10	11	12	13	14	15	16	17	18	19	20	21	22	23
Study ACF									60.7	46.1	51.7	40.9	50.7	38.2	30.7	45.5	40.2	28.5	35.8	35.1	42.6	34.3	30.1
Study MCF									17.0	31.6	23.8	34.4	23.9	33.5	40.9	23.1	23.6	32.4	22.5	21.4	12.1	16.7	17.3
Study PCF									22.2	22.3	24.5	24.7	25.4	28.3	28.3	31.4	36.2	39.2	41.7	43.5	45.3	49.0	52.6
Control ACF	59.6	57.2	54.4	58.6	53.9	54.2	36.4	19.2															
Control MCF	19.6	18.7	20.9	15.4	18.3	15.3	17.6	19.0															
Control PCF	20.8	24.1	24.7	26.0	27.8	30.5	46.0	61.7															

Figure 5: Compensatory growth of the volumes of the MCF (A) and PCF (B) in trigonocephaly patients compared to the control group. Key: ACF – anterior cranial fossa; MCF – middle cranial fossa; PCF – posterior cranial fossa

Intra-observer reliability

The intra-observer reliability test results indicated that the mean or median measurements used were very reliable and the ICC values are indicated in Table 6.

Table 6: Intra-observer reliability test expressed as ICC values

Measurement	ICC (95%CI)	p-value
ACF Parameters		
ACF length (mm)	1	<0.001
ACF width (mm)	1	<0.001
ACF height (mm)	1	<0.001
ACF volume (mm^3)	1 (0.990-1.000)	<0.001
EBA (°)	1	<0.001
FA (°)	1	<0.001
Additional Volumetric Parameters		
MCF volume (mm^3)	1	<0.001
PCF volume (mm^3)	1	<0.001

Abbreviations: ACF – Anterior cranial fossa. EBA – Endocranial bifrontal angle. FA – Frontal angle. ICC – intraclass coefficient. MCF – Middle cranial fossa. PCF – Posterior cranial fossa

Inter-observer reliability

The ICC values of the inter-observer reliability test are indicated in Table 7.

Table 7: Inter-observer reliability test expressed as ICC values

Measurement	ICC (95%CI)	p-value
ACF Parameters		
ACF length (mm)	0.64 (0.330-0.920)	<0.001
ACF width (mm)	0.81 (0.570-0.960)	<0.001
ACF height (mm)	0.94 (0.850-0.990)	<0.001
ACF volume (mm^3)	0.89 (0.730-0.980)	<0.001
EBA (°)	0.30 (0.040-0.770)	0.023
FA (°)	0.32 (0.053-0.780)	0.018
Additional Volumetric Parameters		
MCF volume (mm^3)	0.00 (-0.122-0.440)	0.430
PCF volume (mm^3)	0.87 (0.690-0.980)	<0.001

Abbreviations: ACF – Anterior cranial fossa. EBA – Endocranial bifrontal angle. FA – Frontal angle. ICC – intraclass coefficient. MCF – Middle cranial fossa. PCF – Posterior cranial fossa

2.5. Discussion

Non-syndromic craniosynostoses make up approximately 79% of all craniosynostosis occurrences[15,16]. In the past two decades, a rise in the prevalence of trigonocephaly has been documented across Europe, the United States of America, and South Africa (Table 7) making it the second most common type of non-syndromic, isolated craniosynostosis to date[1-4,17-20]. Furthermore, in the present study, trigonocephaly was observed to be more predominant in males compared to females with a male to female ratio of 6.5:1. Due to the small sample size of the present study, it is expected that this ratio will be larger, however, this finding is similar to findings by Maltese *et al*. (2014) who observed the male to female trigonocephaly ratio in their sample size to be 5.4:1. Additionally, previous studies by Van der Meulen (2012), Cornelissen *et al*. (2016), Ghizoni *et al*. (2016), and Baş *et al*. (2021) also observed trigonocephaly to be more predominant in males compared to females with a male to female ratio of 3-3.5:1.

Table 8: First reported case and the evolution of non-syndromic, isolated trigonocephaly within the last two decades

Study	Country	Description	Prevalence (isolated trigonocephaly/non-syndromic craniosynostoses)	Time period
Welcker (1862)	Germany	First reported case of trigonocephaly	-	-
Di Rocco *et al*. (2009)	France, Paris	Isolated trigonocephaly	598 (21%) out of 2808	1988 - 2007
Van der Meulen (2009)	Pan-European	Isolated trigonocephaly	756 (23%) out of 3240	1997 – 2006
Kolar (2011)	United States of America, Texas	Isolated trigonocephaly	173 (25%) out of 690	1987 – 2009
Van der Meulen (2012)	Netherlands	Isolated trigonocephaly	238 (31.4%) out of 757	2002 – 2012
Cornelissen *et al*. (2016)	Netherlands	Isolated trigonocephaly	240 (36%) out of 666	2008 – 2013
Baş *et al*. (2021)	Turkey, Istanbul	Isolated trigonocephaly	18 (20.1 – 25.5 %)	2010 – 2020
Present study	South Africa, KwaZulu-Natal	Isolated trigonocephaly	15 (44%) out of 34	2012 – 2023

In the present study, the overall ACF length, width, height, and volume were smaller in patients with trigonocephaly compared to the control group. These findings were similar to findings by Chandler *et al*. (2021) who observed that the anterior cranial width and volume in trigonocephaly patients were also smaller compared to the control group ($p=<0.001$ and $p=0.294$, respectively), however, the anterior cranial length and height was larger in trigonocephaly patients compared to the control group ($p=0.003$ and $p=0.010$, respectively). It is expected that the width of the ACF is observed to be smaller in trigonocephaly patients, due to the characteristic shortening of the ACF in patients with this condition, which was observed in both of the above-mentioned studies. Additionally, factors such as age and degree of severity could have an influence on the different ACF and anterior cranium lengths and heights that were observed in the present study and the study by Chandler *et al*. (2021).

2.5.1. Age and degree of severity comparison

In the present study, the median age of trigonocephaly patients was 11 months, with majority of patients grouped in the <12 months age group. A similar trend was observed between the FA and EBA classifications that were used to assess the severity of trigonocephaly. In the FA classification, the majority of patients were classified into the moderate type, followed by the severe type, and the mild type. In the <12 and 12-<36 months age group, patients were further categorised into the three different types of severity, with the majority of patients grouped into the moderate type. In the EBA classification, the majority of patients were classified into the severe type, followed by the moderate type, and the mild type. In the <12 months age group, patients were further categorised into the three different types of severity, with the majority of patients grouped into the moderate type, whilst the majority of patients in the 12-<36 months age group were grouped into the severe type. Only one patient was analysed in the 36-<72 months age group, and was grouped into the severe type using both the FA and EBA classifications of severity. Additionally, the dimensions of the ACF in younger age groups were larger in trigonocephaly patients compared to controls, which follows the same pattern as the study by Chandler *et al*. (2021) who evaluated 167 trigonocephaly patients with a mean age of 7.2 months. These trends could indicate that more severe trigonocephaly cases are observed in younger pediatric patients compared to older pediatric patients. Moreover, smaller dimensions of the ACF were observed in older trigonocephaly patients in the present study, which could be a possible consequence of the skull adjustment and compensatory growth of other areas of the cranium due to the affected anterior region of the skull in patients with this condition.

2.5.2. Compensatory growth of the cranial base

There is only one previous study[2] that recorded the compensatory growth of the middle and posterior thirds of the skull in trigonocephaly patients via volumetric analysis. Naran *et al*. (2017) observed a significantly smaller volumetric ratio when the volume of the anterior third of the skull was compared to the total cranial skull volume in trigonocephaly patients (p=0.0128) compared to controls; a significantly larger volumetric ratio when the volume of the middle third of the skull was compared to the total cranial skull volume was observed in trigonocephaly patients (p=0.0128) compared to controls; however, no significant difference was observed in the ratio of the volume of the posterior third of the skull to the total cranial skull volume when trigonocephaly patients were compared to controls. An interesting observation in the present study, which differs from the study by Naran *et al*. (2017), is that the majority of the cranial base in trigonocephaly patients showed evidence of compensatory growth via volumetric analysis of the MCF and PCF. The PCF showed the most compensatory growth when trigonocephaly patients (30.4%) were compared to the control group (15.7%), whilst the MCF also showed compensatory growth of 28.8% in trigonocephaly patients and only 5.6% in the control group. A direct comparison of the present study with Naran *et al*. (2017) does not yield substantial significant results as volumetric analyses of different regions of the skull were evaluated. However, due to the characteristic occipitoparietal widening[6,10] and the restricted growth of the frontal bones causing an increased compensatory growth of the cranial sutures that are unaffected[11], compensatory growth of the MCF, PCF, as well as the middle and posterior cranial thirds is evident in trigonocephaly patients in order to assist with the growth of the skull and the developing brain.

Furthermore, the present study also observed differences in the compensatory growth of the MCF and PCF according to the different degrees of severity of trigonocephaly. In the FA severity classification, the MCF showed the most amount of compensatory growth in mild patients, then in moderate patients, and the least amount was observed in severe patients; the PCF showed the most amount of compensatory growth in moderate patients, then in mild patients, and the least amount in severe patients. In the EBA severity classification, the MCF showed the most and same amount of compensatory growth as the FA severity in mild patients, then in moderate patients, and the least amount in severe patients; whilst significant differences were observed in the PCF, which showed the most amount of compensatory growth in severe patients, then in moderate patients, and the least amount in mild patients, but not statistically significant ($p=0.581$). The same amount of compensatory growth observed in the MCF in mild trigonocephaly patients indicate that both the FA and EBA classifications of severity could be very effective indices to use in assessing the degree of severity in patients with this condition.

2.5.3. Assessment of degree of severity

Numerous studies have assessed the severity of trigonocephaly using multiple craniometric measurements of the ACF, however, the assessment of the degree of severity still remains controversial as to which method is the most accurate and reliable. Beckett *et al*. (2012) used the EBA to classify trigonocephaly patients into severe (100°-124°) and moderate (124°-148°) on 3D CT scan reconstructions. Van der Meulen (2012) conducted measurements on axial CT scans using the FA to classify the severity of trigonocephaly patients into severe (<89°), moderate (90°-95°), and mild (96°-103°). Ezaldein *et al*. (2014) used the EBA on 2D and 3D CT scans to classify the degree of orbital dysmorphology in trigonocephaly patients and concluded that severe patients had an EBA of <124° and moderate patients had an EBA between 124°-148°. A study by Wang *et al*. (2016) utilised the metopic index on 3D reconstructions to determine a grading system for the degree of severity of trigonocephaly. The metopic index was observed to be significant ($p<0.001$) when comparisons were made between trigonocephaly patients and controls[10]. Naran *et al*. (2017) measured six angles on 3D CT scan reconstructions of patients diagnosed with single suture, non-syndromic trigonocephaly. These angles were standard measurements and were not used to assess the severity of the deformity, however, out of the six angles evaluated, the EBA was significantly more acute in trigonocephaly patients (128.6°±10.4°) compared to controls (141.4°±7.6°) ($p=0.0001$)[2]. Chandler *et al*. (2021) compared previous studies using various craniometric measurements to assess the severity of trigonocephaly to their own proposed severity metric. It was concluded that findings from previous studies were too variable and were limited due to the smaller sample sizes, thus, the FA on 3D CT scan reconstructions showed the most significance in assessing the degree of severity in 167 trigonocephaly patients (98.6°±5.7°) compared to 44 control patients (105.5°±5.0°)[3]. In another study by Baş *et al*. (2021), the severity of trigonocephaly was assessed using measurements of the metopic angle and patients were classified into severe (111°-123°), moderate (124°-135°), and mild (136°-147°).

In the present study, which had a larger median age of trigonocephaly patients and used 2D axial CT scans, the FA and EBA were both used to classify the degree of severity of patients with trigonocephaly. Similar trends were noted when classifying patients into different degrees of severity using both the FA and EBA severity classifications. According to the FA severity classification, five patients were classified into the severe type (<90°), seven patients were classified into the moderate type (91°-99°), and three patients were classified into the mild type (100°-109°); compared to the EBA severity classification with seven patients classified into the severe type (82°-90°), five patients classified into the moderate type (91°-99°), and three patients classified into the mild type (100°-110°). Statistically significant comparisons between the different degrees of severity in trigonocephaly patients and the control group could not be determined as the control group was not classified into different degrees of severity. Moreover, the FA and EBA classifications in the present study are somewhat smaller compared to previous literature. This could be attributed to the larger median age of the present study compared to smaller mean ages of previous studies. Additionally, in the present study, the majority of trigonocephaly patients in older age groups (12-<36 and 36-<72 months) were further classified as moderate and severe types, which indicates that in the current South African population, these patients are only being reported and diagnosed at a later age when the deformity is at its most severe stage.

Furthermore, the CI is another parameter that has been determined in a few previous studies in patients with trigonocephaly. Naran *et al*. (2017) recorded a larger CI in trigonocephaly patients of 81.9±5.9% compared to controls with a CI of 80.9±10.4%, however, no significance was found between the two groups ($p=0.694$). In another study by Applegren *et al*. (2018), the cephalic ratio was calculated to determine the overall head shape in patients with trigonocephaly and was observed to be 0.88 in trigonocephaly patients and 0.90 in controls, with also no significance observed between the two groups ($p=0.224$). In the present study, the mean CI was also observed to be larger in trigonocephaly patients (75.7±8.0%) compared to controls (74.5±3.7%).

The prevalence of trigonocephaly is on the rise across numerous countries due to an unknown cause. Overall, the dimensions of the ACF were smaller in trigonocephaly patients compared to the control group. Slightly larger dimensions of the ACF were observed when younger more severe trigonocephaly patients were compared to the control group, whilst smaller dimensions of the ACF were observed when older moderate and severe trigonocephaly patients were compared to the control group. Thus, age and degree of severity both influence the morphometric changes of the ACF in patients with trigonocephaly. The volume of the MCF was observed to be the most significant, and the volume of the PCF was larger when patients with trigonocephaly were compared to the control group. The PCF showed the most overall amount of compensatory growth followed by the MCF in trigonocephaly patients. The FA and EBA severity classifications were observed to be slightly similar and are valuable indicators to assess the different degrees of severity in patients with trigonocephaly. More moderate and severe patients were observed in older compared to younger age groups, indicating that patients with this condition, in the present population group, are only being reported and diagnosed later on in life.

A limitation of this study is the small sample size, which limited the comparison of substantial significant results between trigonocephaly and control patients. Another limitation is the difficulty in obtaining age- and sex-matched control patients. Although control patients who had met the inclusion criteria were only selected and chosen for analysis, these patients had undergone scanning of the head for a certain type of pathology. However, no skull abnormalities were detected and due to the risk of exposing completely normal pediatric patients to unnecessary radiation, the patients that formed the control group were the only patients available for comparison.

This study provides a novel insight to the morphometric changes of the ACF in non-syndromic, isolated trigonocephaly patients in a specific South African population compared to the normal anatomy observed in control patients. Of the morphometric dimensions of the ACF obtained, the length and volume were the most affected in patients with trigonocephaly. The volume of the PCF was larger in trigonocephaly patients compared to control patients, thus, evidence of compensatory growth was mostly observed in the PCF. The FA and EBA severity classifications could assist craniofacial surgeons by providing an improved grading system in the severity of trigonocephaly, thus increasing the accuracy of which type of surgical treatment is best suited for the different degrees of severity observed in this condition. This study differs from previous literature on trigonocephaly by providing morphometric data on the ACF and volumes of the MCF and PCF which has not been previously documented. The majority of previous available literature that has analysed the morphometry of the skull in trigonocephaly has recorded changes to the entire anterior, middle, and posterior regions of the skull and has not focused on the cranial base.

2.6. Future recommendations

Future studies with a larger sample size of non-syndromic, isolated trigonocephaly patients from multiple craniofacial units across South Africa need to be conducted in order to determine if similar or more significant results can be observed. Further research on the specific dimensions of the ACF of patients with trigonocephaly in a South African population also needs to be conducted, in order for a more significant comparison to the results of the present study. CT scans of normal patients from other institutions should be included in future studies in order to increase the control group database to ensure a comparable number of control patients to trigonocephaly patients, thus allowing the possibility of more significant results.

2.7. Declarations

2.7.1. Acknowledgements

The authors wish to acknowledge the financial assistance of the College of Health Sciences (CHS) for part funding of this project.

The authors with to acknowledge Dr Partson Tinarwo for his assistance with the statistical data analysis.

2.7.2. Author contributions

C Barnes: Project development, Data collection, Data analysis, Manuscript writing and editing

L Lazarus: Project development, Data analysis, Manuscript editing

A Madaree: Project development, Data analysis, Manuscript editing

2.7.3. Conflict of interest

The authors declare that they have no conflicts of interest to report.

2.7.4. Ethical approval

Ethical clearance was obtained from the Biomedical Research Ethics Committee at the University of KwaZulu-Natal (Ethical approval number: BREC/00004342/2022).

2.8. References

1. Beckett JS, Chadha P, Persing JA, et al. Classification of Trigonocephaly in Metopic Synostosis. *Journal of Plastic and Reconstructive Surgery* 2012;130(3):442e-447e.
2. Naran S, Mazzaferro D, Wes A, et al. A Craniometric Analysis of Cranial Base and Cranial Vault Differences in Patients with Metopic Craniosynostosis. *Journal of Craniofacial Surgery* 2017;28(8):2030-2035.
3. Chandler L, Park KE, Allam O, et al. Distinguishing craniomorphometric characteristics and severity in metopic synostosis patients. *International Journal of Oral and Maxillofacial Surgery* 2021;50:1040-1046.
4. Di Rocco F, Arnaud E, Renier D. Evolution in the frequency of nonsyndromic craniosynostosis. *Journal of Neurosurgery Pediatrics* 2009;4(1):21-25.

5. Baş NS, Baş S. Craniometric Measurements and Surgical Outcomes in Trigonocephaly Patients Who Underwent Surgical Treatment. *Cureus Journal of Medical Science* 2021;13(3):e13676.
6. Van der Meulen. Metopic synostosis. *Childs Nervous System* 2012;28:1359-1367.
7. Ghizoni E, Denadai R, Raposo-Amaral CA, et al. Diagnosis of infant synostotic and nonsynostotic cranial deformities: a review for pediatricians. *Revista Paulista De Pediatria* 2016;34(4):495-502.
8. Reefhuis J, Honein MA, Shaw GM, et al. Fertility Treatments and Craniosynostosis: California, Georgia, and Iowa. *American Academy of Pediatrics* 2003;111(1):1163-1166.
9. Kajdic N, Spazzapan P, Velnar T. Craniosynostosis – Recognition, clinical characteristics, and treatment. *Bosnian Journal of Basic Medical Sciences* 2018;18(2):110-116.
10. Wang JY, Dorafshar AH, Liu A, et al. The metopic index: an anthropometric index for the quantitative assessment of trigonocephaly from metopic synostosis. *Journal of Neurosurgery Pediatrics* 2016;18:275-280.
11. Freudlsperger C, Steinmacher S, Bächl H, et al. Metopic synostosis: Measuring intracranial volume change following fronto-orbital advancement using three-dimensional photogrammetry. *Journal of Cranio-Maxillofacial Surgery* 2015;43(5):593-598.
12. Ezaldein HH, Metzler P, Persing JA, et al. Three-dimensional orbital dysmorphology in metopic synostosis. *Journal of Plastic, Reconstructive and Aesthetic Surgery* 2014;67:900-905.
13. Applegren ND, Shock LA, Aldridge KJ, et al. Relationship of a metopic ridge and anterior cranial volume measured by a non-invasive laser shape digitizer. *Journal of Craniofacial Surgery* 2018;29(1):76-81.
14. Waitzman AA, Posnick JC, Armstrong DC, et al. Craniofacial skeletal measurements based on computed tomography: Part II. Normal values and growth trends. *The Cleft Palate Craniofacial Journal* 1992;29(2):118-128.
15. Wilkie AOM, Byren JC, Hurst JA, et al. Prevalence and Complications of Single-Gene and Chromosomal Disorders in Craniosynostosis. *American Academy of Pediatrics* 2010;126(2): e391-e400.
16. Sharma R. Craniosynostosis. *Indian Journal of Plastic Surgery* 2013;46(1):18-27.
17. Welcker, H. 1862. Untersuchungen über Wachsthum und Bau des menschlichen Schädels. Vol. 1. Engelmann. English Edition.
18. Van der Meulen. The Increase of Metopic Synostosis: A Pan-European Observation. *Journal of Craniofacial Surgery* 2009;20(2):283-286.
19. Kolar JC. An epidemiological study of nonsyndromal craniosynostoses. *The Journal of Craniofacial Surgery* 2011;22(1):47-49.
20. Cornelissen M, Den Ottelander B, Rizopoulos D, et al. Increase of prevalence of craniosynostosis. *Journal of Cranio-Maxillofacial Surgery* 2016;44:1273-1279.

INTERFACE PAGE

Chapter 2 comprised of a morphometric analysis of the ACF, a volumetric comparison of all three cranial fossae in patients with trigonocephaly compared to an age-matched control group, and an improved grading system in the severity assessment of trigonocephaly patients. The data acquired provided an understanding of the changes in the anatomy of the cranial base in patients with trigonocephaly compared to the normal anatomy in the control group.

CHAPTER 3: SCIENTIFIC MANUSCRIPT 2

Contributions of this chapter

This chapter included an original manuscript that investigated and recorded the morphometry and morphology of the orbits in trigonocephaly patients within a select South African population. The results of this study were assessed across demographic variables in order to determine statistically significant relationships.

The following manuscript has been submitted and is currently under review by the International Journal of Oral and Maxillofacial Surgery.

Title: Hypotelorism-associated orbital morphometry and morphology in trigonocephaly
Authors: C Barnes, A Madaree, L Lazarus
Journal: International Journal of Oral and Maxillofacial Surgery
Manuscript Number: Pending

This manuscript has been written and structured according to the author guidelines defined by the International Journal of Oral and Maxillofacial Surgery. The American Medical Association (AMA) style was used to format references, as required by the journal.

Title: Hypotelorism-associated orbital morphometry and morphology in trigonocephaly

Authors: Courtney Barnes B. Med Sci; H. Med Sci[1], Anil Madaree MBChB; FRCS; FCS; PhD[2], Lelika Lazarus M Med Sci; PD Dip in HE, PhD[1]

Affiliations: [1]Department of Clinical Anatomy, School of Laboratory Medicine and Medical Sciences, University of KwaZulu-Natal, Durban, South Africa.

[2]Department of Plastic and Reconstructive Surgery, University of KwaZulu-Natal, Durban, South Africa.

Corresponding Author: Lelika Lazarus M Med Sci; PD Dip in HE, PhD
Department of Clinical Anatomy
School of Laboratory Medicine and Medical Sciences
College of Health Sciences
University of KwaZulu-Natal
Durban, South Africa
Ramsaroopl@ukzn.ac.za
+27 (0)31 260 7899, +27 (0)83 275 1910

Funding: The authors wish to acknowledge the financial assistance of the College of Health Sciences (CHS) for part funding of this project.

Keywords: Dysmorphology, hypotelorism, morphology, trigonocephaly

3.1. Abstract

Trigonocephaly occurs when the metopic suture fuses prematurely, and is characterised by a triangular-shaped forehead, shortening of the anterior cranial fossa, supra-orbital retrusion, hypotelorism, narrowing of the bitemporal region, and widening of the occipitoparietal region. This study aims to document the orbital morphometry in patients with trigonocephaly when compared to normal age-matched patients, and to introduce a classification system for the different morphological appearances of the orbits visualized in trigonocephaly. Preoperative two dimensional computed tomography scans of 15 non-syndromic, isolated trigonocephaly patients (13 males and two females) and eight normal age-matched controls (four males and four females) were digitized and analysed. Median ages were 11 months in trigonocephaly and 22 months in normal patients. The degrees of severity of trigonocephaly patients were classified into mild, moderate, and severe types according to the frontal and endocranial bifrontal angles. Orbital height, width, surface area on both left and right sides, and interorbital distance was measured. Orbital morphology of trigonocephaly patients was classified into various groups according to different ages. Statistical tests (t-test and Ranksum test) and correlation analysis were used, and significance was established as $p>0.05$. More complex orbital morphologies were observed in younger age groups, compared to less complex ones in older age groups. Orbital height on both left and right sides showed weak but significant correlations to the interorbital distance between trigonocephaly and control groups ($r=-0.057$ left, $r=-0.024$ right). Orbital surface area on the right side showed a weak but significant correlation to the interorbital distance between trigonocephaly and control groups ($r=-0.056$).

3.2. Introduction

Trigonocephaly, otherwise known as metopic synostosis, is classified as the second most common type of craniosynostosis, forming approximately 25% of all non-syndromic, isolated craniosynostosis occurrences[1-3]. Trigonocephaly occurs when the metopic suture fuses prematurely[4,5]. The occurrence of this premature fusion results in a number of cranial and facial abnormalities, such as a ridge over the middle of the forehead, creating a triangular-shaped forehead, shortening of the anterior cranial fossa (ACF), supra-orbital retrusion, hypotelorism, narrowing of the bitemporal region, and widening of the occipitoparietal region[4,5]. Hypotelorism (an abnormally decreased distance between the orbits that are typically described as being tear-drop in shape) and both orbital rims laterally displaced is evident in trigonocephaly. Most surgical treatment methods for trigonocephaly mainly focus on the surgical correction of the forehead and not on the orbital dysmorphology, therefore, there is sparse literature and understanding of the correlation between the bony orbital structure and trigonocephaly patients[6]. Additionally, previous literature has described the morphology of the orbits in trigonocephaly typically as tear-drop shaped without taking into account different degrees of severity of trigonocephaly, age groups, and growth rate of the skull. Furthermore, it is expected that orbital dysmorphology declines with increasing severity of trigonocephaly, thus introducing more functional defects of the eye[6]. The modification of the supraorbital bar and lateral orbital wall is a crucial aspect in the surgical reconstruction of trigonocephaly. To the author's knowledge, there is no known study that has classified the different morphological appearances of the orbits in trigonocephaly patients in relationship to different degrees of severity, and pediatric age groups. Thus, the aim of this investigation is to document the orbital morphometry in trigonocephaly patients compared to the normal orbital morphometry, as well as to classify the different morphological appearances of the orbits in relationship to different degrees of severity of this condition, and in different pediatric age groups. This study could provide an insight into the evolution of the deformity in older pediatric patients with trigonocephaly in a specific South African population, which could assist craniofacial surgeons in the type of surgical correction to undertake in order to obtain as near to normal orbital features.

3.3. Materials and Methods

3.3.1. Patients

This study was conducted using two dimensional (2D) preoperative computed tomography (CT) scans obtained from the database of the Department of Plastic and Reconstructive Surgery at the Inkosi Albert Luthuli Central Hospital (IALCH), Durban, South Africa. Ethical approval for this study was obtained from the Biomedical Research Ethics Committee (BREC) at the University of KwaZulu-Natal (Ethical approval number: BREC/00004342/2022). A total of 15 patients with a radiographic confirmed diagnosis of non-syndromic, isolated trigonocephaly who presented to the craniofacial unit at IALCH between 2012 and 2023 were included in this study. CT scans of 8 normal age-matched pediatric patients who had undergone scanning of the head for conditions where the skull was unaffected were selected as the control group. Only patients who had meet the inclusion criteria were included in this study, and pediatric patients who were diagnosed with syndromic craniosynostosis and/or who had undergone surgical treatment were excluded. For the control group, pediatric patients who had an abnormally shaped skull, poor imaging quality of the CT scans where the anatomy of the skull and orbits could not be clearly identified, and CT scans with a slice thickness of less than or greater than 0.6mm were excluded.

3.3.2. Image acquirement and analysis

CT scans of selected patients were retrieved from a Picture Archiving and Communication System (PACS) at the IALCH and saved onto a hard drive in the DICOM (Digital Imaging and Communication in Medicine) format. CT scans were obtained during routine scanning of the head using either a 128-slice SOMATOM Definition Adaptive scanner or SOMATOM Definition Flash CT Scanner (Siemens Healthineers, Forcheim, Germany, 2007). The CT scans of the selected patients had a slice thickness ranging from 1 to 5mm, and CT scans of the control group had a slice thickness of 0.6mm. CT scans were examined and analysed using the Horos Software version 3.3.6 (Horos Project, Annapolis, MD, USA, 2019) on an external MacBook computer unit. The DICOM viewer was used to calibrate and manually verify the CT scan images. CT scans were aligned in the orbitomeatal plane. All measurements on the CT scan images were completed on the bone window setting and three dimensional (3D) multiplanar reconstruction setting using the built-in length, angle and closed polygon tools. Measurements were taken three times and intra-observer and inter-observer correlation coefficients were produced in order to ensure maximum accuracy and reliability.

3.3.3. Morphometric and morphological analysis

Specific anatomical landmarks were determined and used to measure the morphometry of the orbits in trigonocephaly and normal pediatric patients (Fig. 1, Table 1). The morphology of the orbits in trigonocephaly patients were determined using the orbital index. The orbital index was calculated according to the equation: mean orbital height/mean orbital width x 100. Thereafter, the morphology of the orbits were classified into various morphological appearances according to the different age groups, and differences in the morphology of the orbits pertaining to laterality was also observed and recorded. Additionally, specific anatomical landmarks were determined and used to measure the metopic indices of the ACF, in order to assess the severity of trigonocephaly and to document any correlation between the interorbital distance and the angles of the ACF in such patients (Fig. 2, Table 1).

Table 1: Description of parameters measured

Parameter	Description
Orbits	
Orbital height	The superior-inferior distance was measured by extrapolating a perpendicular line vertically from a point on the inferior orbital margin towards a point on the superior orbital margin, at the level at which the inferior orbital margin and zygomaticofrontal suture were observed to be the most prominent.
Orbital width	The transverse distance was measured by constructing a horizontal line from the zygomaticofrontal suture to the dacryon (medial orbital wall) of the same orbit, at the level at which the inferior orbital margin and zygomaticofrontal suture were observed to be the most prominent.
Surface area	The surface area of each orbit was calculated by manually outlining the orbital rim using the closed polygon tool, which thereafter automatically calculated the surface area of each orbit, at the level at which the zygomaticofrontal suture was observed to be the most prominent.
Interorbital distance	The interorbital distance was measured by constructing a horizontal line from the dacryon of one orbit to the dacryon of the opposite orbit, at the level at which the dacryon (medial orbital wall) of each orbit was observed to be the most prominent.
Metopic indices of the ACF	
Frontal angle (FA)	The angle of the frontal bone in a single axial plane with the vertex located on the exocranial aspect on the most anterior point of the frontal bone and terminal points at which the lesser wings of the sphenoid bone were observed to be the most prominent.
Endocranial bifrontal angle (EBA)	The angle of the frontal bone in a single axial plane with the vertex located on the endocranial aspect on the most anterior point of the frontal bone and terminal points at which the lesser wings of the sphenoid bone were observed to be the most prominent.

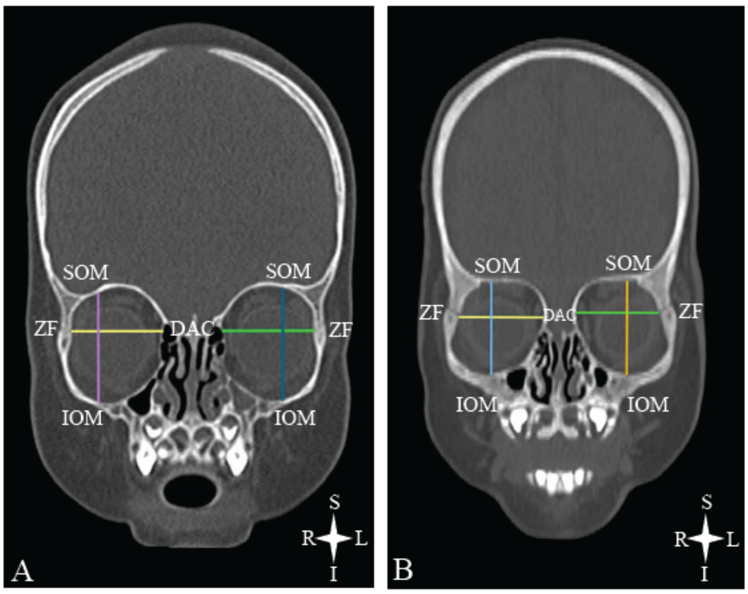

Figure 1: Orbital measurements on a coronal CT scan of a normal patient (A) and trigonocephaly patient (B) (height: IOM to SOM; width: ZF to DAC). Key: IOM – inferior orbital margin; SOM – superior orbital margin; ZF – zygomaticofrontal suture; DAC – dacryon

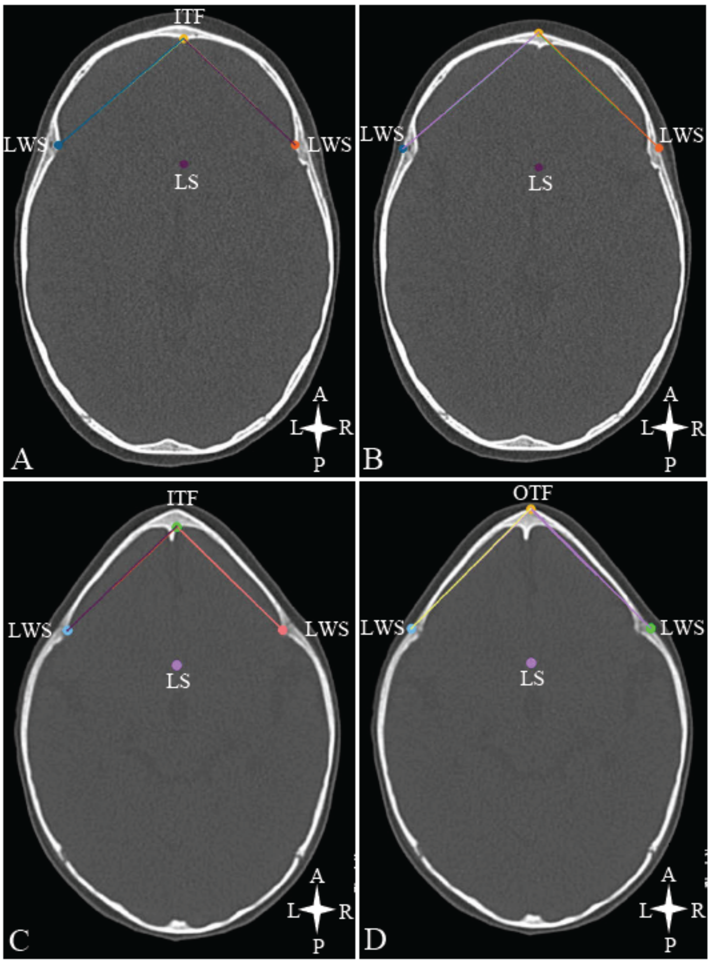

Figure 2: Metopic indices of the ACF on an axial CT scan of a normal patient (A and B) and a trigonocephaly patient (C and D) (EBA: vertex at ITF and terminal points at LWS; FA: vertex at OTF and terminal points at LWS). Key: ITF – inner table of frontal bone; OTF – outer table of frontal bone; LWS – lesser wings of sphenoid bone; LS – midpoint of limbus sphenoidale (transcended landmark used as a reference plane)

Demographics, viz., age, sex, population group, and laterality were recorded, and any significant findings pertaining to the above-mentioned parameters were documented. The various severities of trigonocephaly and pediatric age groups were taken into account when classifying the different morphological appearances of the orbits, in order to determine the relationship between these factors and the orbital morphology in trigonocephaly patients.

Trigonocephaly patients and controls were further grouped by age in order to ensure a more accurate comparative assessment. There were three age groups, viz., <12 months, 12-<36 months, and 36-<72 months. Trigonocephaly patients were classified into three severity groups according to the FA, viz., severe (<90°), moderate (91°-99°), and mild (100°-109°); and according to the EBA, viz., severe (82°-

90°), moderate (91°-99°), and mild (100°-110°). A FA between 84°-96° and a EBA between 81°-97° was observed in the control group.

3.3.4. Statistical analysis

The results were expressed as descriptive statistics, and data was analysed for normality by means of the appropriate statistical test (t-test and Ranksum test). Descriptive statistics were recorded as minimum, maximum, standard deviation, means and medians. Mean or median differences were respectively applied to morphometrical data to indicate a normal or skewed distribution of data. The t-test and Ranksum test were used to describe comparisons between trigonocephaly patients and the control group, whilst the Fischer's exact test was used to determine relationships between demographic variables. The correlation between metopic indices and orbital measurements was determined using Pearson's correlation coefficient. Each measurement was measured three times, and intra-observer and inter-observer correlation coefficient values were calculated in order to assess the accuracy and reliability of the data that was recorded. The R Statistical Computing Software of the R Core Team (R Studio, Boston, MA, USA, 2021) was used to perform statistical data analysis. A p-value of less than 0.05 was considered statistically significant.

3.4. Results

A total of 15 patients diagnosed with trigonocephaly and eight control patients with no abnormal skull shapes or craniofacial diagnosis were selected for data analysis in this study. The median age at the time the CT scan was taken was 11 months (age range: 5-36 months) in trigonocephaly patients with a male to female ratio of 6.5:1, and 22 months (age range: 1-48 months) in control patients, respectively. The majority of patients with trigonocephaly were male (86.7%), whilst only 50% of patients in the control group were male. A total of four population groups were identified in the select South African population, viz., Black, White, Indian/Asian, and Coloured. The majority of patients with trigonocephaly were Black (40%), followed by White (33.3%), Indian/Asian (20%), and Coloured (6.7%). In the control patients, the majority of patients were Black (87.5%), and Indian/Asian (12.5%). Regarding degree of severity, three (20%) patients were assigned to the mild type, seven patients (46.7%) were assigned to the moderate type, and five (33.3%) patients were assigned to the severe type according to the FA classification; whilst three (20%) patients were assigned to the mild type, five (33.3%) patients were assigned to the moderate type, and seven (46.7%) patients were assigned to the severe type according to the EBA classification.

3.4.1. Morphometry of the orbits

The comparison of the morphometry of the orbits between trigonocephaly and control patients is indicated in Table 2. Orbital height showed no significant difference when trigonocephaly patients were compared to controls (p=0.429 left, p=0.397 right) (Fig. 3A). Orbital width showed no significant difference between trigonocephaly and control patients (p=0.966 left, p=0.977 right) (Fig. 3B). No significant difference was observed in the surface area of the orbits between trigonocephaly and control patients (p=0.681 left, p=0.658 right) (Fig. 3C). Interorbital distance showed no significant difference between trigonocephaly and control patients (p=0.758) (Table 2).

Table 2: Measurements in trigonocephaly and control patients

Parameter	Trigonocephaly (n=15)	Control (n=8)	p-value
Orbital height (Median[a])			
Left	31.3(29.4-32.8)mm	32.8(31.8-33.8)mm	0.429
Right	31.2(29.6-32.7)mm	32.8(31.8-33.7)mm	0.397
Orbital width (Mean±SD)			
Left	26.2±1.87mm	26.1±2.43mm	0.966
Right	26.1±1.63mm	26.1±2.73mm	0.977
Surface area (Median[a])			
Left	687(653-760)mm^2	731(721-761)mm^2	0.681
Right	718(645-760)mm^2	736(704-764)mm^2	0.658
Interorbital distance (Mean±SD)	18.2±2.64 mm	18.6±2.79mm	0.758
EBA (Median[a])	91.2(90.4-94.6)°	91.0(89.0-92.6)°	0.324
FA (Median[a])	91.8(90.5-95.7)°	91.1(88.8-92.5)°	0.212

Abbreviations: EBA – Endocranial bifrontal angle. FA – Frontal angle SD – Standard deviation
[a]Ranksum test: Median value (Q1-Q3) is shown due to skewness of data

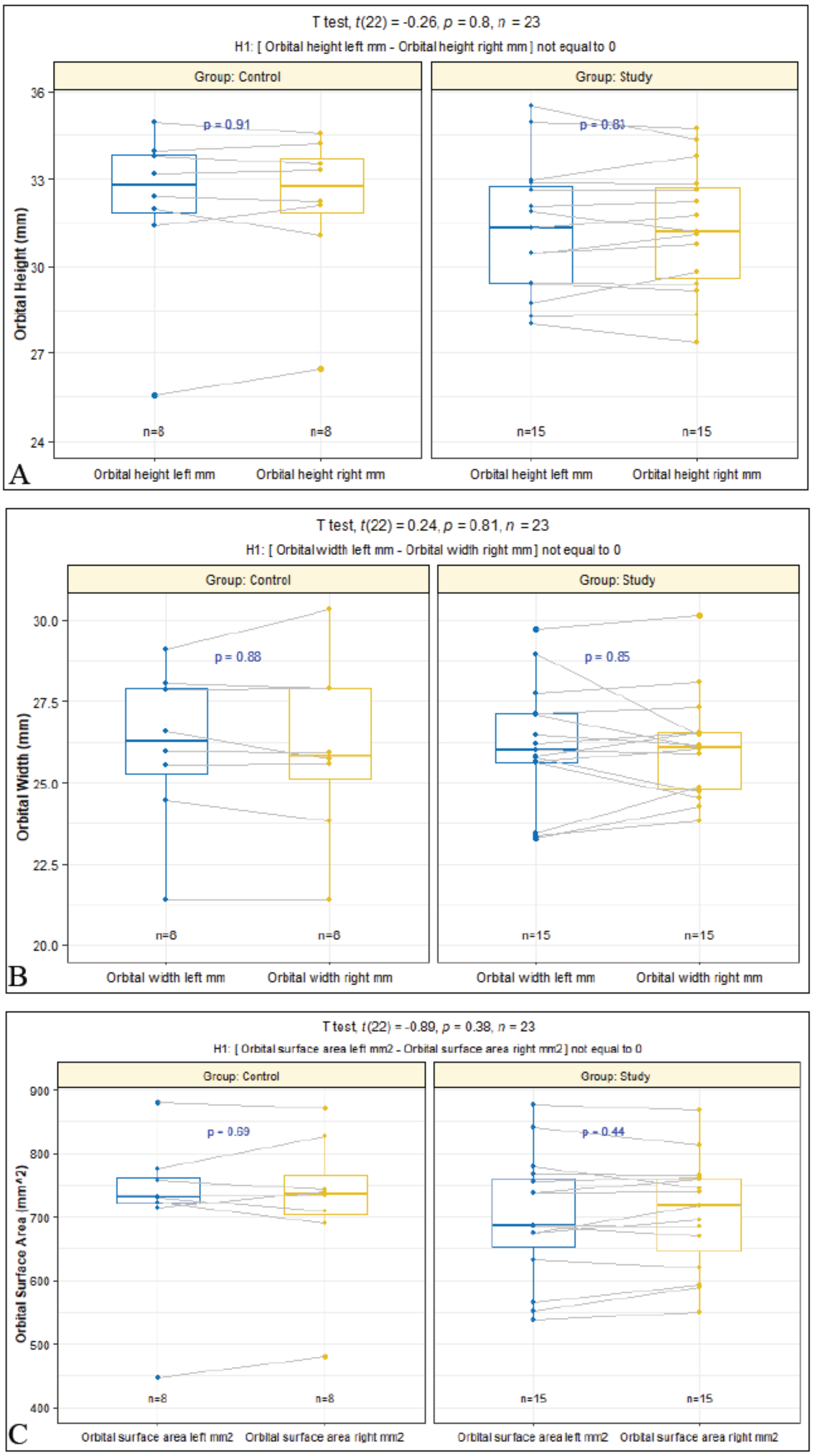

Figure 3: Laterality analysis of orbital height (A), orbital width (B), and orbital surface area (C) between trigonocephaly patients and normal patients

3.4.2. Morphology of the orbits

The classification of the morphology of the orbits in trigonocephaly patients according to the different age groups is indicated in Table 3. In the <12 months age group, kidney bean shaped orbits were the most common in both right and left orbits with a combined orbital index of both orbits ranging from 117 – 125.5 %, followed by rhomboid shaped orbits with a combined orbital index of both orbits ranging from 110 – 115.5%. Differences in morphology of left and right orbits were also observed in 1 patient whose orbital index on the left side was 122.91% which indicated a triangular shaped orbit, compared to the orbital index on the right side of 125.19% which indicated an oval shaped orbit. In the 12-<36 months age group, oval and pear shaped orbits were the most commonly observed with combined orbital indices ranging from 120 – 125% and 116 – 120.5%, respectively. Differences in the morphologies of left and right orbits were also observed in 2 patients. The first patient had an orbital index on the left side of 105.27% which indicated a tear drop shaped orbit, compared to the orbital index on the right side of 116.23% which indicated a pear shaped orbit. The second patient had an orbital index on the left side of 120.17% which indicated an oval shaped orbit, compared to the orbital index on the right side of 112.84% which indicated a rhomboid shaped orbit. In the 36-<72 months age group, 1 patient had an orbital index on the left side of 119.43% which indicated a pear shaped orbit, compared to the orbital index on the right side of 113.83% which indicated an oval shaped orbit (Table 3).

Table 3: Classification of the morphology of the orbits in trigonocephaly patients

Age group (months)	Orbital Index Range (%) *	Morphology
<12 (n=8)		
2	110 – 115.5	Rhomboid
3	117 – 125.5	Kidney bean shaped (laterally notched)
1	118 – 123.5	Tear drop shaped (superolaterally pointed)
1	Left: 122.91	Triangular shaped (medially pointed)
	Right: 125.19	Oval
1	127 – 133	Pentagon (superolaterally pointed)
12-<36 (n=6)		
1	Left: 105.27	Tear drop shaped (inferolaterally pointed)
	Right: 116.23	Pear shaped
1	Left: 120.17	Oval
	Right: 112.84	Rhomboid
1	115 – 116.5	Hexagon
1	118 – 120.5	Pear shaped
1	122 – 125	Oval
1	132 – 133	Pentagon (superolaterally pointed)
36-<72 (n=1)		
1	Left: 119.43	Pear shaped
	Right: 113.83	Oval

**Orbital Index = mean orbital height/mean orbital width x 100*

Intra-observer reliability

The intra-observer reliability test results indicate that the mean or median measurements used were very reliable and the ICC values are indicated in Table 4.

Table 4: Intra-observer reliability test expressed as ICC values

Measurement	Laterality	ICC (95%CI)	p-value
	Orbital Parameters		
Orbital height (mm)	Left	1	<0.001
	Right	1	<0.001
Orbital width (mm)	Left	1 (0.990-1.000)	<0.001
	Right	1 (0.990-1.000)	<0.001
Orbital surface area (mm^2)	Left	1 (0.990-1.000)	<0.001
	Right	0.99 (0.960-1.000)	<0.001
Interorbital distance (mm)	-	1	<0.001
	Metopic indices of the ACF		
Endocranial bifrontal angle (°)	-	1	<0.001
Frontal angle (°)	-	1	<0.001

Inter-observer reliability

The ICC values of the inter-observer reliability test are indicated in Table 5.

Table 5: Inter-observer reliability test expressed as ICC values

Measurement	Laterality	ICC (95%CI)	p-value
	Orbital Parameters		
Orbital height (mm)	Left	0.99 (0.980-1.000)	<0.001
	Right	0.96 (0.870-0.990)	<0.001
Orbital width (mm)	Left	0.71 (0.390-0.960)	<0.001
	Right	0.86 (0.640-0.980)	<0.001
Orbital surface area (mm^2)	Left	0.64 (0.290-0.940)	<0.001
	Right	0.63 (0.290-0.940)	<0.001
Interorbital distance (mm)	-	0.59 (0.246-0.930)	<0.001
	Metopic indices of the ACF		
Endocranial bifrontal angle (°)	-	0.30 (0.040-0.770)	0.023
Frontal angle (°)	-	0.32 (0.053-0.780)	0.018

3.4.3. Correlation analysis

Measurements that were observed to differ significantly between trigonocephaly patients and controls viz., EBA, FA, orbital height, orbital width, orbital surface area, and interorbital distance were compared to each other (Table 6). In trigonocephaly patients, the orbital width on the left side had a positive moderate correlation to the interorbital distance (r=0.376) compared to the orbital width on the right side which had a positive weak correlation (r=0.192); orbital height on both the left and right sides had significant but weak correlations to the interorbital distance (r=-0.057 left, r=-0.024 right); orbital surface area on the left side had a negative weak correlation to the interorbital distance (r=-0.072) compared to the orbital surface area on the right side which had a significant but weak correlation to the interorbital distance (r=-0.056); the EBA and the FA of the ACF showed negative weak correlations to the interorbital distance (r=-0.073 and r=-0.069, respectively). In normal patients, the orbital width on both the left and right sides had a positive strong correlation to the interorbital distance (r=0.799 left, r=0.712 right); orbital height on both the left and right sides had a positive strong correlation to the interorbital distance (r=0.705 left, r=0.736 right); orbital surface area on both the left and right sides had a positive strong correlation to the interorbital distance (r=0.903 left, r=0.853 right); the EBA had a significant but weak correlation to the interorbital distance (r=0.059) compared to the FA which had a positive but weak correlation to the interorbital distance (r=0.104) (Table 6).

Table 6: Correlation of interorbital distance with other measurements in trigonocephaly patients and the control group

Measurements	Trigonocephaly (n=15)	p-value	Controls (n=8)	p-value
	Interorbital distance (mm)			
Orbital width (mm)				
Left	0.376	0.167	0.799	0.017*
Right	0.192	0.492	0.712	0.048*
Orbital height (mm)				
Left	-0.057*	0.841	0.705	0.051*
Right	-0.024*	0.933	0.736	0.037*
Orbital surface area (mm^2)				
Left	-0.072	0.799	0.903	0.002*
Right	-0.056*	0.842	0.853	0.007*
Metopic indices (°)				
EBA	-0.073	0.796	0.059*	0.889
FA	-0.069	0.808	0.104	0.806

Abbreviations: EBA – Endocranial bifrontal angle. FA – Frontal angle
**Correlation is significant at the 0.05 level*
**Indicates statistical significance with a p-value>0.05*

3.5. Discussion

Trigonocephaly is caused by the premature fusion of the metopic suture, and results in a number of cranial and facial abnormalities, viz., a ridge over the middle of the forehead, shortening of the ACF, supra-orbital retrusion, hypotelorism, narrowing of the bitemporal region, and widening of the occipitoparietal region[4,5]. A reduced length and volume of the ACF is typical in trigonocephaly, therefore majority of the literature thus far focuses on restoring both the normal shape and volume of the ACF as one of the primary concerns in treatment of trigonocephaly[2,4]. There is sparse literature addressing the orbital dysmorphology and hypotelorism observed in trigonocephaly[6]. Furthermore, the morphology of the orbits in trigonocephaly have been previously described as tear drop shaped[4] without taking into account the relationship between different pediatric age groups and different degrees of severity of trigonocephaly. Additionally, previous literature has highlighted the importance of utilising metopic indices, such as the FA and EBA, in order to assess the degrees of severity of trigonocephaly[1,3,4].

Thus, this study proceeded to analyse the dimensions of the orbits in trigonocephaly patients and compare these dimensions to an age-matched control group, in order to determine if there is any correlation between orbital dimensions and metopic indices described by previous literature. Additionally, the authors proposed a new classification to categorise the orbital morphology in trigonocephaly patients according to the three pediatric age groups patients were grouped in. Furthermore, the FA and EBA were used to assess the degree of severity of trigonocephaly in order to determine if there was any relationship between the different morphological appearances of the orbits observed and the degrees of severity in trigonocephaly patients.

Orbital height, width, and surface area on both the left and right sides did not show any significance when trigonocephaly patients were compared to the control group. These findings correlate to previous literature in which both the orbital height and width on the left and right sides were also insignificant between trigonocephaly patients and the control gorup[6]. The interorbital distance is also commonly affected in trigonocephaly patients[7]. In the present study, no significance was observed in the interorbital distance between trigonocephaly patients and the control group, however, previous literature has observed a significant decrease in the interorbital distance in non-syndromic, isolated trigonocephaly patients (13.8±1.3mm) compared to the control group (18.6±1.4mm)[7]. A possible factor that could contribute to these significant differences observed in the interorbital distance could be the age of pediatric patients; in previous literature the mean age at the time the CT scan was taken was four months[7] compared to the present study's median age of 11 months. Additionally, the degree of severity could also influence the interorbital distance in trigonocephaly patients, as it is expected that orbital dysmorphology declines with increasing severity of trigonocephaly, thus introducing more functional defects of the eye[6]. Correlation analysis showed that both orbital height on the left ($r=-0.057$) and right ($r=-0.024$) sides and orbital surface area on the right ($r=-0.056$) side were significant when correlated to the interorbital distance in trigonocephaly patients, whilst significance was observed in the orbital height ($p=0.051$ left, $p=0.037$ right), width ($p=0.017$ left, $p=0.048$ right), and surface area ($p=0.002$ left, $p=0.007$ right) on both the left and right sides when correlated to the interorbital distance in the control group. The metopic indices showed no significant correlation to the interorbital distance ($r=-0.073$ EBA, $r=-0.069$ FA) in trigonocephaly patients compared to the control group where the EBA showed significant correlation to the interorbital distance ($r=0.059$). These findings differed to a previous study by Ezaldein *et al*. (2014) where the orbital dysmorphology was classified according to the EBA, and it was observed that the EBA differed significantly when trigonocephaly patients were compared to the control group.

The typical tear drop shaped orbits in trigonocephaly described by previous literature[4] was observed in only a few patients with this condition in the present study, however, different morphological appearances also exist according to different pediatric ages. More complex orbital morphologies, viz., rhomboid, kidney bean, and pentagon shaped orbits were observed in trigonocephaly patients in younger age groups, compared to less complex orbital morphologies, viz., oval and pear shaped orbits which were observed in older age groups. This morphological pattern could possibly coincide with the growth rate of the skull and orbits in pediatric patients, as well as the different degrees of severity.

The insufficient lateral orbital rims in trigonocephaly promotes the supra-orbital retrusion and bitemporal indentations[4,5]. Thus, the orbital morphometry and morphology recorded in this study, of a select South African population, provides a unique insight to craniofacial surgeons during surgical planning and correction of trigonocephaly, especially according to different degrees of severity. Additional to restoring the normal shape and volume of the ACF, the correction of hypotelorism and modification of the supraorbital bar and lateral orbital wall is a crucial aspect in the surgical reconstruction of trigonocephaly in order to restore as near to normal orbital features and functioning of the eyes.

The small sample size of both trigonocephaly patients and the control group, as well as the difficulty in obtaining age- and sex-matched control patients are significant limitations of this study. Additionally, only patients with non-syndromic, isolated trigonocephaly from a single craniofacial unit were included in this study, which also contributed to the small sample size of this study.

This study provides a novel understanding of the morphometric and morphological changes that occur in the orbits in trigonocephaly patients compared to the normal anatomy observed in a control group. Few significances were observed in the morphometry of the orbits when trigonocephaly patients were compared to the control group, however, the orbital height, width and surface area were all observed to have a significant correlation to the interorbital distance. A novel classification system was created in order to classify the different morphologies of the orbits that existed in trigonocephaly patients. The various morphological appearances observed are dependent on both the degrees of severity and age of trigonocephaly patients. These findings could assist craniofacial surgeons in the type of surgical correction needed in order to obtain as near to normal orbital morphology and function.

3.6. Recommendations

Future studies with a larger sample size are recommended by including CT scans of trigonocephaly patients from other craniofacial units in different provinces across South Africa. This will also allow for a more accurate representation of the different orbital morphologies observed in patients with this condition, as the authors introduced a new classification pertaining to this aspect. Additionally, CT scans of normal patients from other institutions should be included in future studies in order to increase the control group database to ensure a comparable number of control patients to trigonocephaly patients, thus allowing the possibility of more significant results.

3.7. Declarations

3.7.1. Acknowledgements

The authors wish to acknowledge the financial assistance of the College of Health Sciences (CHS) towards this research.

The authors wish to acknowledge Dr Partson Tinarwo for his assistance with the statistical data analysis.

3.7.2. Conflict of interest

The authors declare that there are no conflicts of interest to report.

3.7.3. Ethical approval

Ethical clearance was obtained from the Biomedical Research Ethics Committee at the University of KwaZulu-Natal (BREC/00004342/2022).

3.8. References

1. Beckett JS, Chadha P, Persing JA, Steinbacher DM. Classification of Trigonocephaly in Metopic Synostosis. Plast Reconstr Surg 2012: 130(3): 442e-447e. doi: 10.1097/PRS.0b013e31825dc244.
2. Naran S, Mazzaferro D, Wes A, Vossough A, Bartlett S, Taylor, J. 2017. A Craniometric Analysis of Cranial Base and Cranial Vault Differences in Patients with Metopic Craniosynostosis. J Craniofac Surg 2017: 28(8): 2030-2035. doi: 10.1097/SCS.0000000000003888.
3. Chandler L, Park KE, Allam O, Mozaffari MA, Khetpal S, Smetona J, Pourtaheri N, Lu X, Persing JA, Alperovich M. Distinguishing craniomorphometric characteristics and severity in metopic synostosis patients. Int J Oral Maxillofac Surg 2021: 50: 1040-1046. doi: 10.1016/j.ijom.2020.11.022.
4. Van der Meulen J. Metopic synostosis. Childs Nerv Syst 2012: 28: 1359-1367. doi: 10.1007/s00381-012-1803-z.
5. Wang JY, Dorafshar AH, Liu A, Groves ML, Ahu ES. The metopic index: an anthropometric index for the quantitative assessment of trigonocephaly from metopic synostosis. J Neurosurg Pediatr 2016: 18: 275-280. doi: 10.3171/2016.2.PEDS15524.
6. Ezaldein HH, Metzler P, Persing JA, Steinbacher DM. Three-dimensional orbital dysmorphology in metopic synostosis. J of Plast Reconstr Aesthet Surg 2014: 67: 900-905. doi: https://doi.org/10.1016/j.bjps.2014.03.009.
7. Maltese G, Tarnow P, Tovetjärn R, Kölby L. Correction of hypotelorism in isolated metopic synostosis. J Plast Surg Hang Surg 2014: 48(1): 63-66. doi: 10.3109/2000656X.2013.812967.

INTERFACE PAGE

Chapter 3 comprised of a morphometric and morphological analysis of the orbits in patients with trigonocephaly compared to an age-matched control group. The data acquired provided an understanding of the influence of factors such as pediatric age and degree of severity on the changes in the anatomy of the orbits in patients with trigonocephaly compared to the normal orbital anatomy in a control group.

CHAPTER 4: SYNTHESIS

Contributions of this chapter

This chapter discusses the main findings of Chapters 2 and 3 and provides a conclusion on the morphometry of the ACF and orbits, morphology of the orbits, an improved grading system to assess the different degrees of severity of trigonocephaly, and the volumetric compensatory growth of the MCF and PCF in trigonocephaly patients within a select South African population. An explanation of the limitations faced and recommendations for future research is also included in this chapter.

4.1. Synthesis

This study is composed of two manuscripts: the first manuscript analysed the morphometry of the anterior cranial fossa (ACF), viz. length, width, height, and volume, as well as determined the volumes of the middle and posterior cranial fossae (MCF and PCF) to investigate the presence of compensatory growth in these regions of the cranial base in patients with trigonocephaly compared to controls; the second manuscript analysed the morphometry and morphology of the orbits in patients with trigonocephaly compared to controls. Specific craniometric anatomical landmarks were utilised in both manuscripts.

The study sample size for both Manuscripts 1 and 2 included a total of 23 preoperative computed tomography (CT) scans of patients who had presented to the craniofacial unit at the Inkosi Albert Luthuli Central Hospital (IALCH) between 2012 and 2023. A total of 15 patients with a radiographic confirmed diagnosis of non-syndromic, isolated trigonocephaly who had met the inclusion criteria were selected as the patient group of this study; whilst a total of eight patients with no skull abnormalities and who had met the inclusion criteria were selected as the comparable control group of this study. The median age of trigonocephaly patients in the present study was 11 months, which is larger in comparison to previous studies by Beckett *et al*. (2012), Ezaldein *et al*. (2014), Naran *et al*. (2017), Baş *et al*. (2021), and Chandler *et al*. (2021) who had mean ages ranging from 6-7.2 months, respectively. Additionally, patients with trigonocephaly are being reported and diagnosed much earlier in age in first world countries such as the United States of America, Netherlands, and France, therefore resulting in a relatively smaller mean age of patients (Van der Meulen, 2012; Ezaldein *et al*., 2014; Naran *et al*., 2017; Applegren *et al*., 2018; Chandler *et al*., 2021). Whereas in the present study in a South African population, patients with trigonocephaly are being reported and diagnosed later in age, ultimately affecting the overall median age and degree of severity of the present study.

4.1.1. Manuscript 1: A morphometric analysis of the cranial base and severity in trigonocephaly

Previous literature has documented trigonocephaly to be more predominant in males compared to females, with a male to female ratio of 3-3.5:1 (Van der Meulen, 2012; Cornelissen *et al*., 2016; Ghizoni *et al*., 2016; Baş *et al*., 2021). A study by Maltese *et al*. (2014) observed a larger male to female prevalence ratio of 5.4:1. Findings from the present study concur with these previous findings and identified 13 males and two females with a male to female prevalence ratio of 6.5:1.

Selected anatomical landmarks

Anatomically based craniometric landmarks were identified and determined by a plastic and reconstructive surgeon and an anatomist on preoperative two dimensional (2D) axial and sagittal CT scans in order to calculate the dimensions of the ACF. A study by Chandler *et al*. (2021) utilised the midpoint of the sella turcica as a reference landmark to calculate the length, width, and height of the anterior cranium. However, the authors of the present study believed that the sella turcica is too variable in its size and morphology, especially when different age groups and sexes are compared, thus reducing the reproducibility and accuracy of the length, width, and height of the ACF. Therefore, the midpoint of the limbus sphenoidale (the anterior border of the prechiasmatic sulcus) was selected as the reference landmark to calculate the morphometry of the ACF in this study. Similarly, where the lesser wings of the sphenoid bone were observed to be the most prominent, was selected as the lateral boundary to calculate the length and width of the ACF.

Additionally, various studies have used different methods and anatomical landmarks to describe the frontal angle (FA) and endocranial bifrontal angle (EBA) of the ACF. Previously, the superior part of the crista galli was used as a reference landmark, and the lateral borders of the orbital apertures were used as terminal points to measure the EBA; whilst the pterion and nasion were used as reference landmarks and the coronal sutures were used as terminal points to measure the FA (Beckett *et al*., 2012; Van der Meulen, 2012; Ezaldein *et al*., 2014; Naran *et al*., 2017; Chandler *et al*., 2021). These previous studies analysed and calculated the angles of the ACF using three dimensional (3D) reconstructions of CT scans. The present study analysed and calculated the angles of the ACF using radiographic 2D CT scans, thus different landmarks needed to be determined in order to ensure that the analysis of these angles were reliable and accurate according to the type of format available. Therefore, the angles of the ACF were measured in the same plane as the reference landmark (limbus sphenoidale) that was selected, and where the lesser wings of the sphenoid bone were first observed to be the most prominent were chosen as terminal points as this was a more linear landmark as opposed to the curved landmark of the lateral borders of the orbital apertures that were previously described.

Furthermore, no previous studies have documented and recorded the volumes of the cranial base alone. Thus, this study was the first to record the volumes of all three cranial fossae in trigonocephaly patients on 2D CT scans, compared to previous literature which recorded the volumes of the entire anterior, middle, and posterior cranial thirds of the skull using 3D reconstructions of CT scans. Therefore, anatomical landmarks that were visible on the 2D CT scans were selected as specific anterior, posterior and lateral boundaries in order to calculate the volumes of the ACF, MCF and PCF. The most prominent observation of the fused coronal suture was selected as the posterior boundary that separated the ACF from the MCF; the most prominent observation of the superior margin of the petrous part of the temporal bone was selected as the posterior boundary that separated the MCF from the PCF; and the most prominent observation of the inferior margin of the petrous part of the temporal bone was selected as the anterior boundary that separated the PCF from the MCF.

Inter-reliability assessment

The majority of the parameters of the ACF yielded moderate to excellent inter-reliability test results, expect for the EBA and FA. Similarly, the volume of the MCF yielded poor inter-reliability test results. Due to the small sample size and parameters being measured on patients in a 2D format, some anatomical landmarks were not clearly visible. Additionally, due to the limited number of CT scans that were available for analysis, slice thickness and positioning of the patient during scanning could have also influenced the visibility of the selected anatomical landmarks and was thus unavoidable. Furthermore, the volumes of the cranial fossae were all manually outlined on every CT scan slice, and therefore a certain degree of error was to be expected in these measurements.

Main findings

Only one study has documented the length, width, height, and volume of the anterior cranium (Chandler *et al*., 2021) in non-syndromic, isolated trigonocephaly patients, but not the specific dimensions of the ACF alone. Thus, to the authors knowledge, this study is the first to investigate and record the specific dimensions of the ACF as well as the volumes of all three cranial fossae in non-syndromic, isolated trigonocephaly patients. The results from the present study observed that the ACF length, width, height, and volume in trigonocephaly patients in the 12-<36 months age group were smaller when compared to controls in the same age group. However, both the EBA and FA were much larger in trigonocephaly patients compared to controls. In the older 36-<72 months age group, the ACF length, width, and FA were smaller in trigonocephaly patients compared to controls, whilst the ACF height, volume, and EBA were all observed to be larger in trigonocephaly patients compared to controls. The degrees of severity could be attributed to the difference in results in the various age groups, as the more severe the condition of trigonocephaly, the smaller the dimensions and volume of the ACF.

The volume of the MCF was observed to be significantly larger in trigonocephaly patients compared to controls ($p=0.050$). Overall, the PCF showed the most compensatory growth of 30.4%, followed by the MCF of 28.8%. These findings indicate that both the middle and posterior regions of the cranial base compensate for the growth of the skull and developing brain, due to the restricted growth of the ACF in patients with trigonocephaly. This differs from the findings by Naran *et al*. (2017), who observed compensatory growth only in the entire middle third of the skull and not in the posterior third of the skull. Furthermore, in the present study, no significant difference was observed in the total cranial fossae volume when trigonocephaly patients were compared to controls ($p=0.973$). Additionally, different amounts of compensatory growth in the MCF and PCF were observed in trigonocephaly patients when the FA and EBA classifications were used to assess the different degrees of severity. According to the FA severity classification, an overall decrease in the compensatory growth of the MCF was observed throughout mild, moderate, and severe patients; whereas the most amount of compensatory growth in the PCF was observed in moderate compared to mild and severe patients. According to the EBA severity classification, an overall decrease in the compensatory growth of the MCF was also observed throughout mild, moderate, and severe patients, with the same percentage of compensatory growth in mild patients as the FA severity (32.0±9.84%); whereas the most amount of compensatory growth in the PCF was observed in severe compared to mild and moderate patients.

The EBA and FA showed no significance as an assessment of severity when trigonocephaly patients were compared to controls (p=0.324 and p=0.212, respectively). However, when the FA and EBA were used to classify the different degrees of severity, a similar amount of patients were classified in the different groups of severity. In the FA severity classification, the majority of trigonocephaly patients across all three age groups were classified into the moderate group, whereas in the EBA severity classification, the majority of trigonocephaly patients across all three age groups were classified into the severe group. These similar trends between the FA and EBA severity classifications indicate that using both of these classifications are very effective in assessing the severity of patients with trigonocephaly.

4.1.2. Manuscript 2: Hypotelorism-associated orbital morphometry and morphology in trigonocephaly

Selected anatomical landmarks

Selected anatomical landmarks were identified and determined by a plastic and reconstructive surgeon and an anatomist on preoperative two dimensional (2D) axial and coronal CT scans in order to calculate the dimensions of the orbits. The orbital height and width was measured according to the landmarks described by Ezaldein *et al*. (2014), where the infraorbital margin and the zygomaticofrontal suture were observed to be the most prominent. The orbital surface area was manually outlined on each orbit where the zygomaticofrontal suture was observed to be the most prominent. The interorbital distance was measured according to the landmarks described by Maltese *et al*. (2014) and Pala *et al*. (2015), where the dacryon on either medial orbital wall was observed to be the most prominent.

Inter-reliability assessment

The majority of the parameters of the orbits yielded moderate to excellent inter-reliability test results. The orbital surface area of both orbits only yielded moderate inter-reliability test results, as the surface area was manually outlined on the CT scan images and therefore a certain degree of error was to be expected in these measurements.

Main findings

Few studies have recorded the dimensions of the orbits in trigonocephaly patients, however, to the authors knowledge no other study has documented the surface area or different morphologies of the orbits in patients with this condition. Orbital dysmorphology and hypotelorism occurs as a result of both orbital rims being laterally depressed, therefore, the orbits are positioned closer together than normal (Ezaldein *et al*., 2014; Štefánková *et al*., 2015). The results of the present study observed that there was no significant difference between the orbital height, width, and surface area when trigonocephaly patients were compared to controls. The interorbital distance was smaller in trigonocephaly patients (18.2±2.64mm) compared to controls (18.6±2.79mm), albeit it being not significantly smaller (p=0.758). In a study by Maltese *et al*. (2014), the interorbital distance was observed to be significantly smaller in patients with trigonocephaly (13.8±1.3mm) compared to controls (18.6±1.4mm). The mean age of the previous mentioned study was four months as opposed to the median age of 11 months in the present study, which could have contributed to the difference in significant results.

Hypotelorism can vary from mild to severe forms depending on the degree of severity of trigonocephaly (Štefánková *et al*., 2015). Thus, a correlation analysis between the interorbital distance, orbital measurements, and metopic indices was performed in order to determine the impact that the degrees of severity had on the dimensions of the orbits. The orbital height showed a weak but significant correlation to the interorbital distance (r=-0.057 left, r=-0.024 right) in trigonocephaly patients, which indicated that a decreased orbital height and a larger interorbital distance was observed in mild compared to severe trigonocephaly patients. Additionally, the orbital surface area on the right side showed a weak but significant correlation to the interorbital distance (r=-0.056) in trigonocephaly patients, which indicated a smaller orbital surface area on the right side and a larger interorbital distance was observed in mild compared to severe trigonocephaly patients. The metopic indices showed no significant correlation to the interorbital distance in patients with trigonocephaly.

Previous studies have described the orbits in patients with trigonocephaly to be typically tear drop shaped (Van der Meulen, 2012). However, the present study utilised the orbital index to document the different orbital morphologies pertaining to pediatric age, degree of severity and laterality. In each age group, trigonocephaly patients were further categorised into the three different types of severity according to the FA and EBA. In the <12 months age group, rhomboid and kidney bean shaped orbits were observed to be the most common in moderate and severe trigonocephaly patients; whilst in the 12-<36 and 36-<72 months age groups, oval and pear shaped orbits were observed to be the most common in mild and severe trigonocephaly patients, with visible differences in morphologies between right and left sides.

4.2. Limitations

Only non-syndromic, isolated trigonocephaly patients within a retrospective 11 year period were chosen and selected for analysis in this study. Thus, the most significant limitation of this study was the small sample size of patients with this condition, as well as patients being identified with trigonocephaly at only one craniofacial unit in South Africa. Additionally, only a small sample size of controls were available for analysis as it is very difficult to obtain normal age- and sex-matched CT scans of pediatric patients, therefore impacting the statistical significance of results between trigonocephaly and control groups. Regarding the classification of severity in trigonocephaly patients, previous literature analysed non-syndromic, isolated trigonocephaly patients from multiple craniofacial units with a much lower mean age, as well as a larger cohort of normal patients enabling more comparable significant findings. Furthermore, previous studies that assessed the degrees of severity of trigonocephaly patients did not further group the different severities according to different pediatric age groups. Therefore, the overall severity in the literature was classified according to the mean metopic parameters in the entire cohort of trigonocephaly patients. However, in the present study, the overall degrees of severity were further classified in the three different pediatric age groups, which further reduced the sample size in each age group, resulting in statistically insignificant results. Furthermore, the present study analysed parameters on 2D CT scans using the Horos Project Software, compared to previous literature which analysed parameters on 3D reconstructions of CT scans using the Materialise Mimics Software. The difference in analysing software could have significantly impacted the parameters used to assess the degrees of severity in the present study compared to previous literature. Intra-observer reliability assessment yielded excellent results in all parameters measured in this study, however, due to the novelty of many aspects of this study as well as the limited radiographic material available, a certain degree of error was to be expected in the inter-observer reliability assessment and was thus unavoidable.

4.3. Future recommendations

Future studies should still conduct research on non-syndromic, isolated trigonocephaly patients to accurately document the changes in the ACF and orbits without being influenced by syndromic or multiple suture fusion craniosynostoses. Additionally, trigonocephaly patients from multiple craniofacial units across South Africa should be included in future studies in order to document a larger sample size of patients with this condition, thus producing more significant results. Radiographic material of normal patients from other institutions should also be included in future research in order to increase the database of control patients. Further research on the FA and EBA to assess the degree of severity in a much larger sample size of trigonocephaly in a South African population should be conducted in order to determine the reproducibility and significance of these severity classifications. Furthermore, future studies should analyse 3D reconstructions of CT scans of trigonocephaly patients to allow for more direct comparisons to previous studies using the same methodology to determine if similar significant results can be documented.

4.4. Conclusions

The majority of the morphometric and morphological data in this study is novel to a specific South African population of patients with trigonocephaly. The data obtained provides an understanding to craniofacial surgeons on the changes that occur in the ACF in trigonocephaly patients compared to the normal anatomy observed in control patients. The length, height, and volume of the ACF is the most severely affected in trigonocephaly patients, and can be more so according to different pediatric age groups and degrees of severity. The proposed severity assessment using the FA and EBA could assist craniofacial surgeons in providing a more accurate assessment of the severity of trigonocephaly and surgical corrective treatment. However, surgeons need to take into consideration the age of trigonocephaly patients when determining different degrees of severity, as the proposed angle ranges are much smaller in the present South African population compared to other population groups in the United States of America and Europe.

Furthermore, hypotelorism is also a major concern in patients with trigonocephaly with the orbital height, surface area, and interorbital distance being the most affected in patients with this condition. Different orbital morphologies exist in trigonocephaly patients, with more complex orbital morphologies observed in younger pediatric patients that were categorised into the severe type as opposed to older pediatric patients that were categorised into moderate to mild types. The dimensions and morphology of the orbits could provide an insight useful to craniofacial surgeons on the changes that occur to the orbits, and to assist in restoring as near to normal functioning and structure of the eyes.

Overall, this study provides novel approaches to the changes that occur in the cranial base and orbits in patients with trigonocephaly in South Africa. The data obtained from this study will help surgeons to take into consideration the age and different degrees of severity of trigonocephaly patients prior to surgical planning and correction, as well as provide a more accurate and improved assessment of severity of patients with trigonocephaly.

4.5. References

1. Applegren, N. D., Shock, L. A., Aldridge, K. J., Derrick, C. D., Tanaka, T., Baker, C. L., Muzaffar, A. R. 2018. Relationship of a metopic ridge and anterior cranial volume measured by a non-invasive laser shape digitizer. *Journal of Craniofacial Surgery*, 29(1), pp. 76-81. doi: 10.1097/SCS.0000000000004065.
2. Baş, N. S., Baş, S. 2021. Craniometric Measurements and Surgical Outcomes in Trigonocephaly Patients Who Underwent Surgical Treatment. The *Cureus Journal of Medical Science,* 13(3), pp. e13676. doi: 10.7759/cureus.13676.
3. Beckett, J. S., Chadha, P., Persing, J. A., Steinbacher, D. M. 2012. Classification of Trigonocephaly in Metopic Synostosis. *Journal of Plastic and Reconstructive Surgery*, 130(3), pp. 442e-447e. doi: 10.1097/PRS.0b013e31825dc244.
4. Chandler, L., Park, K. E., Allam, O., Mozaffari, M. A., Khetpal, S., Smetona, J., Pourtaheri, N., Lu, X., Persing, J. A., Alperovich, M. 2021. Distinguishing craniomorphometric

characteristics and severity in metopic synostosis patients. *International Journal of Oral and Maxillofacial Surgery*, 50, pp. 1040-1046. doi: 10.1016/j.ijom.2020.11.022.

5. Cornelissen, M., Den Ottelander, B., Rizopoulos, D., Van der Hulst, R., Van der Molen, A. M., Van der Horst, C., Delye, H., Van Veelen, M. L., Bonsel, G., Mathijssen, I. 2016. Increase of prevalence of craniosynostosis. *Journal of Cranio-Maxillo-Facial Surgery*, 44, pp. 1273-1279. doi: 10.1016/j.jcms.2016.07.007.
6. Ezaldein, H. H., Metzler, P., Persing, J. A., Steinbacher, D. M. 2014. Three-dimensional orbital dysmorphology in metopic synostosis. *Journal of Plastic, Reconstructive and Aesthetic Surgery*, 67, pp. 900-905. doi: 10.1016/j.bjps.2014.03.009.
7. Ghizoni, E., Denadai, R., Raposo-Amaral, C. A., Joaquim, A. F., Tedescni, H., Raposo-Amaral, C. E. 2016. Diagnosis of infant synostotic and nonsynostotic cranial deformities: a review for pediatricians. *Revista Paulista De Pediatria*, 34(4), pp. 495-502. doi: 10.1016/j.rpped.2016.01.004.
8. Maltese, G., Tarnow, P., Tovertjärn, R., Kölby, L. 2014. Correction of hypotelorism in isolated metopic synostosis. *Journal of Plastic Surgery and Hand Surgery*, 48(1), pp. 63-66. doi: 10.3109/2000656X.2013.812967.
9. Naran, S., Mazzaferro, D., Wes, A., Vossough, A., Bartlett, S., Taylor, J. 2017. A Craniometric Analysis of Cranial Base and Cranial Vault Differences in Patients with Metopic Craniosynostosis. *Journal of Craniofacial Surgery*, 28(8), pp. 2030-2035. doi: 10.1097/SCS.0000000000003888.
10. Pala, H. G., Artunç-Ülkümen, B., Koyuncu, F. M., Uyar, Y., Bülbül-Baytur, Y. 2015. Normal ranges of biorbital and interorbital distances in healthy Turkish pregnancies at 19-23 weeks of gestation and correlation with craniofacial structures. *Journal of the Turkish-German Gynecological Association*, 16, pp. 170-173. doi: 10.5152/jtgga.2015.15062.
11. Štefánková, E., Horn, F., Neščáková, E., Kabát, M.,Petrík, M., Trnka, J. 2015. Anthropometry of craniosynostosis. *Polish Journal of Neurology and Neurosurgery*, 49(4), pp. 229-238. doi: 10.1016/j.pjnns.2015.05.006.
12. Van der Meulen, J. 2012. Metopic synostosis. *Child's Nervous System*, 28, pp. 1359-1367. doi: 10.1007/s00381-012-1803-z.

Appendix A: Full ethical approval

UNIVERSITY OF KWAZULU-NATAL™
INYUVESI YAKWAZULU-NATALI

11 September 2022

Miss Courtney Barnes (218008430)
School of Lab Med & Medical Sc
Westville

Dear Miss Barnes,

Protocol reference number: BREC/00004342/2022
Project title: Trigonocephaly: A morphometric analysis utilising specific anatomical cranial landmarks in a South African population
Degree: Masters

EXPEDITED APPLICATION: APPROVAL LETTER

A sub-committee of the Biomedical Research Ethics Committee has considered and noted your application.

The conditions have been met and the study is given full ethics approval and may begin as from 11 September 2022. Please ensure that any outstanding site permissions are obtained and forwarded to BREC for approval before commencing research at a site.

Note to PI: A statistician should be consulted at the design stage to ensure that the planned sample size is adequate. Consultation at the analysis stage may be too late to ensure meaningful data.

This approval is valid for one year from 11 September 2022. To ensure uninterrupted approval of this study beyond the approval expiry date, an application for recertification must be submitted to BREC on the appropriate BREC form 2-3 months before the expiry date.

Any amendments to this study, unless urgently required to ensure safety of participants, must be approved by BREC prior to implementation.

Your acceptance of this approval denotes your compliance with South African National Research Ethics Guidelines (2015), South African National Good Clinical Practice Guidelines (2020) (if applicable) and with UKZN BREC ethics requirements as contained in the UKZN BREC Terms of Reference and Standard Operating Procedures, all available at http://research.ukzn.ac.za/Research-Ethics/Biomedical-Research-Ethics.aspx.

BREC is registered with the South African National Health Research Ethics Council (REC-290408-009). BREC has US Office for Human Research Protections (OHRP) Federal-wide Assurance (FWA 678).

The sub-committee's decision will be noted by a full Committee at its next meeting taking place on 11 October 2022.

Yours sincerely,

[redacted]

Prof D Wassenaar
Chair: Biomedical Research Ethics Committee

Biomedical Research Ethics Committee
Chair: Professor D R Wassenaar
UKZN Research Ethics Office Westville Campus, Govan Mbeki Building
Postal Address: Private Bag X54001, Durban 4000
Email: BREC@ukzn.ac.za
Website: http://research.ukzn.ac.za/Research-Ethics/Biomedical-Research-Ethics.aspx

Appendix B: IALCH Gatekeeper permission

KWAZULU-NATAL PROVINCE
HEALTH
REPUBLIC OF SOUTH AFRICA

DIRECTORATE:

Physical Address 800 Vusi Mzimela Road, Mayville - 4058
Postal Address: Private bag X03 Mayville – 4058
Tel: 031 240 1124 Fax: 031 240 1005 Email: linda.mtshali@ialch.co.za
www.kznhealth.gov.za

OFFICE OF THE MEDICAL MANAGER
INKOSI ALBERT LUTHULI CENTRAL HOSPITAL

Reference: BREC/00004342/2022
Enquiries: Dr. A. Harrichandparsad

23 January 2023

Miss C Barnes (218008430)
School of Lab Med & Medical Sc
Westivlle

Dear Ms Barnes

Re: Approved Research: Ref No: BREC/00004342/2022: A morphometric analysis utilising specific anatomical cranial landmarks in a South African population.

As per the policy of the Provincial Health Research Committee (PHRC), you are hereby granted permission to conduct the above-mentioned research once all relevant documentation has been submitted to PHRC inclusive of Full Ethical Approval.

Kindly note the following.

1. The research should adhere to all policies, procedures, protocols and guidelines of the KwaZulu-Natal Department of Health.
2. Research will only commence once the PHRC has granted approval to the researcher.
3. The researcher must ensure that the Medical Manager is informed before the commencement of the research by means of the approval letter by the chairperson of the PHRC.
4. The Medical Manager expects to be provided feedback on the findings of the research.
5. Kindly submit your research to:

- The application is an online process by logging on to: HTTP://NHRD.HEALTH.GOV.ZA and follow the steps as indicated on the Provincial Health Research page.

Yours fai[redacted].........

Dr A Harrichandparsad
Acting Medical Management

GROWING KWAZULU-NATAL TOGETHER

KWAZULU-NATAL PROVINCE
HEALTH
REPUBLIC OF SOUTH AFRICA

DIRECTORATE:

INKOSI ALBERT LUTHULI CENTRAL HOSPITAL
OFFICE OF THE MEDICAL MANAGER
Private Bag X03, Mayville, 4058
800 Vusi Mzimela (Bellair) Road, Mayville,4091
Tel: 031 240 1059 Fax: 031 240 1005 Email: Ursula.john@ialch.co.za

Reference: BREC/00004342/2022
Enquiries: Medical Management

23 January 2023

Miss C Barnes (218008430)
School of Lab Med & Medical Sc
Westville

Dear Ms Barnes

RE: PERMISSION TO CONDUCT RESEARCH AT IALCH

I have pleasure in informing you that permission has been granted to you by the Medical Manager to conduct research on: **A morphometric analysis utilising specific anatomical cranial landmarks in a South African population.**

Kindly take note of the following information before you continue:

1. Please ensure that you adhere to all the policies, procedures, protocols and guidelines of the Department of Health with regards to this research.
2. This research will only commence once this office has received confirmation from the Provincial Health Research Committee in the KZN Department of Health.
3. Kindly ensure that this office is informed before you commence your research.
4. The hospital will not provide any resources for this research.
5. You will be expected to provide feedback once your research is complete to the Medical Manager.

Yours faithfully

....[redacted]......
Dr A Harrichandparsad
Acting Medical Manager

GROWING KWAZULU-NATAL TOGETHER

Appendix C: DOH Gatekeeper permission

KWAZULU-NATAL PROVINCE
HEALTH
REPUBLIC OF SOUTH AFRICA

DIRECTORATE:

Postal Address: Private Bag X9050
Physical Address: 330 Langalibalele Str, PM Burg; 3201
Tel: 0333953189/3123/2805 Fax: 033-3943782
Email address: hrkm@kznhealth.gov.za
www.kznhealth.gov.za

Health Research & Knowledge Management Unit

NHRD Ref: KZ_202208_019

Dear Ms C Barnes
(UKZN)

Approval of research

1. The research proposal titled **'Trigonocephaly: A morphometric analysis utilising specific anatomical cranial landmarks in a South African population'** was reviewed by the KwaZulu-Natal Department of Health (KZN-DoH).

   The proposal is hereby **approved** for research to be undertaken at Inkosi Albert Luthuli Central hospital.

2. You are requested to take note of the following:
   a. *All research conducted in KwaZulu-Natal must comply with government regulations relating to Covid-19. These include but are not limited to: regulations concerning social distancing, the wearing of personal protective equipment, and limitations on meetings and social gatherings.*
   b. *Kindly liaise with the facility manager BEFORE your research begins in order to ensure that conditions in the facility are conducive to the conduct of your research. These include, but are not limited to, an assurance that the numbers of patients attending the facility are sufficient to support your sample size requirements, and that the space and physical infrastructure of the facility can accommodate the research team and any additional equipment required for the research.*
   c. *Please ensure that you provide your letter of ethics re-certification to this unit, when the current approval expires.*
   d. *Provide an interim progress report and final report (electronic and hard copies) when your research is complete to* ***HEALTH RESEARCH AND KNOWLEDGE MANAGEMENT, 10-102, PRIVATE BAG X9051, PIETERMARITZBURG, 3200*** *and e-mail an electronic copy to hrkm@kznhealth.gov.za*
   e. *Please note that the Department of Health shall not be held liable for any injury that occurs as a result of this study.*

For any additional information please contact Ms G Khumalo on 033-395 3189.

Yours Sincerely

[redacted]

Chairperson, Health Research Committee
Date: 30/08/2022

GROWING KWAZULU-NATAL TOGETHER

Appendix D: Datasheet sample 1

Patient ID	Age CT scan was taken (months)	Race	Sex	ACF Length (mm)	ACF Width (mm)	ACF Height (mm)

(Data available on request)

Appendix E: Datasheet sample 2

Patient ID	Age CT scan was taken (months)	Race	Sex	ACF Frontal Angle (°)	ACF Endocranial Bifrontal Angle (°)

(Data available on request)

Appendix F: Datasheet sample 3

Patient ID	Age CT scan was taken (months)	Race	Sex	ACF Volume (mm^3)	MCF Volume (mm^3)	PCF Volume (mm^3)

(Data available on request)

Appendix G: Datasheet sample 4

Patient ID	Age CT scan was taken (months)	Race	Sex	Cephalic Length (mm)	Cephalic Width (mm)	Cephalic Index (%)

(Data available on request)

Appendix H: Datasheet sample 5

Patient ID	Age CT scan was taken (months)	Race	Sex	Left Orbital Height (mm)	Left Orbital Width (mm)	Left Orbital Surface Area (mm^2)

(Data available on request)

Appendix I: Datasheet sample 6

Patient ID	Age CT scan was taken (months)	Race	Sex	Right Orbital Height (mm)	Right Orbital Width (mm)	Right Orbital Surface Area (mm^2)

(Data available on request)

Appendix J: Datasheet sample 7

Patient ID	Age CT scan was taken (months)	Race	Sex	Interorbital Distance (mm)

(Data available on request)

Appendix K: Datasheet sample 8

Patient ID	Age CT scan was taken (months)	Race	Sex	Orbital Height (mm)	Orbital Width (mm)	Orbital Index (%)

(Data available on request)

Appendix L: Turnitin Report

Masters Thesis - Courtney Barnes

ORIGINALITY REPORT

9%	6%	8%	3%
SIMILARITY INDEX	INTERNET SOURCES	PUBLICATIONS	STUDENT PAPERS

PRIMARY SOURCES

1	Submitted to University of KwaZulu-Natal Student Paper	2%
2	"Microscopy Techniques for Biomedical Education and Healthcare Practice", Springer Science and Business Media LLC, 2023 Publication	2%
3	researchspace.ukzn.ac.za Internet Source	2%
4	archive.org Internet Source	1%
5	Sanjay Naran, Daniel Mazzaferro, Ari Wes, Arastoo Vossough, Scott P. Bartlett, Jesse A. Taylor. "A Craniometric Analysis of Cranial Base and Cranial Vault Differences in Patients With Metopic Craniosynostosis", Journal of Craniofacial Surgery, 2017 Publication	<1%
6	"6th World Congress of PGHAN", Journal of Pediatric Gastroenterology and Nutrition, 2021 Publication	<1%

APPENDIX M: Papers and Scientific Presentations Emanating from the Study

The following is an outline of the research outputs from this thesis:

Book Chapter

Madaree, A., Bisetty, V., Mohan, N., **Barnes, C**. and Lazarus, L., 2023. An Exploration of the Practice of CT Modalities to Evaluate Anterior Cranial Deformities in Craniosynostosis. In Microscopy Techniques for Biomedical Education and Healthcare Practice: Principles in Light, Fluorescence, Super-Resolution and Digital Microscopy, and Medical Imaging (pp. 125-142). Cham: *Springer Nature Switzerland.*

Scientific Presentation

A morphometric analysis of the metopic indices and orbits in trigonocephaly.
XXVIII International Symposium on Morphological Sciences; 5 to 8 August 2023; Cape Town
C. Barnes, A. Madaree, L. Lazarus.